CAPITAL UNIVERSITY OF SCIENCE AND
TECHNOLOGY, ISLAMABAD

A Novel Compound Gauge Based on Quartz Tuning Fork

by

Faiz Mustafa

A thesis submitted in partial fulfillment for the
degree of Master of Science

in the

Faculty of Engineering
Department of Electrical and Computer Engineering

2025

I dedicate this work to my dearest parents, my sons (Maarib Mustafa and Maahid Mustafa), my beloved wife and my mentors Munawar Hussain Goraya & Dilawar Hussain Goraya whose unwavering support and encouragement have been the driving force behind my successful academic journey.

CERTIFICATE OF APPROVAL

A Novel Compound Gauge Based on Quartz Tuning Fork

by

Faiz Mustafa

(MEE221001)

THESIS EXAMINING COMMITTEE

S. No.	Examiner	Name	Organization
(a)	External Examiner	Dr. Shabbir Majeed Chaudhry	UET, Taxila
(b)	Internal Examiner	Dr. Muhammad Riaz	CUST, Islamabad
(c)	Supervisor	Dr. Noor Muhammad Khan	CUST, Islamabad

Dr. Noor Muhammad Khan
Thesis Supervisor
April, 2025

Dr. Noor Muhammad Khan
Head
Dept. of Electrical and Computer Engineering
April, 2025

Dr. Imtiaz Ahmad Taj
Dean
Faculty of Engineering
April, 2025

Author's Declaration

I, **Faiz Mustafa** hereby state that my MS thesis titled "**A Novel Compound Gauge Based on Quartz Tuning Fork**" is my own work and has not been submitted previously by me for taking any degree from Capital University of Science and Technology, Islamabad or anywhere else in the country/abroad.

At any time if my statement is found to be incorrect even after my graduation, the University has the right to withdraw my MS Degree.

(Faiz Mustafa)

Registration No: MEE221001

Plagiarism Undertaking

I solemnly declare that research work presented in this thesis titled "**A Novel Compound Gauge Based on Quartz Tuning Fork**" is solely my research work with no significant contribution from any other person. Small contribution/help wherever taken has been duly acknowledged and that complete thesis has been written by me.

I understand the zero tolerance policy of the HEC and Capital University of Science and Technology towards plagiarism. Therefore, I as an author of the above titled thesis declare that no portion of my thesis has been plagiarized and any material used as reference is properly referred/cited.

I undertake that if I am found guilty of any formal plagiarism in the above titled thesis even after award of MS Degree, the University reserves the right to withdraw/revoke my MS degree and that HEC and the University have the right to publish my name on the HEC/University website on which names of students are placed who submitted plagiarized work.

(Faiz Mustafa)

Registration No: MEE221001

Acknowledgement

First of all, immense gratitude to Almighty Allah (SWT) for blessing me with strength, knowledge and guidance, igniting my journey's inspiration and unwavering determination.

I extend my heartfelt gratitude to my supervisor **Dr. Noor Muhammad Khan** for his invaluable guidance, motivation and unwavering support throughout my research. I am also thankful to Dr. Muhammad Ashraf for providing the clarity of various concepts which were very helpful for this research.

I extend my sincere gratitude to Dr. Muhammad Yasin Shami and Dr. Allah Bakhsh as well for providing their valuable guidance and support.

Last but not least, I would like to extend a heartfelt appreciation to my parents and my sisters whose boundless love and unwavering support have been the foundation of my academic journey.

(Faiz Mustafa)

Abstract

This thesis presents the design, development, and validation of a novel compound pressure gauge based on Quartz Tuning Fork (QTF) sensor. The proposed design is capable of measuring pressures across an extensive range—from high vacuum levels to positive pressures region. The goal of this research is to bridge the gap between conventional pressure sensors, which are often specialized for either vacuum or positive pressure measurement, and to develop a unified sensor that can seamlessly work across these two regions. In vacuum region, the sensor measures changes in resonance impedance caused by gas damping, allowing for precise readings down to 10^{-3} mbar. In positive pressure region, mechanical stress induced by external pressure causes a measurable shift in the Quartz Tuning Fork's resonance frequency, enabling pressure measurements up to 10 bar and even beyond. This wide range operation is achieved by careful design, sensor integration, and calibration to ensure seamless working of proposed sensor across vacuum and positive pressure regions. The sensor's performance is negatively impacted by the temperature and gas composition variations. However, these factors are mostly controllable. The sensor's ability to operate effectively in both low and high-pressure environments, combined with its compact design and low power consumption, makes it a promising tool for a wide range of industrial, scientific, and commercial applications.

Contents

List of Figures

List of Tables

Abbreviations

ADC	Analog to Digital Converter
CDG	Capacitance Diaphragm Gauge
EMI	Electromagnetic Interference
GF	Gauge Factor
I/VC	Current to Voltage Converter
I2C	Inter-Integrated Circuit Protocol
ISO	International Organization for Standardization
KB	Kilo Byte
MGQ	Microprocessor Grade Quartz
QTF	Quartz Tuning Fork
RAM	Random Access Memory
SRG	Spinning Rotor Gauge
UART	Universal Asynchronous Receiver/Transmitter

Symbols

g	Acceleration of gravity
ϵ	Strain of material
C	Capacitance
F	Force
k	Specific thermal conductivity of gas
T	Temperature
P	Pressure of gas
M	Molecular mass of gas
n	Number of moles of gas
ρ	Density of gas
η	Viscosity of gas
L	Mean free path of gas particles
R_0	Ideal gas constant
k	Boltzmann constant
f	Flow-regime dependent relation for change in impedance of QTF
V	Amplitude of voltage
η_0	Conversion efficiency of QTF from electrical energy to mechanical energy and vice
θ	Phase difference between current and voltage of QTF
V	Volume of gas
A_m	Mechanical amplitude of the oscillation of QTF
ω	Angular frequency of QTF
f_r	Resonance frequency of QTF
R	Radius of sphere, equal to thickness of QTF

l	Length of QTF prongs
w	Width of QTF prongs
t	Thickness of QTF prongs
Z_0	Intrinsic impedance of QTF at high vacuum
Z	Pressure-dependent impedance of QTF
C_1, C_2, C_3	Millikan's constants

Chapter 1

Introduction

In this chapter, an overall introduction of pressure & vacuum technology along with its applications and measurement techniques is presented.

1.1 Overview

Pressure measurement and control are the most used process variables in industrial and scientific applications. It plays a vital role in the successful and smooth operation of many systems, such as chemical industry, vacuum furnaces, coating systems, electron beam welding machines, pneumatic controls, environmental monitoring, medical devices, gas filling, etc. Atmospheric pressure ranges from 1013 mbar (or 760 mmHg), at sea level, to 310 mbar on Mount Everest (the highest point on Earth) [1]. The pressures below the prevailing atmospheric level are called negative pressures or vacuum, while the pressures above the prevailing atmospheric level are called positive pressures or simply pressure, illustrated in figure 1.1.

The word vacuum is derived from the Latin word 'Vacuus' which means empty [2]. A space utterly devoid of matter is called absolute vacuum, which does not exist in nature and cannot be fully achieved humanly. In modern usage, the word vacuum applies to any space which is at less than prevailing atmospheric pressure.

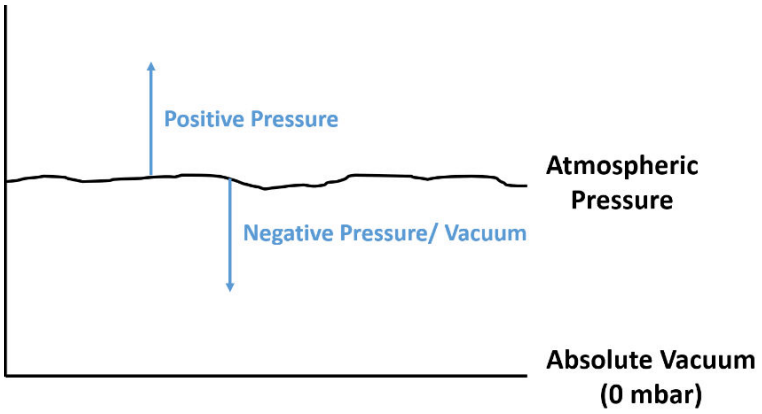

FIGURE 1.1: Illustration of Positive and Negative Pressures

At present, the total range of vacuum available for measurement extends from atmospheric pressure down to less than 10^{-12} mbar, that is, it extends over more than 15 orders of magnitude. International Standards Organization (ISO) has divided this entire vacuum range into vacuum regions [1], enlisted in table 1.1 below:

TABLE 1.1: Classification of Measurable Vacuum Region

Sr. No.	Vacuum Region	Range
1	Rough Vacuum	$1013 - 10^{0}$ mbar
2	Medium Vacuum	$10^{0} - 10^{-3}$ mbar
3	High Vacuum	$10^{-3} - 10^{-7}$ mbar
4	Ultrahigh Vacuum	$10^{-7} - 10^{-12}$ mbar
5	Extremely High Vacuum	$below 10^{-12}$ mbar

The term pressure, in industrial applications, usually denotes a positive pressure region i.e., above 760 mmHg or 1013 mbar. Unlike vacuum, pressure or positive pressure has no ultimate upper limit and is not divided into distinct ranges.

1.2 Vacuum Technology Evolution

Concept of pressure has existed since long, however Torricelli is credited with the conceptual understanding of the vacuum and the very first practical work in

vacuum technology with the invention of barometer, a device used for measuring air pressure, in 1643, shown in figure 1.2. Because we are living submerged in an ocean of air, the atmosphere is pressing down on us. Torricelli found that the pressure of atmosphere at sea level pressing down on a well of mercury would support a nearly 30-inch column of mercury in a tube upended in the reservoir of mercury. The mercury in the column would not flow down into the well because of the counterbalancing atmospheric pressure on the surface of mercury in the well [3].

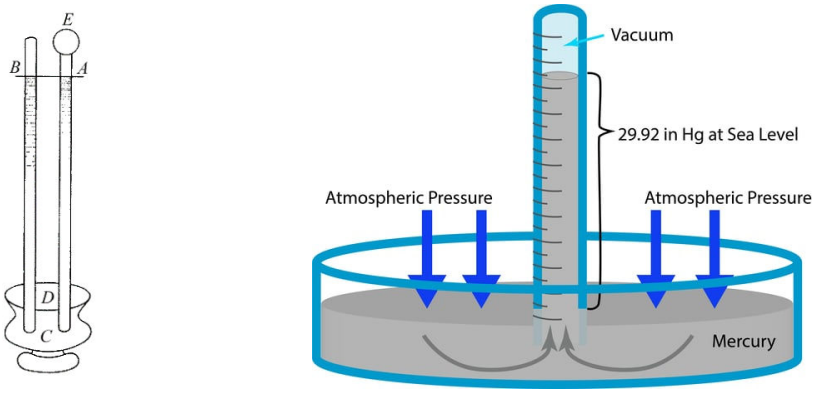

(a) Torricelli's barometer (b) A modern day mercury barometer

FIGURE 1.2: Typical Mercury Barometer

Pascal, in 1648, setup an experiment to measure the height of Torricelli column at different altitudes on a mountain and hence the atmospheric pressures at different altitudes. Followed by this discovery, Otto von Guericke invented piston vacuum pump in 1650s. Using his vacuum pumps, in 1654, Otto von Guericke succeeded in producing sufficient vacuum inside two sealed copper hemispheres to conduct a, now-classic, demonstration in which 16 horses were unable to pull apart the two halves of evacuated chamber until air was readmitted [4] as illustrated in figure 1.3. Interest in vacuum remained at low level for more than 200 years until McLeod's invention of the compression gauge in 1874 which further extended the measurement range to lower pressures range [5]. In 1905, Gaede designed a rotary vacuum pump sealed with mercury [6]. The thermal conductivity vacuum gauge, diffusion pump, ionization vacuum gauge and ion pump soon followed. They formed the basis of a technology that has made possible everything from light bulb to semiconductors, aerospace and efficient functioning of process industry.

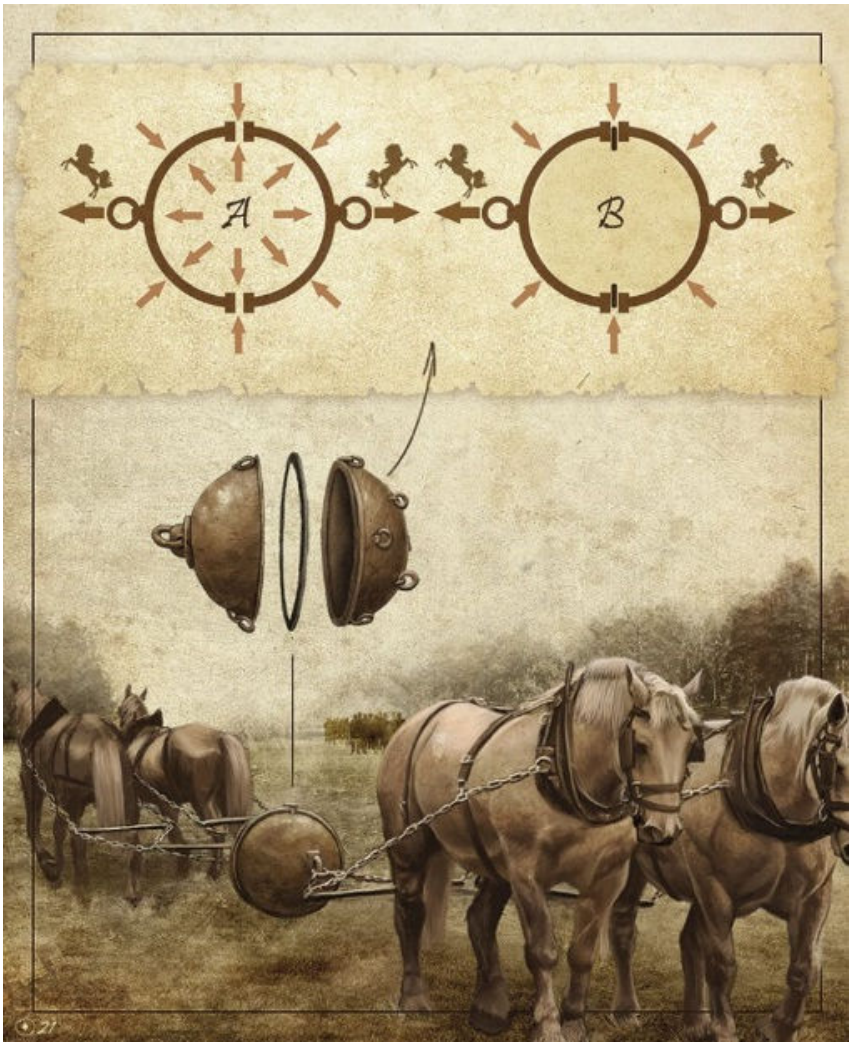

FIGURE 1.3: An Illustration of Otto von Guericke's Experiment [7]

1.3 Pressure Measurement

Accurate measurement of pressure is vital for maintaining optimal performance in processes that rely on controlled environments. Different applications require specific levels of pressure, and as such, a wide range of measurement techniques has been developed [8]. Numerous techniques have been developed for the measurement of pressure. Instruments used to measure positive pressures are called pressure gauges, vacuum gauges and compound gauges (measuring both positive pressures and negative pressures/ vacuum). For physical reasons, it is impossible to develop a single pressure sensor capable to perform quantitative measurements within the entire pressure range available (including positive pressures and vacuum). Therefore, a variety of different pressure, vacuum and compound gauges

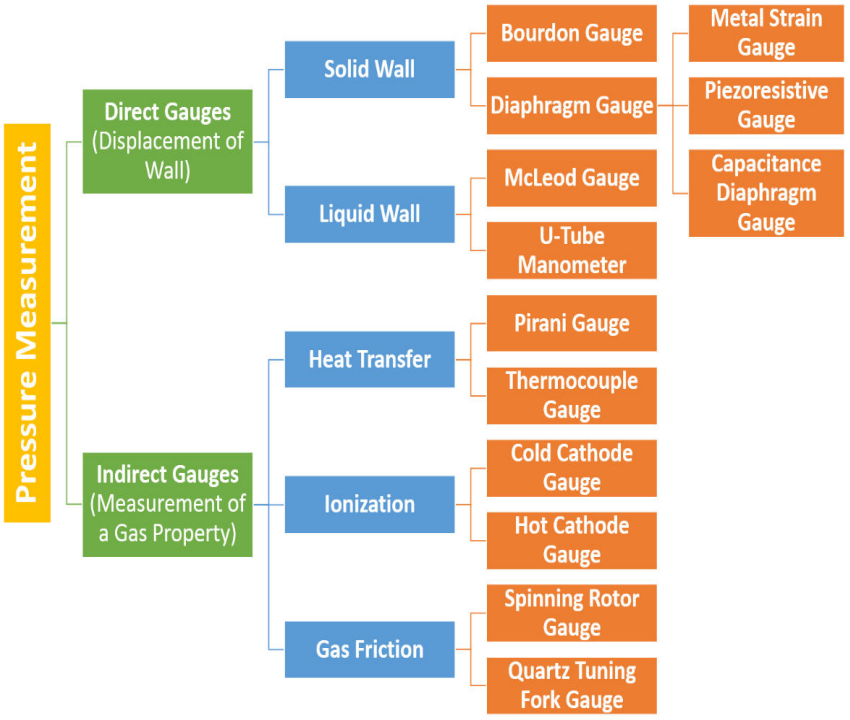

FIGURE 1.4: Classification of Pressure Measurement Techniques

are available, each with their own characteristic measurement range which commonly extends over several decades. Pressure gauges are generally classified into two broad categories: direct and indirect pressure measuring devices [9]. Further classification is shown in figure 1.4. In the case of direct (or absolute) pressure measurements, the readings obtained through the gauge are independent of the type of gas and depend solely on the pressure to be measured e.g. mechanical gauges where the pressure is determined directly by recording the force acting on the surface of a diaphragm. While in the case of indirect pressure measurements, the pressure is determined as a function of a pressure dependent property of the gas (thermal conductivity, ionization probability etc.). These properties do not exclusively depend on the pressure but also on the molar mass of the gasses. For this reason, the pressure reading obtained through gauges which rely on indirect pressure measurements, depends on the types of gas. These readings usually relate to air or nitrogen as the calibration gas. For the measurement of other gases, the corresponding correction factor must be applied. The selection of a particular measuring method depends on the required pressure range, sensitivity, and the environmental conditions in which the measurements are to be made.

1.3.1 Units of Pressure

SI unit of pressure is Pascal ($1Pa = 1Nm^{-2}$) however, some other units are used commonly in industrial and scientific applications like bar, mbar ($1/1000^{th}$ of the bar), psi, and Torr. The interconversion of these units is enlisted below in table 1.2.

TABLE 1.2: Interconversion of Some Common Units of Pressure

Unit	atm	Pa	mmHg	Torr	Bar	mbar	psi
atm	1	101325	760	760	1.013	1013	14.3
Pa	9.87 x 10^{-7}	1	7.5 x 10^{-3}	7.5 x 10^{-3}	1 x 10^{-5}	0.01	1.45x10^{-4}
mmHg	1.32 x 10^{-3}	133.322	1	1	1.33 x 10^{-3}	1.33	0.01934
Torr	1.32 x 10^{-3}	133.322	1	1	1.33 x 10^{-3}	1.33	0.01934
Bar	0.987	1 x 10^{5}	750.062	750.062	1	1000	14.504
mbar	9.87 x 10^{-4}	100	0.75	0.75	1 x 10^{-3}	1	0.014504
psi	0.068	6894.76	51.715	51.715	0.0689	68.95	1

1.4 Direct Measurement Gauges

Direct gauges measure pressure by sensing the force exerted by gas molecules directly on a sensing element. These gauges provide reliable and straightforward pressure measurements, particularly in low to medium vacuum ranges and moderately high pressures, and are often chosen for their simplicity and reliability. Unlike indirect gauges, which infer pressure from secondary effects (like thermal conductivity or ionization), direct gauges offer a more intuitive and often more accurate reading in certain applications.

1.4.1 Hydrostatic Gauges

Hydrostatic gauges are one of the oldest and most fundamental types of pressure measuring instruments. They work based on the principle of balancing the weight

of a liquid column against the pressure exerted by a gas. These gauges are well-known for their precision in low-pressure measurements but become impractical for higher pressures due to physical constraints, such as the need for tall liquid columns.

1.4.1.1 U-Tube Manometer

A U-tube manometer is a simple, yet highly accurate device for measuring low-pressure differentials. It consists of a U-shaped tube filled with a liquid, typically water, mercury, or oil, shown in figure 1.5. When pressure is applied to one side of the tube, the liquid levels in the arms change accordingly. The pressure difference is determined by measuring the height difference between the liquid levels in the two arms of the tube [10].

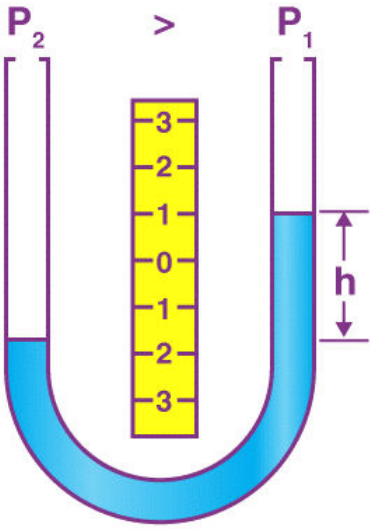

FIGURE 1.5: A Typical U-Tube Manometer

If P_1 is the known reference pressure and P_2 is the pressure/ vacuum to be measured, the relation for the pressure can be given as:

$$P_2 = \rho g h + P_1 \tag{1.1}$$

where ρ is the density of liquid used in manometer, g is the gravitational force and h is the the difference of liquid height in two arms of manometer.

The accuracy of the U-tube manometer makes it ideal for low-pressure environments where high precision is required. However, as the pressure increases, the height of the liquid column required to balance the pressure becomes impractically large. For instance, measuring a pressure of 10 bar using mercury would require a column nearly 7.5 meters high, limiting the use of U-tube manometers to lower pressure applications.

1.4.1.2 McLeod Vacuum Gauge

The McLeod gauge is a liquid column gauge that measures vacuum based on the compression of a known volume of gas i.e., it works on the principle of Boyle's gas law. It consists of a sealed glass tube filled with mercury, where the gas sample is compressed, and the resulting pressure is measured [11].

Working Principle

The working principle of gauge is shown in figure 1.6. The pressure to be measured (P_1) is applied to the top of the reference column of the McLeod Gauge. The mercury level in the gauge is elevated by operating the piston to fill the volume shown by the dark shade in figure 1.6. When this is the case (condition – 1), the gas applying pressure P_1 fills the bulb and the measuring capillary. The piston is operated further so that the mercury level in the gauge increases. When the mercury level reaches the cutoff point, a known volume of gas (V_1) is trapped in the bulb and measuring capillary tube. The piston continues to raise the mercury level so the trapped gas in the bulb and measuring capillary tube is compressed. This is done until the mercury level reaches the "Zero reference Point" marked on the reference capillary (condition – 2). In this condition, the volume and pressure of the gas trapped in measuring capillary tube become V_2 and P_2 respectively.

Let,

Volume of bulb from cutoff point to the start of the measuring capillary tube = V

Area of cross-section of the measuring capillary tube = a

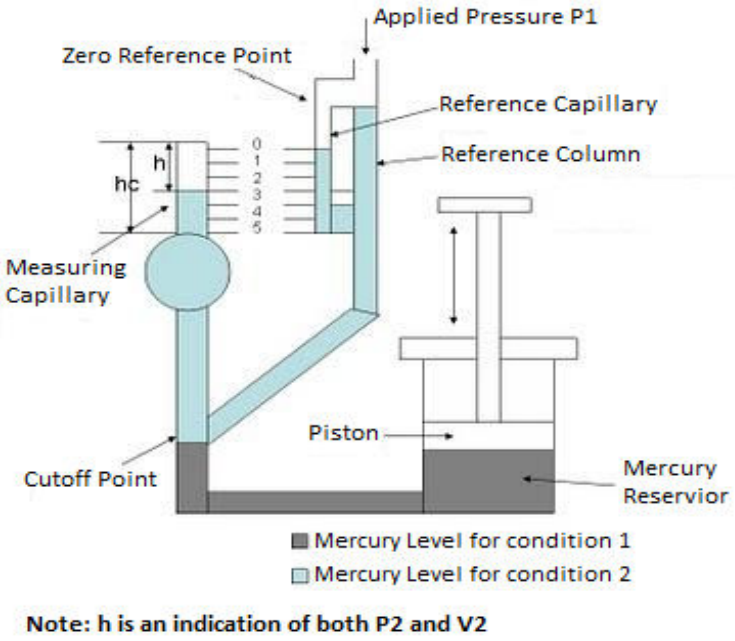

FIGURE 1.6: Working Principle of McLeod Vacuum Gauge

Height of measuring capillary tube = h_c

When the mercury has been forced upwards to reach the zero reference point in the reference capillary, the final volume of the gas = V_2 = ah

h = height of the compressed gas in the measuring capillary tube

P_1 = Applied pressure of the gas unknown.

P_2 = Pressure of gas at final condition, that is, after compression = P_1+h

Now as V_1, V_2 and P_2 are known, the applied pressure P_1 can be calculated using Boyle's Law:

$$P_1V_1 = P_2V_2 \tag{1.2}$$

$$P_1V_1 = (P_1 + h)ah \tag{1.3}$$

Rearranging,

$$P_1 = \frac{ah^2}{V_1 - ah} \tag{1.4}$$

Since ah is very small when compared to V_1, it can be neglected. Therefore:

$$P_1 = \frac{ah^2}{V_1} \tag{1.5}$$

The McLeod gauge is highly accurate for high-vacuum measurements, down to 10^{-6} mbar. However, its use is limited by the need for manual & discontinuous operation and the presence of mercury, a toxic liquid which poses health and environmental risks.

1.4.2 Mechanical Gauges

Mechanical gauges' operation is based on the mechanical deformation of elements like diaphragms or Bourdon-tube in response to pressure changes. As pressure changes, these elements physically move, and the displacement is displayed on a calibrated dial, providing a direct reading of the pressure level. Widely used for low to medium pressure range, mechanical gauges are valued for their simplicity, durability, and cost-effectiveness. They are common in industrial applications where high precision is not critical, but robustness and ease of use are essential. Despite these advantages, mechanical gauges are less suitable for high or ultra-high vacuum measurements due to their limited sensitivity and resolution at lower pressures.

1.4.2.1 Bourdon-Tube Gauge

The Bourdon gauge operates using a flattened tube known as a Bourdon tube which may be a helix, coil or C-shape. A typical C-Shape Bourdon-Tube gauge is shown in figure 1.7. When subjected to a pressure, the tube tends to straighten or regain its circular form in cross-section due to the difference in external and internal pressure across it. The amount of deformation of the tube is proportional to the differential pressure across the tube. This movement is transmitted to a pointer through a mechanical linkage. The pointer moves over a calibrated dial, providing a direct reading of the pressures [12, 13]. Bourdon gauges are rugged, easy to use and can withstand harsh environments, making them suitable for a wide range of industrial applications. Bourdon-Tube gauge is one of the most seen gauges in industry because of its lower cost, ruggedness and easy operation.

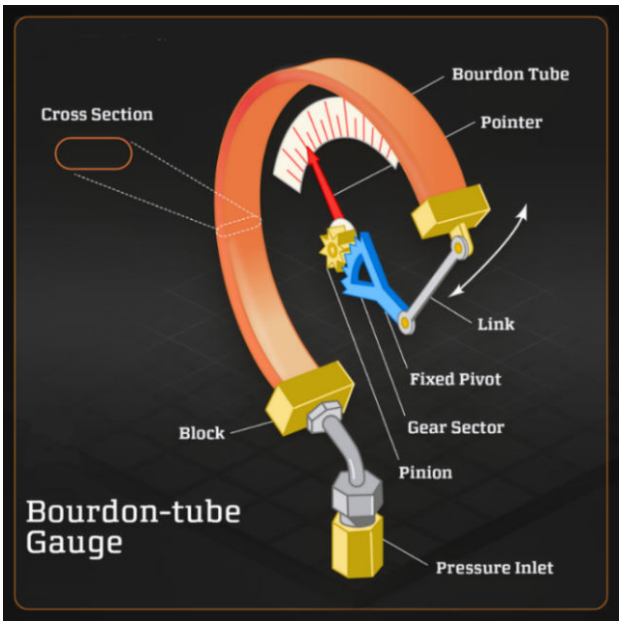

FIGURE 1.7: A Typical C-Shape Bourdon-Tube Gauge

1.4.2.2 Diaphragm Gauges

Diaphragm gauges measure pressure by detecting the deflection of a thin diaphragm under the influence of pressure [14]. If a differential pressure exists across the diaphragm, a net force F causes deflection in the diaphragm.

$$F = (P_1 - P_2)A \tag{1.6}$$

where, A is the area of the diaphragm and P1 & P2 are two pressures on either side of the diaphragm.

A. Metal Strain Gauge

Edward Simmons and Arthur Ruge invented the strain gauge in 1938 [15]. The device consists of a metallic path (usually copper-nickel or platinum-tungsten alloys) deposited on an insulating flexible substrate, shown in figure 1.8 below. The metallic foil shows a resistance change when the element is subjected to a force that causes it to distort. To measure pressure, strain gauge is attached to a diaphragm. A reference pressure/vacuum is created on one side of the diaphragm and is sealed, while the other side is exposed to pressure being measured. The diaphragm deforms under the influence of pressure difference across it, causing the

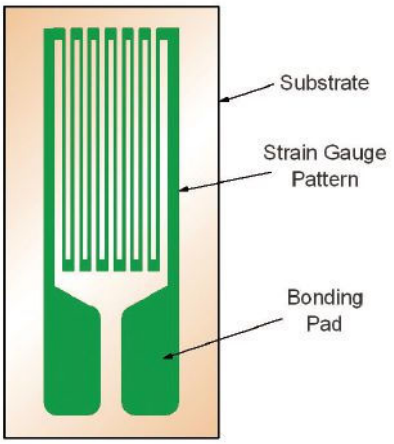

FIGURE 1.8: A Typical Strain Gauge - Consisting of a Metal Pattern on a Flexible Substrate

strain gauge to stretch or compress. This deformation changes the resistance of the strain gauge, which can be measured and correlated with the applied pressure using Wheatstone bridge or any other suitable method. The sensitivity of the strain gauge is called Gauge Factor (GF) and is calculated as:

$$GF = \frac{\Delta R/R_G}{\epsilon} \tag{1.7}$$

where, ΔR is the change in resistance due to strain, R_G is the resistance of the unstressed gauge and ϵ is the strain. Strain sensors are widely used due to their simplicity, robustness, and ability to measure a wide range of pressures. They offer good linearity and repeatability, making them suitable for many industrial applications. However, they can be sensitive to temperature changes, so temperature compensation is often required to maintain accuracy.

B. Piezoresistive Gauge

These sensors work on the same principle which strain gauges work on. However in place of strain element, a piezoresistive material (usually silicon) is integrated into a diaphragm whose electrical resistance changes in response to mechanical strain. Similar to metal strain gauges, a reference pressure is created on one side of the diaphragm and the other side is exposed to the pressure being measured. Under the influence of pressure diaphragm deforms, inducing strain in the piezoresistive

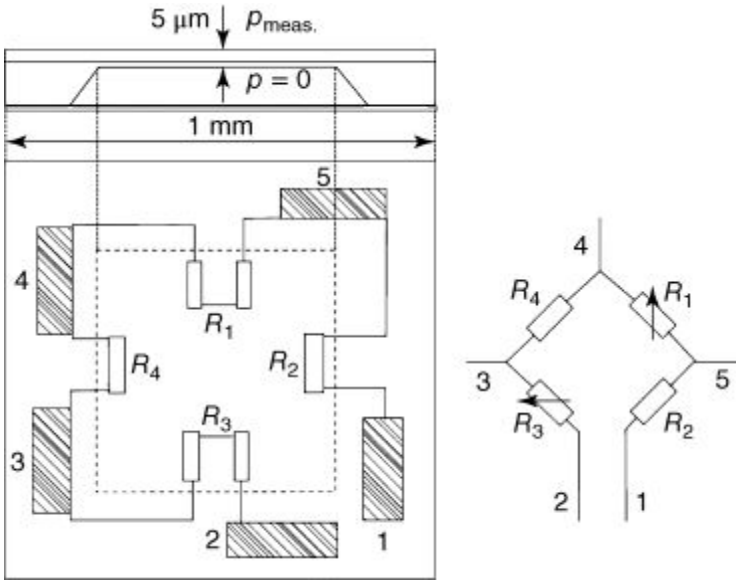

FIGURE 1.9: Typical Construction of a Piezoresistive Sensor

material and altering its resistance. This change in resistance is then measured using Wheatstone bridge and converted into, an electronically adjusted, pressure reading, as shown in figure 1.9. In metals, the change in resistance is determined by the geometrical change of the conductor i.e., cross section, length etc. Semiconductors, on the other hand, show a change in the resistivity of the material as well in addition to geometrical resistance changes, thus increasing the strain effect. Therefore, semiconductor materials are preferred for pressure measurements relying on this principle. One of the key advantages of piezoresistive sensors is their compatibility with microelectromechanical systems (MEMS) technology, enabling the production of miniaturized sensors with low power consumption. Depending on the gauge construction the pressure reading covers a wide range of 0.1 to 200 mbar or 1 to 2000 mbar [16] and up to 1000 bar on positive pressure side [17].

C. Capacitive Diaphragm Gauge

Capacitive diaphragm gauges (CDG) operate on the principle of capacitance change due to the deformation of a diaphragm under pressure. These sensors consist of a diaphragm located between two conductive plates, forming a capacitor. When pressure is applied, the diaphragm deforms, changing the distance between the plates, thus changing the capacitance. This change in capacitance is directly proportional to the applied pressure and can be measured and converted into an

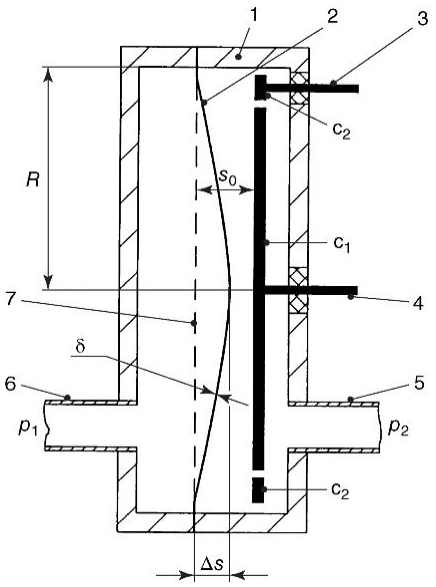

FIGURE 1.10: A Typical Construction of a Capacitance Diaphragm Gauge

electrical signal.

$$C = \frac{A\epsilon}{d} \tag{1.8}$$

where, C is capacitance of the sensor, A is the surface area of sensing diaphragm, d is the distance between the diaphragm and fixed electrode, and ϵ is permittivity of dielectric between electrodes. CDGs may have ports on both sides of the diaphragm so that the instrument can be used for differential pressure measurements, or one side may be evacuated to 10^{-7} mbar and sealed so that the gauge is for absolute pressure sensing. Getter material placed on the reference side to maintain long-term low pressure. The measuring range of the pressure sensor is varied by using diaphragms of different thickness, keeping the dimensions of the sensor constant. Hasse [18] was the first one to describe a functional single-sided CDG in 1936 followed by Lilly, Legallais, and Cherry [19], Alpert, Matland, and McCoubrey [20], Drawin [21], Hecht [22], and Macdonald & King [23] before availability of commercial instruments.

Figure 1.10 shows the construction of a typical CDG with (1) Housing, (2) diaphragm, (3) feed-through to capacitor ring c_2, (4) feed-through to capacitor ring c_1, (5) gas inlet (reference pressure p_2), (6) connecting port to vessel with measured pressure p_1, and (7) diaphragm in zero position ($p_1 = p_2$), δ: diaphragm thickness; Δs: deflection of diaphragm; s_0: distance between diaphragm and

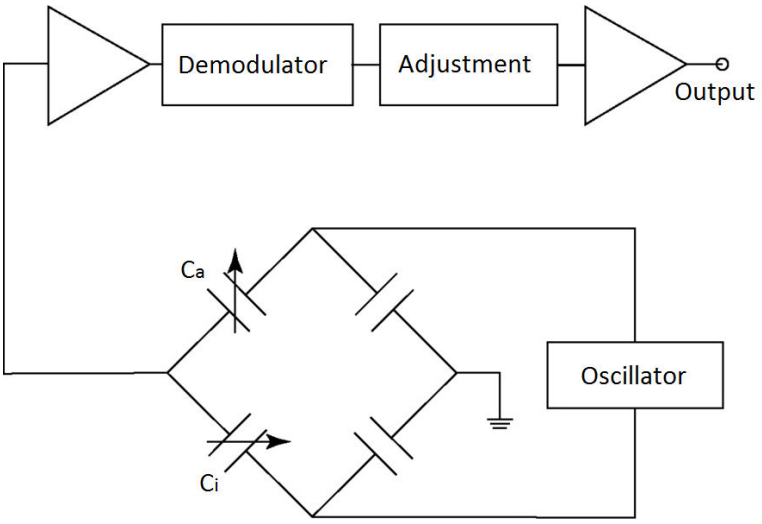

FIGURE 1.11: Wheatstone Bridge based Capacitance Measurement Circuit

capacitor plate c_1. The diaphragm, exposed to the pressure, to be measured, is usually a round disk made of low thermal-expansion coefficient material, e.g., ceramic. Thickness of diaphragm is determined by the desired ultimate pressure level to be measured and can be as low as 25μm [24]. For improved zero-point stability, the membrane forms two capacitors with the circular electrode c_1 and the annular electrode c_2. The difference in capacitance of the two capacitors gives measure of pressure. Figure 1.11 shows capacitance measurement setup. Both capacitors (c_1 and c_2) are part of a Wheatstone bridge consisting of four capacitors. The oscillator sends a high-frequency signal (commonly 10 to 100 kHz) to the pressure sensor. The bridge changes the amplitude and phase of the oscillator signal with the pressure. For negative pressures ($p_2 > p_1$ in Figure 1.10), the phase position is shifted by 180° compared with positive pressure ($p_2 < p_1$). Demodulation of the signal produces a DC voltage signal, which is linearized and amplified.

Alternatively, a capacitance to digital converter can be used to measure the pressure dependent capacitance (Figure 1.12). A square wave voltage excitation source, of amplitude V, is connected to the sensing capacitance C_x which injects a charge Q according to $\mathrm{Q} = C_x\mathrm{V}$. This charge is fed into the integrator which tries to offset the introduced charge. The comparator compares at high frequency if the output of integrator is higher or lower than ground potential and sends a binary signal that is filtered for noise. The filtered output is used for measurement of unknown

capacitance and hence pressure.

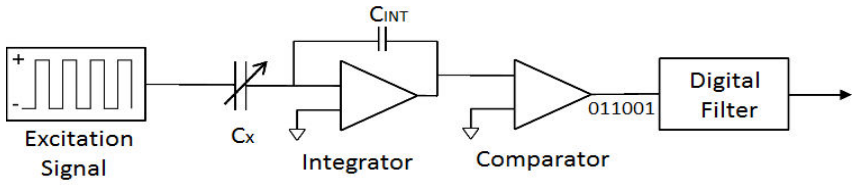

FIGURE 1.12: Capacitance to Digital Converter Circuit

Capacitive pressure sensors are known for their high sensitivity, accuracy, and linearity. They have a claimed accuracy ± 0.5% of reading. These uncertainties are due to causes like non-linearity and hysteresis [25]. A dynamic range of four orders of magnitude can be obtained using a single gauge head with an overall range up to as low as 10^{-5} mbar from atmospheric pressure [26]. If the applied pressure exceeds the gauge measuring pressure (by 20% approx.), the deflectable diaphragm touches the opposite end and in this manner prevents damage to the diaphragm. However, such an overload may invalidate the calibration of gauge.

1.5 Indirect Vacuum Gauges

Indirect vacuum gauges measure pressure by observing the physical properties of a gas, such as thermal conductivity or ionization potential, which vary with pressure. These gauges are typically used for measuring medium to high vacuum levels.

1.5.1 Thermal-Conductivity Gauges

Thermal conductivity of a gas refers to its ability to transfer (conduct) heat from a hotter body to a colder body.

$$Q_{heat-conduction} = kA\frac{(T_1 - T_2)}{d} \tag{1.9}$$

where, $Q_{heat_conduction}$ is the quantity of heat transferred, k is specific thermal conductivity of gas, A is surface area of hot object, T_1 is temperature of hotter object

and T_2 is the temperature of cooler object. Gauges working on this principle, measure vacuum by detecting changes in the thermal conductivity of a gas, which decreases as the pressure drops.

1.5.1.1 Pirani Vacuum Gauge

Marcello S. Pirani, in 1906, studied the pressure dependent thermal conductivity of gasses and invented a wide range vacuum gauge using this principle which was later named after him, "Pirani vacuum gauge" [27]. The Pirani gauge consists of a heated filament (approx. 100° C) enclosed in a metal tube, exposed to vacuum being measured. When gas molecules collide with the filament, they transport heat away from the hot wire. The heat loss from filament is a function of gas pressure. As the pressure decreases, the thermal conductivity of the gas surrounding the filament decreases i.e., heat loss from filament decreases. The Pirani sensor filament is typically a thin wire (<25 μm) made of a metal having high temperature coefficient of resistance, like Nickel, Tungsten, Platinum etc., to ensures a high pressure sensitivity. Pirani gauges are widely used for measuring vacuum ranges from 1000 mbar to as low as 10^{-4} mbar with an accuracy of 20-10%. Marcello S. Pirani described three modes of operation for Pirani sensor in his publication:

1. Constant Voltage mode
2. Constant Current mode
3. Constant Temperature (Resistance) mode

The hot filament is part of a Wheatstone bridge which may operate in a self-balancing condition, supplying variable energy to keep the filament at constant temperature. The energy supplied to keep the temperature or resistance of filament is constant is a measure of vacuum. Alternatively, it may operate in imbalance mode where the energy supplied to filament is constant (constant voltage or current) and Wheatstone bridge measures out-of-balance resistance of the filament as a measure of vacuum.

A. Constant Voltage mode Operation:

In this mode, a constant voltage is applied to the bridge. As the pressure changes, the filament temperature, and thus its resistance, changes due to change in thermal conductivity of gas. Wheatstone bridge measures the change in resistance of filament and the signal conditioning circuitry relates the output to vacuum level, as illustrated in figure 1.13 below.

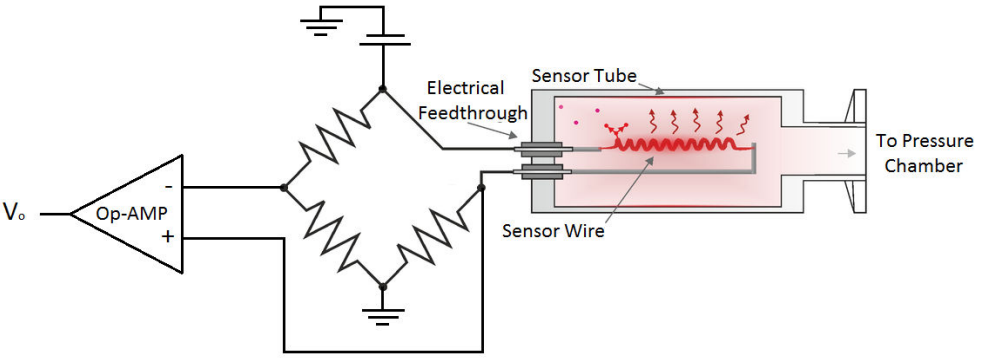

FIGURE 1.13: Constant-Voltage Operation of Pirani Gauge

B. Constant Current mode Operation:

In this mode, a constant current is supplied to the bridge. As the pressure changes, the filament temperature, and thus its resistance, changes due to change in thermal conductivity of gas. Wheatstone bridge measures the change in resistance of filament and the signal conditioning circuitry relates the output to vacuum level, as illustrated in figure 1.14 below.

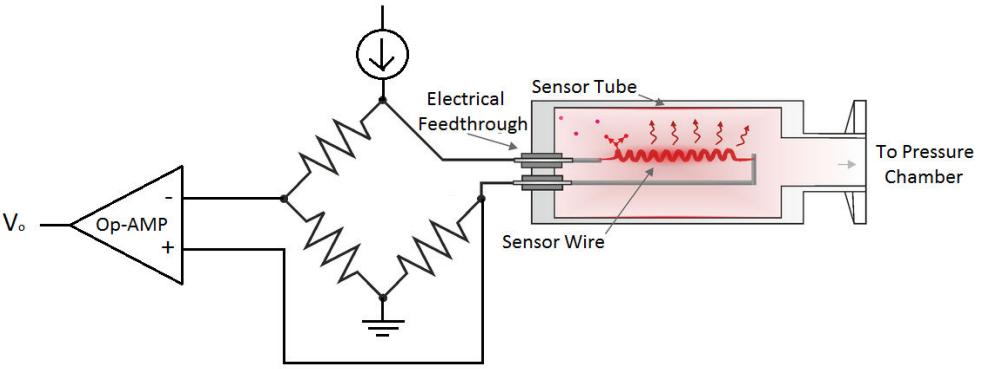

FIGURE 1.14: Constant-Current Operation of Pirani Gauge

C. Constant Temperature (Resistance) mode Operation:

In this mode, Wheatstone bridge is used in feedback loop of an op-amp. As soon as pressure changes, the filament resistance changes and the bridge goes out of balance. The op-amp changes its output level accordingly to bring the bridge into balance again. In doing so, it supplies the enough energy to filament to maintain it at a constant temperature and keep the bridge at balanced condition. The signal conditioning circuitry relates the energy supplied to filament with vacuum level, as illustrated in figure 1.15 below.

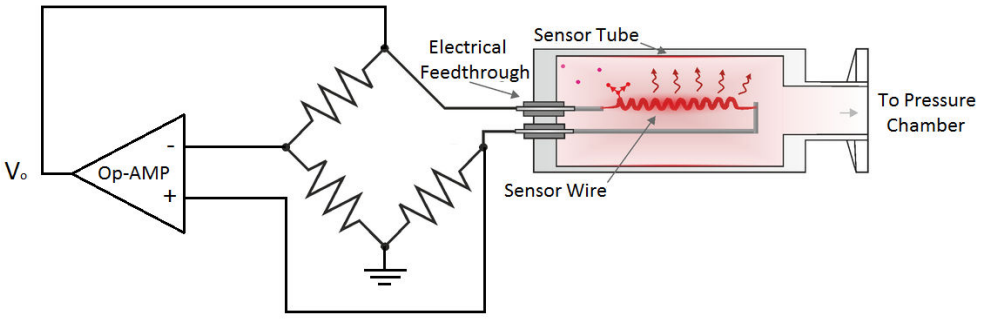

FIGURE 1.15: Constant-Temperature Operation of Pirani Gauge

1.5.1.2 MEMS Pirani Sensor:

In modern Pirani gauges, filament wire has been replaced with a MEMS type sensor as shown in figure 1.16. This has several advantages over conventional Pirani gauges (filament type) like smaller size, wider measurement range, low power consumption and higher resistance to mechanical shocks which may damage the filament.

1.5.1.3 Thermocouple Vacuum Gauge

Thermocouple gauge has similar construction to Pirani gauge with the exception that filament temperature is directly monitored using a thermocouple attached to

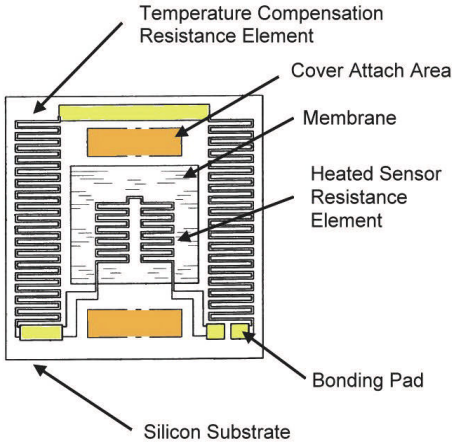

FIGURE 1.16: MEMS Pirani Gauge [28]

the heated filament. The output of thermocouple, usually in millivolts, is used as a function of vacuum, as demonstrated in figure 1.17 below.

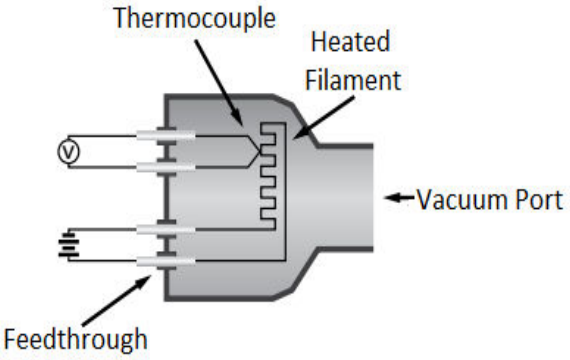

FIGURE 1.17: A Typical Thermocouple Vacuum Gauge

Thermocouple has a measuring range approximately 10^{-3} to 1000 mbar, a decade lower than Pirani gauge with an accuracy similar to Pirani gauge. It has almost same advantages and disadvantages as the Pirani gauge.

1.5.1.4 Thermistor Vacuum Gauge

Thermistor gauge has similar construction and working principle as the Pirani gauge with the difference that metal filament is replaced with a semiconductor-oxide thermistor like TaN. Thermistor type gauge has similar accuracy and measuring range as a thermocouple gauge, however it is more rugged and used in harsh environments.

1.5.2 Ionization Gauges

When the pressure drops into high vacuum region, all the previously discussed pressure measuring techniques fail to detect change in pressure any further and the only reliable pressure measuring technique in this region is through gas ionization. Ionization gauges measure vacuum by ionizing gas molecules and then quantifying the ions current as a measure of gas pressure. These gauges are extremely sensitive and are used to measure high to ultra-high vacuum levels.

1.5.2.1 Hot Cathode Vacuum Gauges

During early 20th century, vacuum tube based electronic devices were common before the invention of semiconductor based electronics. One of such devices was a triode vacuum tube, equivalent to modern day silicone transistor. Using the structure similar to triode vacuum tube, in 1921, Saul Duschman and G.C. Found invented the very first hot-cathode ionization gauge. As shown in Figure 1.18, the gauge consists of three electrodes: a hot filament (cathode), a grid screen and an ion collector. This whole assembly is enclosed in a glass tube which has a port for attachment to vacuum chamber. The filament when heated, throws electrons into the space around it, a process called thermionic emission. The temperature of the filament is regulated by monitoring the emission current I_e, of electrons emitted from the filament, at the grid electrode. The grid is held at a positive potential (180 V in the figure 1.18) than that of the filament to accelerate the electrons towards it. However, since the grid highly perforated, most of the electrons pass through the holes and continue radially outward. Upon reaching the ion collector, electrons encounter a reverse electric force because the ion collector is at a negative potential w.r.t the grid (actually ground). After taking about five trips back and forth through the grid openings, emitted electron is crashed into a grid wire and becomes part of the emission current. But during its journey, the accelerated electron may bombards a gas molecule that comes across its path and might remove one (or more) of the molecule's electrons, rendering it as a positively charged ion. If this incident happens outside the grid, the positively charged ion

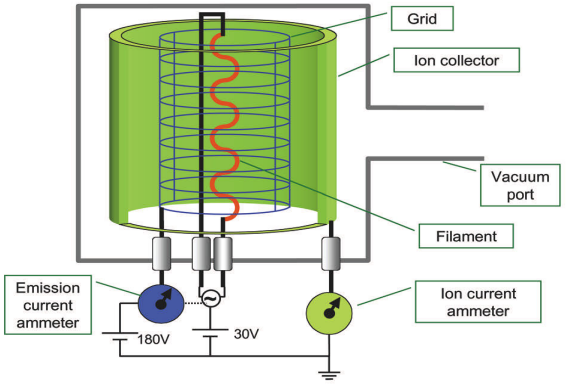

FIGURE 1.18: Construction of Triode Type Hot-Cathode Gauge

will be attracted to the ion collector and becomes a part of the collector current I_c. Higher the pressure, higher the number of molecules present in the vicinity of gauge and greater the chances of molecules being ionized by accelerated electrons i.e., higher ion current and vice versa. So the ion collector current is proportional to the pressure.

But this type of gauge cannot measure beyond $10-7$ mbar. Initially the reason for this barrier was unknown however in 1947, Nottingham identified the source of the problem [29]. When an electron, emitted from the filament, crashes into grid it sometimes causes the release of an X-ray, which then strikes the ion collector and may knocks an electron from the ion collector (photo-emission). The problem with all this is that the ion collector ammeter does not differentiate between the pressure-related ions current and X-ray generated current. This effect was later termed as "X-ray limit". Once the X-ray limit was understood a solution was proposed in the name of Bayard-Alpert gauge as shown in figure 1.19. In 1950, Bayard and Alpert from the Westinghouse research lab suggested a new design to dramatically reduce the X-ray limit and extend the gauge's measurement down to 10^{-10} mbar [30]. The ion collector was converted into a thin wire to reduce its area and therefore its chance of being struck by X-rays. The ion collector was moved inside at the gauge axis and the filament was moved to outside the grid cylinder. This new design by Bayard-Alpert significantly reduced the X-ray effect making the gauge capable of measuring further lower pressures, however the vacuum measuring principle of gauge remained unaltered.

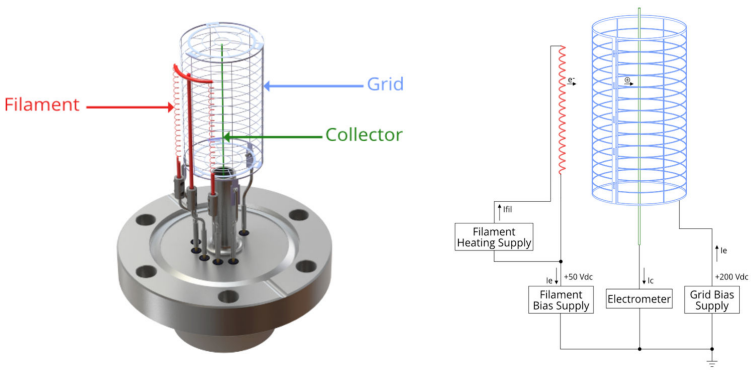

(a) Typical Bayard-Alpert gauge (b) Illustration of the gauge

FIGURE 1.19: Construction of a Bayard-Alpert Type Hot-Cathode Gauge

1.5.2.2 Cold Cathode Vacuum Gauges

Penning [31] is considered the inventor of cold cathode type ionization gauge. Penning gauge ignite a gas discharge between a cathode and anode pair using a high DC voltage of 3 kV. A magnetic field, perpendicular to the electrical field, is used which forces the emitted electrons onto spiral paths and thus considerably increase their path length before being absorbed by the anode. These electrons, on their way, further ionize the gas molecules and thus increase the ion current. The resulting ions are collected on cathode, and the current generated is proportional to the vacuum level. The ion current I through collector at a pressure level of P are related as:

$$P = I^m \tag{1.10}$$

where, m is dependent on gauge design and is usually in the range 1 – 1.4. The original Penning type cold cathode had a lower limit of 10^{-7} mbar because only few molecules are available for ionization and therefore gas discharge distinguishes at lower pressures. Peter Hobson and Paul Redhead in 1958, overcame this limit with the introduction of the inverted magnetron gauge [32]. The gauge consists of a central anode, a cylindrical cathode (serving as an ion collector) and a magnetic field perpendicular to electric field as shown in figure 1.20. Today most of the commercial cold cathode gauges are inverted magnetron type because of their superior performance.

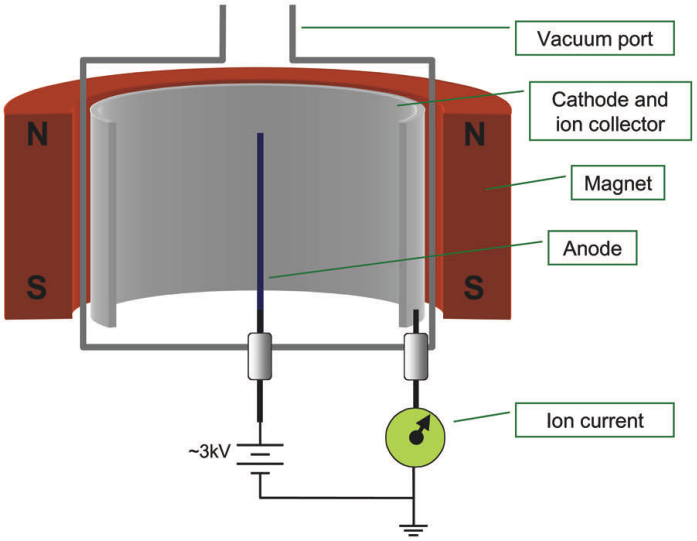

FIGURE 1.20: A Typical Cold-Cathode Vacuum Gauge

Cold cathode gauges are robust and can measure very low pressures, down to about 10^{-9} mbar from 10^{-2} mbar, but they require a strong electromagnetic field for operation. The most obvious advantage of a cold cathode gauge is the absence of filament making it more rugged and harsh-environment friendly. However, high voltage and strong magnetic field might be a concern for some applications.

1.5.3 Friction/ Viscosity Gauges

Friction gauges measure vacuum by detecting changes in movement due to frictional forces of gas that vary with pressure. The idea of measuring pressure by means of molecular drag on moving objects dates back to 1865, introduced by Meyer [33] and Maxwell [34]. These gauges are used for special applications where ionization gauges are not suitable e.g. cryogenics etc.

1.5.3.1 Spinning Rotor Vacuum Gauge (SRG)

In 1962, Beams and coworkers suggested that gas friction could be measured by observing the deceleration of a magnetically suspended spinning ball [35]. Fremerey and his colleagues used this concept to develop a vacuum gauge at Jülich,

Germany [36] named spinning rotor gauge.

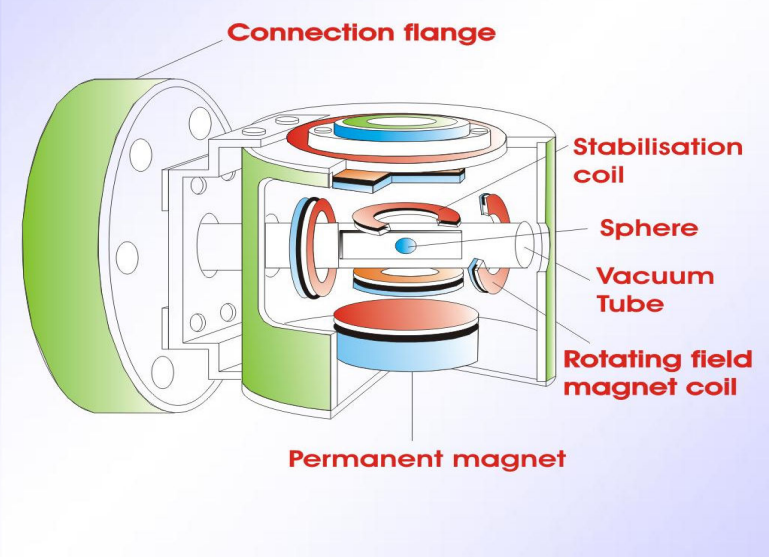

FIGURE 1.21: Illustration of a Spinning Rotor Gauge

A diagram of spinning rotor gauge is shown in figure 1.21. A steel ball is enclosed in a vacuum tube. The stabilization coils around the steel ball levitate it magnetically. Rotating field magnet coils, connected to an AC source, generate a rotating magnetic field causing the ball to spin about its axis. When the ball achieves its rated rotational speed (400 Hz), the AC source is cut-off causing the ball to decelerate at a rate depending on the amount of gas present around it. The magnetized steel ball induces voltage in pick-up coils present around it. The output of these coils is used to calculate the deceleration rate which is then used to estimate the pressure level around the ball, shown in figure 1.22.

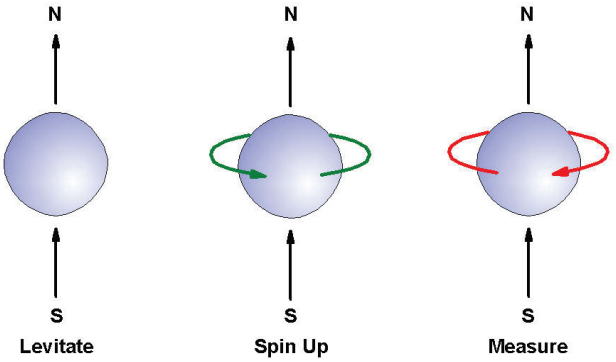

FIGURE 1.22: Operation Principle of the Spinning Rotor Gauge

Spinning rotor gauges are highly sensitive and accurate, capable of measuring pressures in the range 1 mbar to as low as 10^{-7} mbar. Because of high accuracy and reproducibility, these gauges are often used as secondary standards in calibration laboratories. However, just like most of the indirect gauges, SRG is also gas dependent and hence a gas-dependent factor is incorporated into the gauge's reading if the gas being measured is other than test gas in order to take accurate measurements from the gauge.

1.5.3.2 Quartz Tuning Fork Gauge

Tuning fork shaped quartz oscillators, shown in figure 1.23, are commonly used as frequency references in modern watches and microcontrollers because of their high stability, environmental resistance and a very high quality factor of the order of 10^5. Mass-produced, these devices are very inexpensive and ubiquitous. In 1984, Kokubun et al. [37] found that electrical impedance of quartz tuning fork crystals vary with frictional force of gas and thus can be used as a vacuum measuring instrument. The gauge had a measurement range of 10^{-2} mbar to atmospheric pressure i.e. 1000 mbar. Later, the team from Seiko Instruments further investigated the device as a potential vacuum sensor and had been the main theme of their research, towards the end of 20^{th} century. This gauge is particular interest of this research and would be discussed in detail in the proceeding chapters.

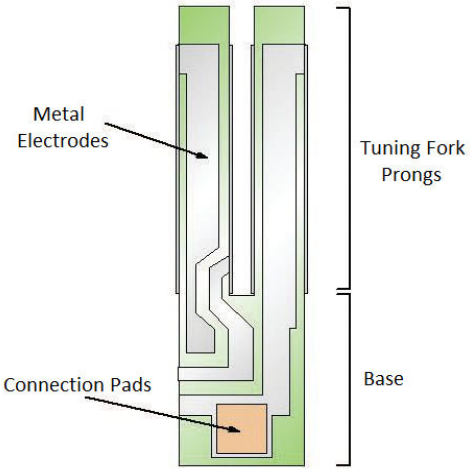

FIGURE 1.23: A Sketch of Quartz Tuning Fork crystal[38]

1.6 Potential Compound Sensing Technologies

As discussed in above section Bourdon gauge, capacitance diaphragm gauge, piezoresistive gauge and quartz tuning fork sensor are the only technologies capable of pressure measurement in both vacuum and positive pressure regions. Among them Bourdon gauge is a mechanical type gauge with analog output which is not suitable for modern world applications. The rest of the sensors are discussed in detail in chapter 5 where possibilities and limitations of each sensor is discussed.

1.7 Thesis Motivation

Pressure measurement is one of the basic requirement of most industries and scientific laboratories. Traditional pressure gauges, which include mechanical (such as Bourdon gauges and diaphragm gauges) and electronic types (for example piezoelectric and capacitive sensors) have been widely used for decades. While these technologies have served well for many years, there is growing need for more precise, miniature, durable and reliable pressure measurement solutions. Quartz tuning forks have emerged as a promising technology for enhancing the performance of pressure measurement approaches. Unlike conventional pressure sensors, quartz tuning fork sensors offer enhanced performance characteristics such as higher accuracy, greater durability and broader operational ranges.

The use of quartz tuning fork in pressure measurement is motivated by their inherent benefits, including:

1. **Compound sensing capability:**

   Most of the existing gauges are either pressure gauges (capable of measuring positive pressures only) or vacuum gauges (capable of measuring negative pressures only). Quartz tuning fork sensors on the other hand, can measure both positive and negative pressures accurately. This unique feature of quartz tuning fork make it ideal for development of a compound pressure gauge.

2. **Miniaturization:**

   Quartz tuning fork sensors are extremely small in size, these sensors are therefore well-suited for MEMS technology (the sensor used for this research is enclosed in a chamber of dia. 2mm and length 6mm).

3. **Wide availability:**

   Unlike other pressure or vacuum sensors, which are custom-made and usually are expensive, quartz tuning fork sensors are commonly available in the market at much lower costs.

4. **High accuracy:**

   Quartz tuning fork sensors offer exceptional sensitivity to pressure changes, allowing extremely accurate measurements.

1.8 Thesis Objectives

The primary aim of this research is to develop a compound pressure gauge that utilizes quartz tuning fork crystal as a versatile sensor. The research seeks to achieve following objectives:

1. **Design and Development of a Compound Gauge:**

   To design a compound pressure gauge that integrates a single quartz tuning fork sensor in a manner that enhances the measurement range, accuracy and reliability. The design focuses on optimizing the configuration and integration of quartz tuning fork in such a way that enables both vacuum and positive pressure measurement with a single sensor and circuitry.

2. **Broad Pressure Range Measurement:**

   To develop a gauge capable of measuring a wide range of pressures ranging from high vacuum to positive pressure region. This would be the first gauge of this kind having such an extensive measuring range and specialize in both vacuum and positive pressure region.

1.9 Thesis Organization

The rest of the thesis is organized as follows:

- **Chapter 2: Literature Review and Problem Formulation**

  This chapter provides a comprehensive review of existing technologies and research related to pressure measurement and quartz tuning fork sensors. It also highlights the advancements in the field and identify gaps that this research aims to address.

- **Chapter 3: Design and Methodology**

  Detailed description of the design, development and testing procedures for the quartz tuning fork based compound pressure gauge is provided in this chapter. This chapter outlines the experimental setup, calibration processes and data acquisition methods used in the study.

- **Chapter 4: Results and Discussion**

  This chapter presents and analyze the experimental results including performance metrics such as accuracy, sensitivity and stability in the context of research's objectives. Comparisons with conventional pressure gauges will be made to highlight the advantages of new technology.

- **Chapter 5: Alternatives Considered**

  This chapter deliberates the alternative technologies which could be potentially used in compound pressure sensing and discuss their limitations and pros & cons as compared to the quartz tuning fork based compound pressure gauge.

- **Chapter 6: Conclusion and Future Work**

  The final chapter summarizes the key findings of the research, address any limitations encountered and provide recommendations for future work and potential applications of the quartz tuning fork based compound pressure gauge.

1.10 Summary

This introduction has outlined the background and motivation for developing a quartz tuning fork based compound pressure gauge, set forth the research objectives and discussed possible applications of developed gauge. The following chapters delve into the literature review, methodologies and results of the research, culminating in comprehensive evaluation of the developed compound pressure gauge. By addressing the limitation of current pressure measurement technologies and leveraging the unique properties of quartz tuning fork sensor, this research aims to make a meaningful contribution to the field of pressure instrumentation and sensor technology.

Chapter 2

Literature Review and Problem Formulation

This chapter offers a comprehensive overview of friction type pressure sensors. It further explores the fundamentals of quartz tuning fork oscillator and offers a comprehensive literature review of previous research on their application as a pressure and vacuum sensor. A detailed examination identify the gaps that this research aims to address.

2.1 Literature Survey

Our literature review consists of a fourfold analysis. First, we examine friction-based gauges. Next, we explore the previous work on pressure and gas sensing applications of quartz tuning fork.

2.1.1 Friction Gauges

It is a well-known concept that fluids (liquids and gasses) resist the motion of objects through them. This resisting-force is called viscosity or friction of the fluid. For gasses, this resisting force is dependent on the number of particles

around the object in motion. By ideal gas law, pressure is also proportional to the number of gas particles present in a space:

$$P = nkT \tag{2.1}$$

By this theory, we can establish a relation between viscosity and the pressure of a gas.

In 1875, Kundt and Warburg [39] studied the frictional effects of gasses on moving objects at low pressures and Maxwell [40] discussed these effects in relation to kinetic theory of gasses in his paper, published in 1879. Sutherland [41] used these studies to suggest the very first gauge based on the principles of viscosity and later Hogg [42] further investigated Sutherland's instrument and suggested some improvements. The device consisted of a thin disk which is set into oscillations using an external magnet and the time required for oscillation amplitude to decrease to half its initial value is a measure of vacuum. This gauge had a measurement range of 10^{-4} mbar to 10^{-1} mbar. Langmuir [43] is credited for the development of very first practical viscosity vacuum gauge based on a quartz fiber, suspended in the gas. The fiber was manually actuated and the damping rate of oscillation amplitude was an indication of pressure. However, he provided no theoretical analysis or calibration of his instrument. Later on, F. Haber and F. Kirschbaum [44] developed the earliest theoretical concept of a quartz fiber gauge based on Langmuir's work and developed their own quartz fiber gauge. The gauge had a measuring range of 10^{-5} mbar to 10^{-1} mbar. E. B. King [45] also developed a similar quartz fiber based gauge with measurement range extended down to 2 x 10^{-6} mbar. In 1913, Langmuir [46] suggested the first continuous measuring friction gauge which was later built by S. Dushmann in 1975 [47]. The gauge consisted of a disk which rotates at high frequency by means of a motor. The motor's rotor was inside the bulb while stator was located outside. This rotating disk exerts a tangential force on a second disk through momentum transfer of gas molecules and deflection angle of second gauge provides information about pressure inside the bulb. This gauge had a measurement range of 10^{-6} mbar to 10^{+1} mbar. J. A.

Roberts [48] developed a commercial vacuum gauge by replacing rotating disks in Dushman's gauge with two coaxially aligned cylinders with a measurement range of 10^{-3} mbar to 20 mbar. W. Becker [49] developed the first friction type gauge with an electrical output in 1961. Becker's gauge consisted of a metal ribbon mounted between two pole pieces of magnets. The current through the ribbon to keep its oscillation amplitude constant was a measure of pressure. The gauge had a measurement range of 10^{-4} mbar to 1000 mbar.

However in all the above discussed instruments, sensor element was usually suspended in gas by physically attaching its one end to a support resulting in the suspension friction being too high. It was only after 1937, when magnetic suspension allowed frictionless mounting [50], the effect of gas friction was positively exploited for pressure measurements. Beams [35, 51] was the first to develop gas friction type pressure measuring devices using magnetic suspension however, his instruments were hard to operate. Later, Fremerey [52–55] developed a better vacuum gauge, the spinning rotor gauge (discussed in detail in section 1.5.3.1), based on magnetic suspension and gas friction.

2.1.2 Quartz Tuning Fork as Vacuum Sensor

In 1959, Pacey [56] reported the very first vacuum gauge based on a quartz crystal oscillator. The sensor he used was a 200 KHz, DT-cut quartz crystal driven by a triode-based circuit. The gauge could measure vacuum in the range of 10^{-1} to 10^{+3} mbar. About 25 years later, quartz based friction gauge was revived by the vacuum group of Electrotechnical Laboratory Japan and Seiko Instruments and has been subject of number their papers published during the latter part of 20^{th} century. Hirata et al. [57] in 1983, measured the resonance impedance of tuning fork-shaped quartz crystal, oscillating in bending mode vibration, as a function of gas pressure from 10^{-2} mbar to ambient atmospheric pressures. The experimental results showed that the resonance impedance increases monotonically from lower to higher pressures, and the variation in impedance is similar to the calibration curves of other friction vacuum gauges available at the time thus concluding that the

quartz tuning fork crystal has potential application as a small and low-cost pressure sensor. In 1984, Kokubun et al. [37] theocratically analyzed pressure dependence of electrical impedance of quartz tuning fork crystal. Kokubun developed a simple mathematical model for pressure-dependent resonance impedance of quartz tuning fork based on string-of-bead model.

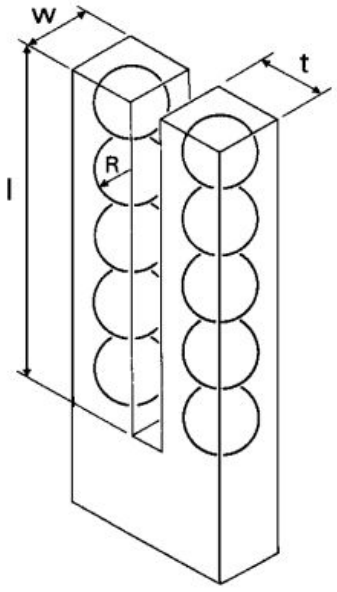

FIGURE 2.1: String-of-Bead Model of Quartz Tuning Fork [58]

According to string-of-bead model, quartz tuning fork crystal is thought to be made up of two bars and each bar is further made up of a string of beads (spheres) as shown in figure 2.1, and each sphere is in same vibration mode as the whole quartz tuning fork crystal. According to this model, resonance impedance of quartz tuning fork caused by gas friction can be calculated as:

$$Z = C_Q.f \tag{2.2}$$

where, C_Q is gas and QTF dependent constant and f is flow-regime dependent relation for change in impedance of quartz tuning fork with pressure.

For molecular flow region (P $\geq$ 6 x 10^{-1} mbar):

$$f = R^2\sqrt{\frac{8\pi M}{R_0 T}}.P \tag{2.3}$$

For viscous flow region (P $\leq$ 1.3 x 10^{-2} mbar):

$$f = 6\pi\eta R + 3\pi R^2\sqrt{2\eta\rho\omega} \tag{2.4}$$

The results calculated using this model demonstrated good agreement with the experimental values.

Ono et al. [59] built and tested the first model of QTF-based friction vacuum gauge along with its controller. The gauge had an overall measurement range from 10^{-2} mbar to atmospheric pressure with an accuracy better than 10%. The quartz oscillator was driven at its resonance frequency by a constant amplitude voltage using a phase locked loop oscillation circuit. The resonance current of oscillator was rectified and measured as a function of gas pressure. The pressure readings for several gasses were made and found to be in agreement with the theoretical results. Also, the gauge showed stability over a long period of 3000 hours. Hirata et al. [58] studied the electrical impedance of various types and sizes of quartz crystal oscillators as a function of pressure. Among the quartz oscillators, tuning fork type oscillators showed the highest sensitivity in terms of impedance change, about 10 times higher than other type of oscillators as shown in figure 2.2.

Secondly, the relation between pressure dependent change in impedance and size of quartz tuning fork was studied and it suggested that a crystal with higher length to width ratio or length to thickness ratio performs better in terms of sensitivity towards pressure measurement. They measured the pressure dependent change in resonance impedance of 33 quartz tuning fork crystals of different sizes with frequencies between 24 and 150 KHz. The experimental results showed that pressure sensitivity of impedance to the length l, width w and thickness t of quartz tuning fork is as follows:

$$Z \propto \frac{l^3}{wt^3}.f \tag{2.5}$$

Ono et al. [60] used the similar sensor and control setup used by him and his team earlier [59] with pressure measurement range 10^{-3} mbar to atmospheric pressure. In order to lower the measurable range, a temperature-stabilized sensor housing

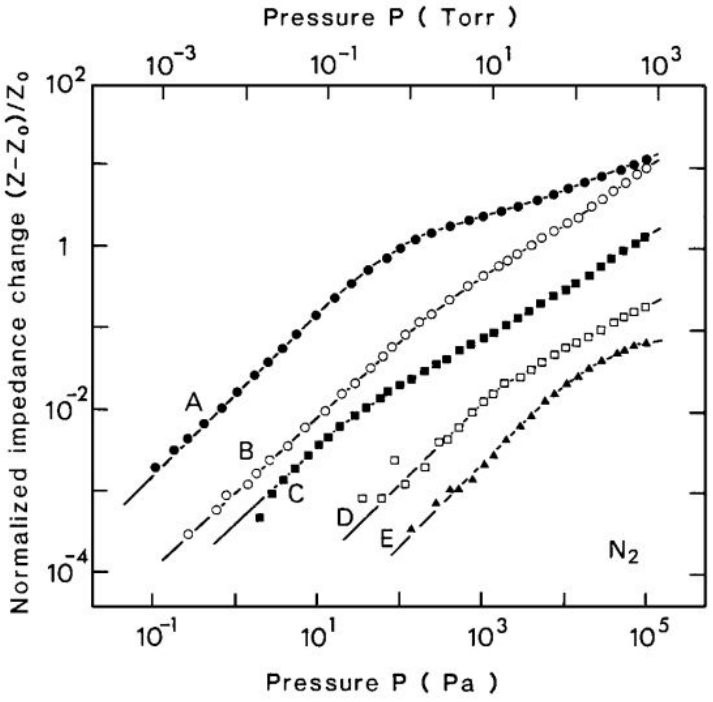

FIGURE 2.2: Pressure-dependent Change in Electrical Impedance for Oscillators of Various Oscillation Modes. **A:** Tuning Fork, **B:** MGQ, **C:** AT cut, **D:** NT cut, **E:** Ultra-sonic Microphone made of Ceramics [58]

was used where a thermo-control setup measures the temperature of housing using thermocouple and based on this temperature value controls the current through a transistor (being used as a heater) to maintain the temperature at 50 ± 0.2 °C. Additionally, the gauge readout was digital (consisting of a 12-bit, 10 V full scale ADC) instead of an analog meter used previously.

Hirata et al. [61] developed a PLL-less self-oscillation circuit which drives the quartz tuning fork oscillator at its resonance. The gauge had a measurement range of 10^{-3} to 10^{+3} mbar with an accuracy of 10% and a better response time of 0.2 s and resolution of 5 x 10^{-3} mbar. Kokubun [37] theoretically analyzed pressure dependence of electrical impedance of quartz tuning fork oscillator in molecular and viscous flow regions based on string-of-beads model. However, this model did not discuss the behavior of QTF oscillator's impedance in intermediate or transition flow region (1.3 x 10^{-2} mbar $\geq$ P $\leq$ 6 x 10^{-1} mbar). Kokubun et al. [62] studied the behavior of QTF impedance in intermediate flow region by making use of theory of slip effect. By extending this formula for intermediate

flow region into molecular flow region , a single unified formula describing the pressure dependence of impedance over the whole pressure region was obtained, but there was an error of 20% between theoretical and experimental results. In order to remove this discrepancy, Millikan's empirical formula was adopted and the unified formula thus obtained was inn better agreement with experimental data for various gasses.

Rudolph Stocker [63] tried to find a solution for the limitations of QTF-based vacuum gauge namely: gas dependence, temperature disturbance, contamination effects and slow response time. Stocker designed a QTF driving circuit which keeps the mechanical/ physical amplitude of vibration of oscillator constant and measures the energy required to do so as pressure indication. As the pressure around QTF increases, more energy is required by the QTF to overcome friction of gas to keep its amplitude of vibration constant. This mode of operation had a much faster response time as compared to previous developments. Secondly, he included a temperature sensitive element in his circuit to cancel out the effect of temperature-induced variations in the impedance of oscillator. In order to compensate for contamination effects on the pressure readings of QTF, both resonance impedance and frequency were measured since both of these quantities behave in a different manner to pressure changes and contamination. Like all other indirect type vacuum gauges, QTF is also gas dependent i.e., the pressure reading is dependent on the molecular weight of the gas. Stocker compensated thi by combining QTF sensor with Pirani sensor as both are impacted differently but equally by the molecular mass of the gas. The change in electrical impedance of quartz tuning fork oscillator is dependent on molecular mass as:

$$\Delta Z \propto \sqrt{M}\rho \tag{2.6}$$

While for Pirani gauge, the electrical energy N, required to keep the filament temperature constant is given as:

$$\Delta N \propto \frac{aC_s}{\sqrt{M}}\rho \tag{2.7}$$

where, a is gas dependent constant and C_s is the molecular specific heat of the gas. From equations (2.6) and (2.7), we can see that two sensors are dependent on molecular weight of gas in equal but opposite manner. Therefore, by joining the output of both, a gas-independent gauge was developed.

Until the early 1990s, all QTF sensors were developed and tested in a controlled laboratory environment, however Kobayashi et al. [64] in 1993, developed the first QTF-based friction-type vacuum gauge meant to be used on commercial scale. The wristwatch quartz oscillator and temperature controlled housing used in previous studies [60–62] were replaced with a new quartz oscillator, named T-oscillator, designed to sense temperature as function of resonance frequency of oscillator. T-oscillator has a linear relation between temperature change and frequency shift with a slope of 1 Hz/°C. The major difference between T-oscillator and wristwatch-oscillator was in crystal cut angle. The angle θ between the longitudinal direction of oscillator and z-axis of crystal for wristwatch oscillator is selected to be +5° while for T-oscillator, it is -15° to -30° as shown in figure 2.3. By measuring the frequency

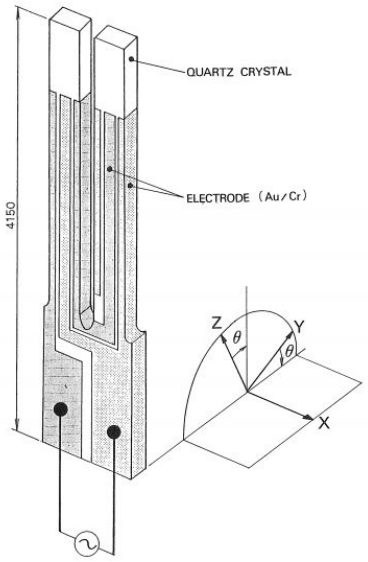

FIGURE 2.3: The Axis (x, y, z) of Quartz Crystal Relative to Oscillator Configuration

of oscillator, it was possible to estimate the temperature of oscillator and hence thermal variation of impedance with an accuracy of 2Ω. This oscillator allowed to estimate the pressure from measured value of impedance (Z) and frequency (f)

of T-oscillator with an error of less than 10% in the range of 10^{-3} mbar to 10^{+3} mbar.

2.1.3 Quartz Tuning Fork as Positive Pressure Sensor

Henry E Karrer and Jerry G Leach [65] in 1969 described that quartz resonators change frequency when subjected to pressure and developed a fluid pressure measurement gauge using quartz resonator. Ward [66] developed a quartz tuning fork-based friction gauge primarily intended for positive pressure measurements of corrosive gasses. The tuning fork is enclosed in a sealed bellow which in turn is exposed to gas pressure being measured. The bellow setup was used to protect the quartz tuning fork sensor from high pressures and corrosive gasses. This gauge has a measurement range of 250 bar with Nitrogen gas. Downie and Behrens [67] used quartz tuning fork for measurement of high gas pressures using a different approach. Their sensor was meant to measure pressure of non-reactive gases in the pressure range to 900 bar.

2.1.4 Gas Sensing Applications of Quartz Tuning Fork

The pressure-induced change in impedance of quartz tuning fork oscillator is dependent on the molecular weight of the gas being measured [58–63]. Furthermore, frequency and impedance dependence of on the molecular weight of gas is somewhat different. T. Kobayashi et al. [68] exploited these facts to develop a binary gas concentration analysis device using quartz friction vacuum gauge. Kobayashi established an algorithm for calculation of pressure as function of quartz oscillator's impedance using the relation developed [62]. The reduction in frequency of quartz tuning fork is proportional to the ρ (or molecular weight M) of the gas while change in impedance is proportional to the square root of the product ρ and η at a given pressure in viscous region. This characteristics made it possible to analyze the concentration of binary mixture of gasses with considerable difference in molecular masses e.g. Hydrogen & Nitrogen mixture or Argon & Helium mixture.

However, it was difficult to discriminate between gasses of closer molecular mass values, like Argon & Nitrogen, on the basis of relation between ΔZ and Δf_r of quartz friction gauge. For these mixtures, a gas independent gauge (capacitance diaphragm gauge) in combination with quartz friction gauge was used and the difference in output pressure values is analyzed to determine the concentration of gasses. Kurokawa et al. [69] further investigated the partial-pressure measurement capability of quartz friction vacuum gauge at near atmospheric pressure conditions. The partial pressure of a binary gas was estimated by measuring the impedance change of a quartz friction vacuum gauge, which depends on both viscosity and total pressure of a binary gas, where the total pressure values were provided by a capacitance manometer (which is gas-independent). They successfully measured partial pressure of ozone in ozone-oxygen mixture with a resolution of 20 mbar. Later on, A. Suzuki et al. [70] used the method of [68] and [69] to measure the concentration of hydrogen in air with a resolution of 0.05 %vol. in air. Later, Suzuki et al. [71] enhanced the range of hydrogen detection from 0.1 – 100 %vol. in air with a response time ¡ 1s and discussed it in detail [72].

All the above discussed gas sensing setups were intended to use in controlled laboratories environment. However, for outdoor hydrogen sensing with quartz friction gas, Suzuki et al. [73] studied the influence of temperature on the output of QTF sensor and tried to minimize it. The temperature induced changes in the range of 15 – 50 °C were equivalent to 6 %vol. in air concentration of hydrogen, much above the critical limit of 4 %vol. in air concentration of hydrogen. The influence of temperature was reduced below the point corresponding to 1 %vol. in air hydrogen concentration. In 2016, Suzuki et al. [74] used a temperature stable quartz oscillator (TSQO) to eliminate the influence of temperature on the output of quartz friction vacuum gauge in order to enhance the accuracy of hydrogen sensing. The TSQO exhibited improved temperature stability with a fluctuation of only 0.22% in the temperature range 30 – 100 °C as compared to 2.0% by the conventional quartz oscillator in the temperature range 15 – 85 °C. An error of 0.22% is acceptable for outdoor hydrogen sensing because the fluctuations are smaller than the 0.33% change induced by the hydrogen concentration of 0.33

%vol. in air, which is considered the minimum safe limit for hydrogen leakage in air. Above this limit, hydrogen leakage may cause explosion. In 2019, Suzuki et al. [75] accounted for environmental pressure based output changes of QTF sensor along with temperature stability to further enhance the usability of quartz friction gauge as outdoor hydrogen sensor. The accuracy of this setup was much better than the desirable minimum accuracy of 0.33%.

2.2 Gap Analysis and Problem Statement

Current vacuum sensors are predominantly designed to function within low-pressure ranges and are ill-equipped to measure higher (positive) pressures. Exposing these sensors to higher pressures can lead to irreversible damage, making them unsuitable for applications that demand a wide range of pressure measurements. On the other hand, pressure sensors that excel in high-pressure environments often fall short in vacuum conditions, becoming impractical for measurements beyond a few millibar. These sensors are also tailor-made and therefore cost higher. This creates a significant challenge in critical applications such as industrial chamber leak testing, chemical processes that require both a pristine vacuum condition for clean environments and high-pressure environments for chemical reactions to occur, and specialized applications like rocket fueling. These scenarios necessitate a sensor that can seamlessly work in both vacuum and high-pressure measurements, something that existing sensor technologies struggle to provide.

Quartz tuning fork crystal, readily available in the market at very low cost, has demonstrated its capability in both vacuum and positive pressure measurements, but traditionally, this has required use of custom-made quartz tuning fork sensors, each with distinct driving and signal conditioning circuitry tailored to specific pressure ranges. This dual setup adds complexity and limits the efficiency of the measurement systems. Therefore a versatile, accurate, and robust sensing solution that can seamlessly work in both vacuum and high-pressure environments is required.

2.3 Proposed Solution

This research investigates the development and potential of such a solution that can address the limitations of current technologies and offering a new approach to wide range pressure measurement in demanding industrial and scientific applications. The introduction of a novel gauge that leverages quartz tuning fork technology to measure both vacuum and positive pressure levels using a single, unified setup not only enhances the pressure measuring range but also simplifies the hardware requirements as well as enhances the accuracy and reliability of measurements across this broad pressure spectrum.

2.4 Thesis Contribution

This research contributes significantly to the advancement of pressure measurement technology by developing and characterizing a compound sensor capable of operating across a wide range of pressures. The primary contributions of this research, with a focus on the compound nature of the sensor, are as follows:

1. **Design and development of a quartz tuning fork based compound pressure gauge:**

   This research introduces a novel compound pressure gauge that utilizes quartz tuning fork sensor to measure pressures from high vacuum levels (down to 10^{-3} mbar) to high pressures (up to 10 bar) within a single device. This innovation merges the capabilities of separate vacuum and high-pressure sensors into a unified system, significantly simplifying pressure measurement across a wide range.

2. **Optimization and Integration of Dual Measurement Ranges:**

   The research focuses on the seamless integration and optimization of vacuum and high-pressure measurement within the compound sensor. By developing unified signal conditioning and calibration techniques, this research ensures

that the sensor maintains high accuracy, sensitivity, and robustness across its entire operating range, thereby eliminating the need for multiple sensor setups and enhancing the overall system efficiency.

Chapter 3

Design and Methodology

3.1 Design of Quartz Tuning Fork Compound Gauge

The development of a compound gauge that can operate effectively across a wide pressure range accurately, is certainly a challenge since no gauge is available which is equally specialized both in vacuum and positive pressures. The quartz tuning fork-based sensor was selected for this purpose because of its capability to provide precise frequency and electrical impedance shifts in response to changes in external pressure. The preferred parameter of quartz tuning fork for pressure measurement is frequency however in vacuum region, changes in pressure around the tuning fork affect its resonance frequency very little (of the order of few Hz) and hence electrical impedance of quartz tuning fork is only viable option. While in positive pressures, the force exerted on the tuning fork's prongs causes a measurable change in its resonance frequency. The design objective of this research is to create a system that not only offers high sensitivity in vacuum conditions but also maintains the same sensitivity and accuracy in positive pressure regions. This requires a careful design which provides both mechanical robustness and electronic precision. The following sections detail the various stages of the design and methodology adopted in this research.

3.1.1 Quartz Tuning Fork Specifications

In this section, the key specifications of the quartz tuning fork sensor, selected for the development of compound gauge, are outlined with primary focus on highlighting the factors which are critical for compound sensing capabilities of the quartz tuning fork sensor.

3.1.1.1 Material

The quartz tuning fork crystal is made from high-purity quartz (silicon dioxide), a material well known for its excellent piezoelectric properties. Quartz is favored for several reasons:

1. **Frequency Stability:**

   Quartz based resonator exhibits remarkable stability in maintaining its natural resonance frequency, even under varying environmental conditions, primarily temperature and humidity. This property is crucial in pressure measurement applications where small frequency shifts need to be detected with high precision for measuring the pressure with better resolution and accuracy, which may get affected from other environmental factors.

2. **Low Thermal Expansion:**

   Quartz has a low coefficient of thermal expansion, meaning that it is fairly resistant to frequency drift caused by temperature changes. This ensures that the sensor maintains accurate readings over a wide range of temperatures, minimizing the need for external temperature compensation in most operating environments.

3. **Chemical Resistance:**

   Quartz is chemically inert, allowing the tuning fork to operate in harsh environments without affecting the gases and other materials that may be present in the measuring chamber.

3.1.1.2 Size

The physical dimensions of the quartz tuning fork play a pivotal role in determining its resonant frequency and sensitivity. The size of the tuning fork influences the mechanical stiffness of its prongs, which in turn dictates the sensor's response to applied pressure. Quartz tuning forks are available in various sizes and packages. For this research however, a 2 x 6 mm cylindrical package was selected, based on the following considerations:

1. **Prong Length, Width, and Thickness:**

   The length and thickness of the prongs determine the tuning fork's ability to oscillate under external forces. A longer prong length results in lower resonant frequency and increased sensitivity to external pressure. Conversely, thicker prongs increase the tuning fork's stiffness, leading to higher resonant frequencies but reduced sensitivity.

2. **Package Type:**

   While quartz tuning forks are available in multiple packages, such as cylindrical packages (ϕ3 x 8 mm and ϕ2 x 6 mm) and SMD (surface mount devices) package, the 2 x 6 mm cylindrical package was chosen for this study. This particular size offers an optimal balance between pressure sensitivity and compactness, making it suitable for integration into a wide range of measuring setups.

   - Better Sensitivity: Compared to larger cylindrical packages (e.g., 3 x 8 mm), the 2 x 6 mm variant is slightly more sensitive to pressure changes, making it ideal for detecting even small variations in both vacuum and positive pressure conditions.
   - Wide Availability: The 2 x 6 mm cylindrical package is one of the most widely available and cost-effective quartz tuning fork packages in the market, ensuring affordable accessibility for future research or commercial applications.

3.1.1.3 Resonance Frequency

One of the critical parameters of a quartz tuning fork is its resonance frequency, which defines its natural oscillation rate when no external forces are applied. The selected QTF has a resonance frequency of 32.768 KHz, a frequency commonly used in watches, clocks, and timing devices. This frequency was chosen for several reasons:

1. **Wide Availability at Low Cost:**

   32.768 KHz tuning forks are mass-produced for timekeeping applications, making them widely available and affordable. Their low cost allows for the use of multiple sensors or replacements without significantly increasing the overall cost of the system.

2. **Sensitivity to Pressure:**

   At 32.768 KHz, the QTF offers a good balance between frequency stability and sensitivity to pressure changes. This frequency range is ideal for measuring the pressure range targeted in this study. Higher frequency tuning forks may offer increased sensitivity, but they are generally more expensive (due to low availability) and more vulnerable to environmental influences.

3.1.1.4 Quality Factor (Q-factor)

The Quality Factor (Q-factor) is a measure of the tuning fork's energy loss per cycle of oscillation, or more simply, its oscillation efficiency. It indicates how well the tuning fork can maintain its oscillation when subjected to external disturbances, such as changes in pressure. The Q-factor is a key parameter in determining the tuning fork's sensitivity, particularly in vacuum conditions.

1. **Q-Factor in Vacuum:**

   In a vacuum, the QTF exhibits a high Q-factor, typically around the order of 105. This means that the tuning fork can oscillate with minimal damping

from air molecules. A higher Q-factor corresponds to higher sensitivity to pressure changes in vacuum, as even small shifts in air damping will cause noticeable changes in the amplitude of oscillation.

2. **Q-Factor in Positive Pressure:**

   At atmospheric pressure, the Q-factor is lower due to the increased damping effect of air or gas molecules on the tuning fork prongs and hence changes very little with any further increase in pressure. However, the tuning fork remains sensitive to pressure-induced mechanical strain, with changes in resonance frequency being the primary measurement indicator in these conditions.

3. **Impact on Sensitivity:**

   The high Q-factor (quality factor) in vacuum environment ensures that the quartz tuning fork is capable of detecting minute changes in pressure, making it an ideal sensor for applications that require precise vacuum measurements. Meanwhile, in positive pressure environments, the Q-factor degrades however it has very limited role in pressure measurement in this region. In positive pressure region, the sensor's sensitivity to frequency shifts remains high enough to provide accurate measurements across the desired pressure range.

3.1.1.5 Additional Specifications

1. **Operating Temperature Range:**

   The selected tuning fork can operate reliably across a temperature range of -40°C to +85°C. This temperature stability is crucial for maintaining accurate pressure readings in varying experimental conditions.

2. **Aging Rate:** Quartz crystals typically exhibit low aging rates, with the selected tuning fork showing a frequency drift of only ±3 ppm/year as specified by its datasheet. This low aging rate ensures that the sensor maintains its accuracy over extended periods of use, making it suitable for long-term pressure monitoring applications.

These specifications highlight the quartz tuning fork's ability to perform reliably as a compound pressure sensor. Its low cost, compound sensing capability, and wide availability further enhance its suitability for commercial and industrial applications.

3.1.2 Principles of Operation

The quartz tuning fork operates on the principle of piezoelectric mechanical resonance, wherein the tuning fork vibrates at its natural frequency when excited by an external electrical signal. The friction of gas particles around the quartz tuning fork impact its resonance properties i.e., impedance and frequency. The schematic of compound gauge is shown in figure 3.1. The sensor's response to external pressure is manifested through changes in both electrical impedance and resonance frequency, depending on whether the sensor is exposed to vacuum or positive pressure. The operation of the quartz tuning fork sensor can be divided into two distinct modes based on the pressure conditions: Vacuum Mode and Positive Pressure Mode. Each mode exploits different mechanical and electrical behaviors of the tuning fork to achieve precise measurements over the desired pressure range.

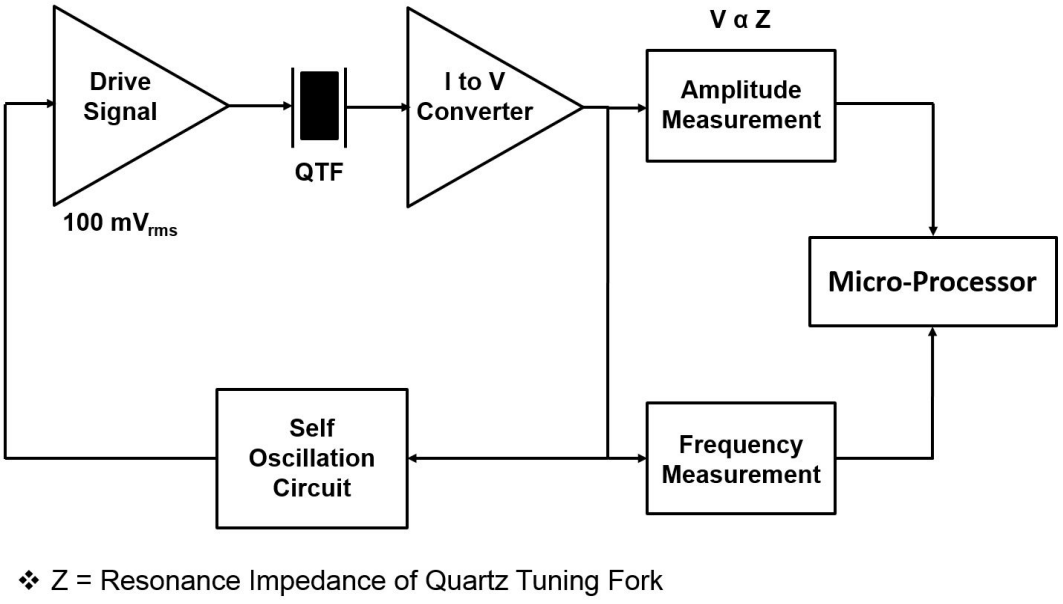

FIGURE 3.1: Schematic of QTF based Compound Gauge

3.1.2.1 Vacuum Mode (Oscillation Amplitude Detection)

In vacuum conditions, the quartz tuning fork operates by detecting changes in electrical impedance, and hence oscillation amplitude, which is directly influenced by the level of vacuum surrounding the sensor. The key principles in vacuum mode are as follows:

A. Air Damping Effect

Under normal atmospheric pressure, air molecules surrounding the tuning fork prongs exert a damping force on their oscillations. This force is due to the interaction between the oscillating prongs and the surrounding air, which resists the vibration of QTF. This results in increased resonance impedance and reduced oscillation amplitude. As the pressure decreases and approaches a vacuum state, the number of air molecules around the prongs is significantly reduced, and thus the damping effect diminishes. With less resistance from air molecules, the tuning fork prongs are able to oscillate with greater freedom, resulting in decreased resonance impedance and increased oscillation amplitude. The resonance impedance is primarily affected by the gas friction force, which can be quantified through the following relationship:

$$\Delta Z = Z - Z_0 \tag{3.1}$$

$$\Delta Z = \frac{2\eta_0 V^2 cos\theta}{A_m^2}.f \tag{3.2}$$

Where:

- Z is the impedance of the quartz tuning fork due to an ambient gas
- Z_0 is intrinsic impedance of QTF at high vacuum
- V is the excitation voltage of the oscillator
- η_0 is the conversion efficiency of the electric energy to the mechanical energy
- θ is the phase difference between voltage and current

- A_m is the amplitude of the forced vibration of quartz tuning fork's prongs
- f is the friction drag coefficient representing the gas friction force acting on the prongs

For a specific quartz tuning fork oscillator, the term $\frac{2\eta_0 V^2 cos\theta}{A_m^2}$ is constant, so change in Z depends on f given by:

$$f = 6\pi\eta' R + 3\pi R^2\sqrt{2\eta'\rho\omega} \tag{3.3}$$

$$\eta' = \frac{\eta}{1 + (\frac{L}{R})(C_1 + C_2 e^{(-C_3\frac{R}{L})})} \tag{3.4}$$

Where:

- R is the radius of the sphere, which is nearly equal to the thickness of the quartz tuning fork
- M is the molecular weight of the ambient gas
- R_0 is the gas constant
- T is the temperature
- η is the coefficient of viscosity of gas
- ρ is the density of the gas, proportional to the molecular weight and pressure P
- ω is the resonance frequency
- L is mean free path of gas particles
- C_1 is constant for Millikan's formula
- C_2 is constant for Millikan's formula
- C_3 is constant for Millikan's formula

B. Damping Mechanism

1. At atmospheric pressure, air molecules create significant damping, which reduces the amplitude of the oscillations. This is because the air friction increases the overall impedance, causing energy loss in the oscillating system.

2. As the pressure decreases and approaches vacuum conditions, the damping force becomes negligible, allowing the tuning fork to oscillate more freely with minimal energy loss. This leads to a measurable increase in oscillation amplitude as the air drag on the prongs is significantly reduced.

3. In the high vacuum range, where the pressure reaches less than 10^{-3} mbar, the tuning fork experiences almost no damping from residual gas molecules, resulting in its highest oscillation amplitude and the lowest resonance impedance.

C. Vacuum Measurement

When driven by a self-oscillating circuit, the QTF's resonance impedance directly affects its oscillation amplitude. Changes in the air damping effect, caused by variations in ambient pressure, lead to corresponding changes in the amplitude of oscillation. At higher pressures, the damping effect reduces the oscillation amplitude, while at lower pressures, particularly in vacuum conditions, the amplitude increases as the damping effect is diminished.

- **Atmospheric Pressure:** Maximum damping occurs due to air molecules resisting the tuning fork's motion, resulting in low oscillation amplitude.

- **Medium Vacuum:** As pressure decreases, damping is reduced, leading to a gradual increase in oscillation amplitude.

- **High Vacuum:** Minimal damping allows the tuning fork to oscillate freely with very high amplitude, corresponding to very low resonance impedance.

Thus vacuum measurement process relies on the real-time monitoring of the QTF's oscillation amplitude. As the vacuum level increases (i.e., the pressure decreases),

the amplitude of oscillation grows, providing a precise indication of the degree of vacuum. The system continuously tracks these amplitude changes, translating them into corresponding vacuum levels.

3.1.2.2 Positive Pressure Mode (Frequency Detection)

When the quartz tuning fork is exposed to positive pressures, the prongs of the tuning fork undergo mechanical stress, which either compress or elongate them slightly. This stress alters the prongs' stiffness, which in turn changes the natural frequency of oscillation. The magnitude of the frequency shift is directly proportional to the amount of pressure applied i.e., as pressure increases, the resonant frequency shifts away from the nominal 32.768 KHz. This frequency shift is detected by frequency measurement system, employed using PIC18F4550 microcontroller's built-in counter, which monitors the real-time oscillation frequency and correlates it to the applied pressure. The relationship between pressure and change in frequency is linear within range of interest, making it easy to map frequency shifts to specific pressure values using a simple linear relation. This linear response also contributes to the sensor's reliability and repeatability, making it suitable for industrial and scientific applications.

$$\Delta f_r = A_f P \tag{3.5}$$

where, A_f is gas and QTF dependent constant (slope of the linear equation) and P is pressure to be sensed

3.1.2.3 Dual-Mode Operation and Transition

The quartz tuning fork compound gauge is designed to operate seamlessly across a broad pressure spectrum, from high vacuum conditions to high positive pressures up to 10 bar. The microprocessor-based dual-mode operation enables the sensor to switch effortlessly between detecting amplitude changes in vacuum conditions

and frequency shifts in positive pressure environments. The ability to function in two distinct modes is one of the key innovations of this gauge, making it suitable for industrial and scientific applications that demand precise measurements over a wide range of pressures.

A. Measurement Mode Transition

The transition between vacuum mode and positive pressure mode is automatic, triggered by the external pressure conditions. The sensor is pre-calibrated to identify the threshold (both in terms of oscillation amplitude and frequency) between vacuum and positive pressure, ensuring a smooth shift in measurement of interest. This transition is essential to maintain accuracy and ensure optimal sensor performance.

1. **Vacuum Mode Activation**

   In vacuum conditions, when the pressure falls below a specific threshold (below 1000 mbar), the system switches to amplitude-based detection. As the pressure continues to drop, the sensor measures oscillation amplitude changes, which increase as the air damping on the QTF prongs decreases. This mode is highly sensitive to small changes in vacuum levels, and the conversion algorithm for amplitude to vacuum level, discussed in section 3.1.2.1, is used to deliver precise readings from 1000 mbar down to 10^{-3} mbar.

2. **Positive Pressure Mode Activation**

   As the pressure rises above the threshold (around 1000 mbar), the system transitions to frequency-based detection. In this mode, the tuning fork's resonant frequency shifts in response to the mechanical stress caused by the increasing pressure. The sensor's frequency counter tracks these shifts, and a calibrated frequency-to-pressure conversion algorithm, discussed in section 3.1.2.2, is applied to determine the positive pressure, with high accuracy, up to 10 bar.

3. **Dual-Mode Data Handling**

   The sensor's microcontroller is programmed to continuously monitor both amplitude and frequency, allowing it to determine which parameter to prioritize based on the current pressure conditions. This real-time decision-making ensures that the most relevant measurement mode is used at all times. The system is designed to prevent overlaps or gaps in measurement, making the sensor highly responsive to pressure changes in both directions (from vacuum to positive pressure and vice versa) as shown by the flowchart in figure 3.2

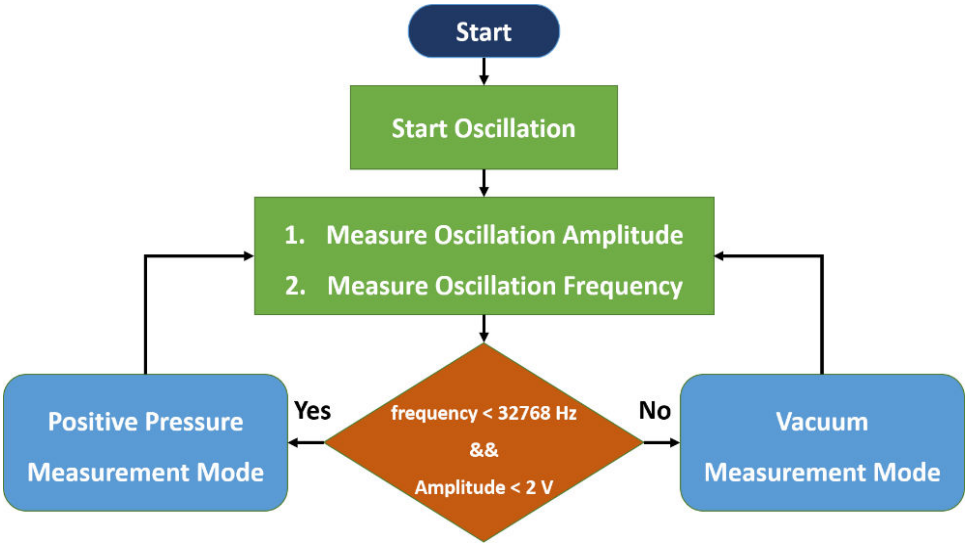

FIGURE 3.2: Flowchart of Dual Transition Mode

3.1.3 Mechanical Design

The mechanical design of the quartz tuning fork-based compound gauge plays a critical role in ensuring both the safe functionality and longevity of the sensor in varying pressure environments. The housing of sensor, the major mechanical part, not only serves to protect the quartz tuning fork from external environmental factors but also provides structural integrity under extreme conditions—both high vacuum and high pressure. The design must balance the need for robustness with precision, ensuring that the sensor remains sensitive to minute pressure changes while operating safely under high mechanical stress.

3.1.3.1 Material Selection

Stainless steel was selected as the primary material for the sensor housing due to its excellent combination of mechanical strength, corrosion resistance, and its ability to withstand high mechanical stress. Stainless steel is well-suited for ensuring long-term durability and reliable performance in a compound gauge operating across a wide pressure range.

1. **Vacuum Compatibility**

   Stainless steel is highly compatible with vacuum environments, making it an ideal choice for applications requiring ultra-low pressures. Its impermeability ensures that it does not allow gas penetration, preventing contamination that could interfere with the process under measurement. One of the critical factors in vacuum systems is outgassing, where trapped gases are released from the material's surface, potentially compromising vacuum integrity. Stainless steel exhibits minimal outgassing, preserving the vacuum quality and ensuring consistent, reliable readings, even at 10^{-3} mbar.

2. **Pressure Compatibility**

   Stainless steel offers exceptional mechanical strength and durability, making it well-suited for handling positive pressures up to 10 bar. Its ability to withstand repeated cycles of pressurization and depressurization without deformation is essential for maintaining the integrity of the sensor housing. The high tensile strength of stainless steel prevents structural failures under extreme pressures, while its corrosion resistance protects the housing from environmental factors such as moisture or corrosive gases. This ensures that the sensor maintains its structural and functional integrity over long periods, reducing the need for frequent maintenance or re-calibrations.

3. **Temperature Compatibility**

   Stainless steel can withstand wide range of temperatures often present in tough industrial conditions.

3.1.3.2 Sealing Mechanism

To ensure the sensor's operation and systems' safety in both vacuum and high-pressure environments, a vacuum-tight seal was required. The sealing mechanism is critical in preventing any gas ingress or egress, which could not only disturb the sensor's measurements but also the system, particularly in vacuum mode where even minute leaks can disturb the system.

- **O-ring Seals** High-precision O-rings made from fluoroelastomer (such as Viton) are chosen due to their excellent sealing properties in a wide range of temperatures and pressures. These O-rings, shown in figure 3.3, are designed to create a hermetic seal, maintaining vacuum integrity while also withstanding the stress of high-pressure environments. The same O-ring ensures the leak-free operation of the sensor under both vacuum and high-pressure conditions, providing a dual-purpose seal that simplifies the design. O-rings are placed at all the key joints, ensuring that there are no weak points where leaks could occur.

FIGURE 3.3: Viton O-ring

3.1.3.3 Feedthrough

The mechanical design also incorporates a two-conductor nickel feedthrough (8175-01-W from Ceramaseal) shown in figure 3.4, which serves as interface between the sensor's internal environment and external data acquisition electronics but maintains the pressure isolation.

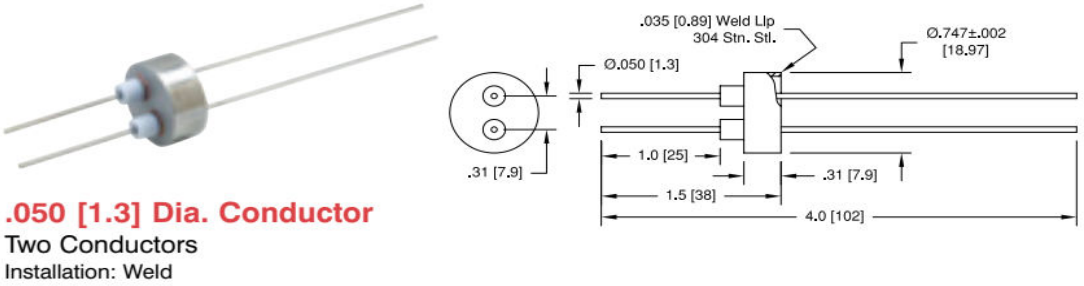

FIGURE 3.4: Electrical Feedthrough (Ceramseal 8175-01-W)

- **Pressure Isolation** The primary purpose of feedthrough is to pass electrical signals to the sensor without compromising the vacuum or pressure integrity i.e., isolate the internal sensor environment physically from the external environment, which is required in extreme conditions i.e., high vacuum or high pressure.

3.1.3.4 Connection Port

To mount the quartz tuning fork sensor into a process chamber, whose pressure is to be measure, a KF-10 (Klein Flange) port, shown in figure 3.5 was incorporated into the sensor's tube. The KF flange is widely used in vacuum systems due to its ease of use, reliability, and ability to make or break connection with minimal effort.

FIGURE 3.5: Steel Housing for Sensor with KF-10 Mounting Flange

- **Range of Operation**

  The connection port can comfortably handle pressure range of interest, from 10^{-3} mbar to 10 bar, allowing for the full range of pressures. The port allows the gauge to be easily integrated into various experimental setups and pressure chambers.

- **Modular Design**

  The KF flange system was selected due to its modular nature, enabling the sensor to be easily connected and disconnected from different pressure systems. This flexibility is particularly useful in experimental settings, where the sensor may need to be removed and reinstalled frequently between tests.

3.1.4 Electronic Design

The electronic part of the quartz tuning fork-based compound gauge is the most critical one as it directly defines how accurately the changes in frequency and amplitude are measured and converted into pressure readings. The design is centered on exciting the tuning fork at its resonance frequency, tracking its resonance frequency, and detecting oscillation amplitude with high precision. Several key components and circuits are combined to ensure reliable, accurate, and real-time measurements. The main elements of the electronic design are described as follows:

3.1.4.1 Self-Oscillation Circuit

The heart of the electronic system is the self-oscillation circuit, optimized for frequency of 32.768 KHz. Self-oscillation circuit, shown in figure 3.6 uses QTF in feedback and, in this way, continuously tracks and keep driving the QTF at its resonance frequency. This circuit was designed using a low-noise, wide bandwidth operational amplifier (TL082), ensuring stable oscillation of the tuning fork without external frequency interference. The drive signal to QTF is limited to a constant amplitude of $\pm$100mV to avoid any damage to sensor caused by high

power dissipation and at the same time constant drive signal makes it easy to estimate the resonance impedance of sensor by measuring the output current. A current-to-voltage converter (I/V converter) transforms the resonance impedance-dependent current to measurable voltage which is then fed to analog-to-digital converter (ADC) after necessary signal-conditioning. This digital data is then converted to vacuum readings by the microcontroller using pre-embedded lookup table.

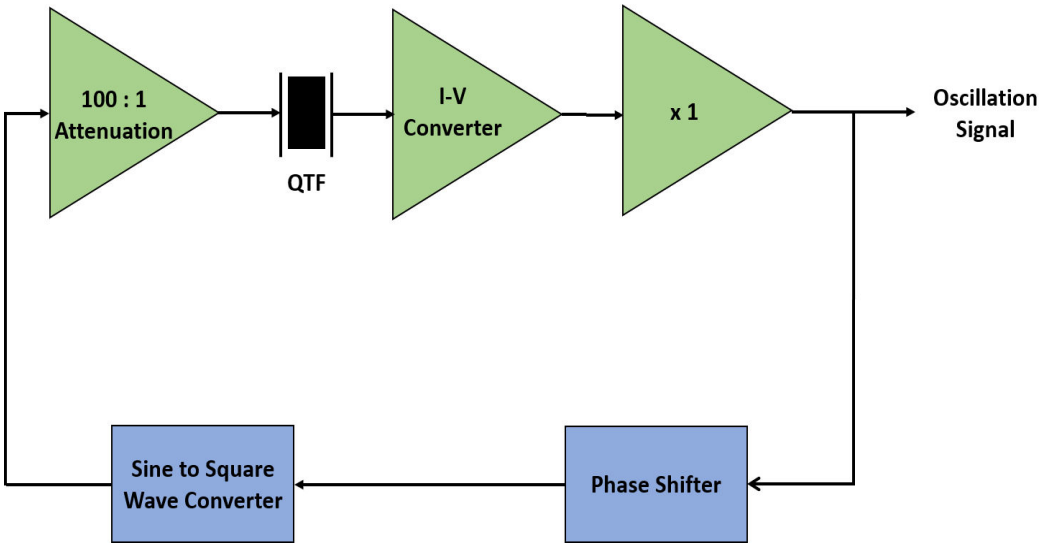

FIGURE 3.6: Schematic of Self-Oscillation Circuit for Driving QTF Sensor

3.1.4.2 Frequency Counter

The PIC18F4550 microcontroller's built-in timer modules, shown in figure 3.7 can also function as counter, when operated using an external clock source. In our case, the external clock source is resonance frequency of quartz tuning fork sensor. This way timer/counter module serves as the frequency measuring device for this research, offering high enough resolutions (at least 0.1 Hz) to detect even small shifts in frequency. A minimum resolution of $1/10^{th}$ of Hz is essential for capturing minor frequency variations that correspond to minute pressure changes in the positive pressure regime (1 to 10 bar). The frequency shifts are captured in real-time and processed by the microcontroller, which uses pre-calibrated conversion curve (in the form of lookup table embedded in microcontroller) to convert frequency changes into pressure readings.

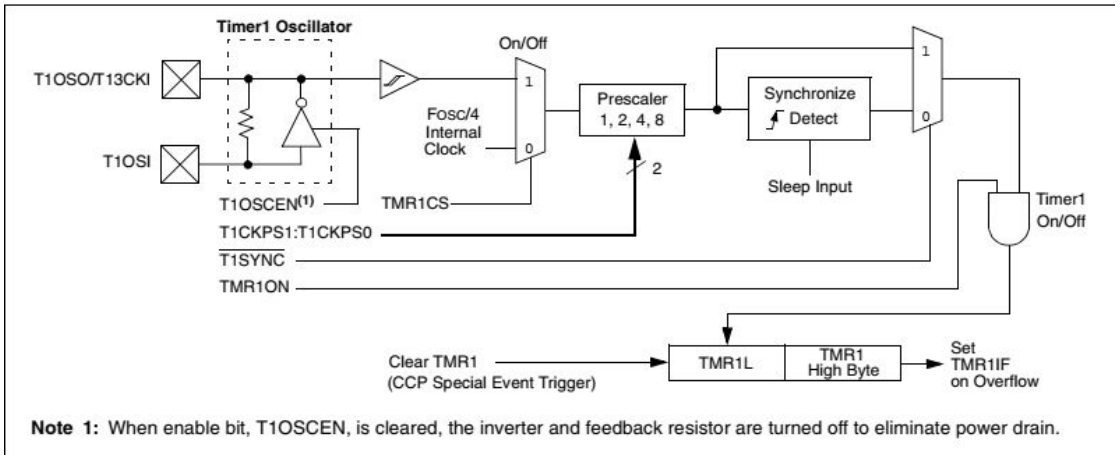

FIGURE 3.7: Timer 1 Module of PIC18F4550

3.1.4.3 Amplitude Measurement Circuit

In vacuum environments, the quartz tuning fork's oscillation amplitude is dependent on pressure around it. To capture these pressure-dependent changes in amplitude level, a precision rectifier circuit is designed, shown in figure 3.8, which converts the high-frequency AC signal from the QTF into a microcontroller-readable DC voltage.

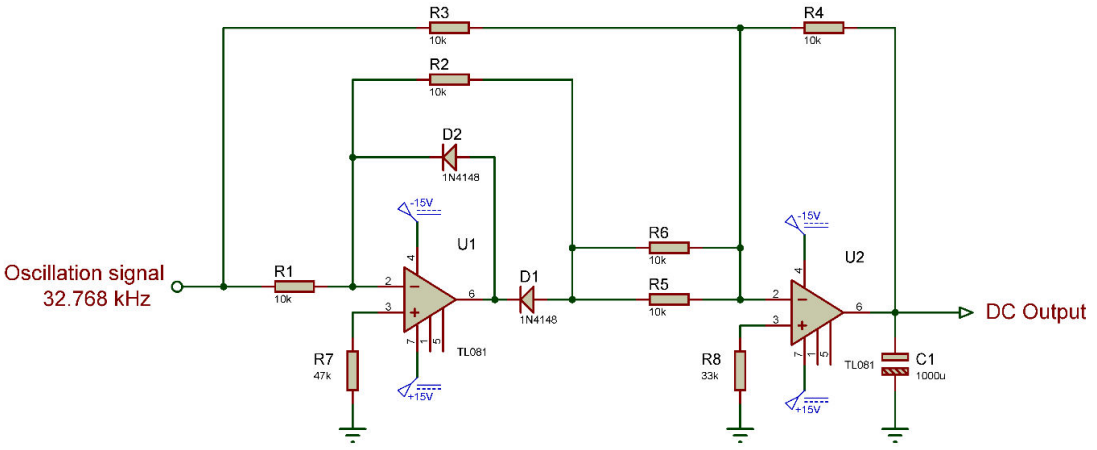

FIGURE 3.8: Full-Wave Precision Rectifier

This rectified signal is then digitized using a 16-bit analog-to-digital converter (ADS1115) shown in figure 3.9, providing high-resolution digital values of the amplitude changes. The high-resolution ADC ensures that even tiny variations in oscillation amplitude—corresponding to minute changes in vacuum levels—are captured. This data is processed by the microcontroller to generate accurate

vacuum readings according to equation (3.1). By employing high-precision rectification and digitization, the system can reliably measure vacuum levels down to 10^{-3} mbar, offering excellent performance in low-pressure environments.

3.1.4.4 Microcontroller Interface

The PIC18F4550 microcontroller, shown in figure 3.10 from PIC18 family of Microchip Technology, serves as the brain for this entire system, handling data acquisition, signal processing, and system control. Specifications like 32 KB program memory along with 2 KB RAM, 33 I/O pins and peripherals such as I2C, UART and Timers (16-bit and 8-bit) make it a good choice for this application.

FIGURE 3.9: ADS1115, 16-bit Analog to Digital Converter

It ensures precise handling of both frequency and amplitude data as well as pressure calculations using the most suitable parameter among two. The microcontroller converts these signals into pressure readings through pre-determined calibration curves or algorithms.

1. **Data Processing**

   The microcontroller is programmed to convert the frequency and amplitude data into pressure readings using pre-calibrated conversion curves and algorithms. The relationship between frequency shift and positive pressure as well as amplitude and vacuum was developed through extensive testing and calibration, discussed in detail in chapter 4.

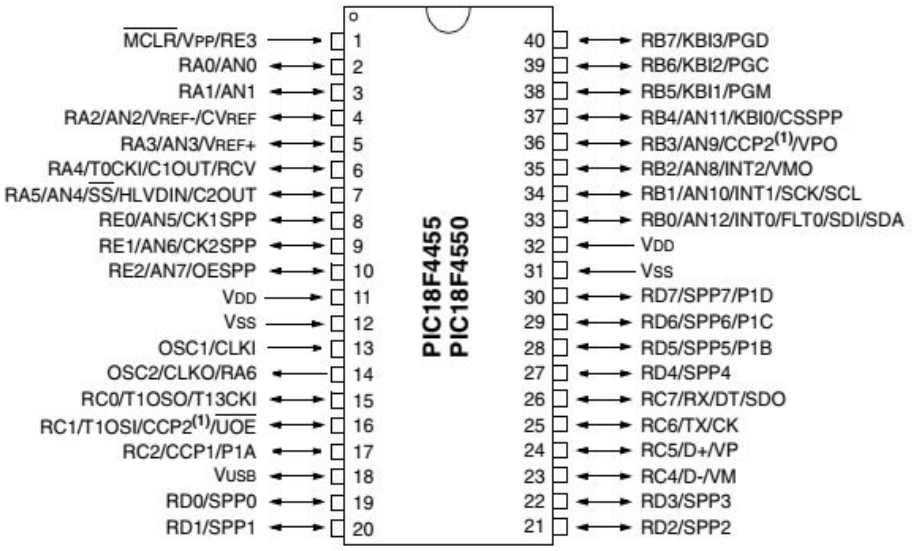

FIGURE 3.10: PIC18F4550 Pin Diagram

2. **Communication Protocol** To facilitate real-time data acquisition and external monitoring, the microcontroller features an RS-232 communication interface. This allows the sensor to interface with external systems, enabling continuous data logging, remote diagnostics, and real-time monitoring of pressure data during both laboratory testing and field applications.

3.1.4.5 Display and User Interface

The system incorporates a UART communication based 4.3-inch TFT touchscreen display (model: NX4827T043, Nextion made) shown in figure 3.11 to enable real-time interaction between the user and quartz tuning fork compound pressure gauge and displaying real-time pressure values.

A. Features and Capabilities:

1. **Pressure Display**

   The primary purpose of display is real-time pressure data visualization, with options to select between units such as mbar, bar, and Pa, and human-machine interface.

FIGURE 3.11: Nextion TFT Display 4.3-inch

2. **User Interface and Control**

   The touch interface allows users to interact directly with the device, offering control over key settings such as sensor's parameters, unit selection, and diagnostic tests. Additionally, the display provides intuitive controls for adjusting measurement parameters or switching between different operational modes, enhancing user convenience and system versatility.

3.1.4.6 Noise Filtering

To enhance the accuracy of the quartz tuning fork sensor, noise reduction techniques are implemented within the self-oscillation circuit. A low-pass filter (with cut-off frequency 33 kHz) as shown in figure 3.12 was integrated to eliminate high-frequency noise, ensuring that only the relevant oscillation amplitude signals are captured. This filtering helped in minimizing signal distortions, which is particularly critical in vacuum measurements where small amplitude changes need to be detected with precision.

Additionally, copper shielding was applied to the self-oscillation circuit, in order to protect against external electromagnetic interference (EMI). The shielding served to isolate the circuit from stray electromagnetic fields that could otherwise introduce noise and affect the QTF's oscillation behavior. This dual approach of low-pass filtering and EMI shielding ensured stable and noise-free readings, leading to more reliable vacuum and pressure measurements.

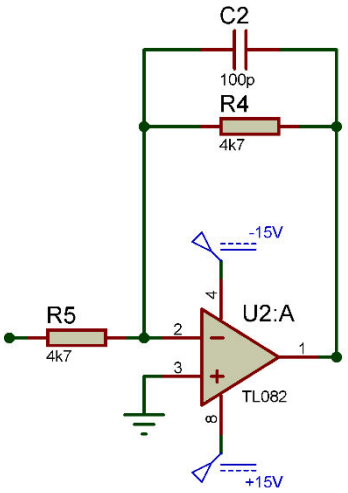

FIGURE 3.12: Low-pass Filter Incorporated into Self-Oscillation Circuit

3.2 Methodology

This section discuss the development and validation of the quartz tuning fork-based compound pressure sensor. The process was divided into several critical steps, covering initial calibration, pressure measurement procedures, vacuum testing, performance validation, and data analysis.

3.2.1 Test Environment

A controlled test environment was established to verify the QTF sensor's performance across both vacuum and high-pressure conditions. The test setup was designed to eliminate environmental variables such as temperature fluctuations, vibration, and gas contamination that could affect the accuracy of the pressure measurements. A schematic of the complete testing setup is shown below in figure 3.13.

1. **Test Chamber**

   A test chamber capable to withstand high differential pressures was incorporated into the system for testing the sensor. The chamber is made up of stainless steel (SS-316L) and equipped with KF ports for mounting sensors,

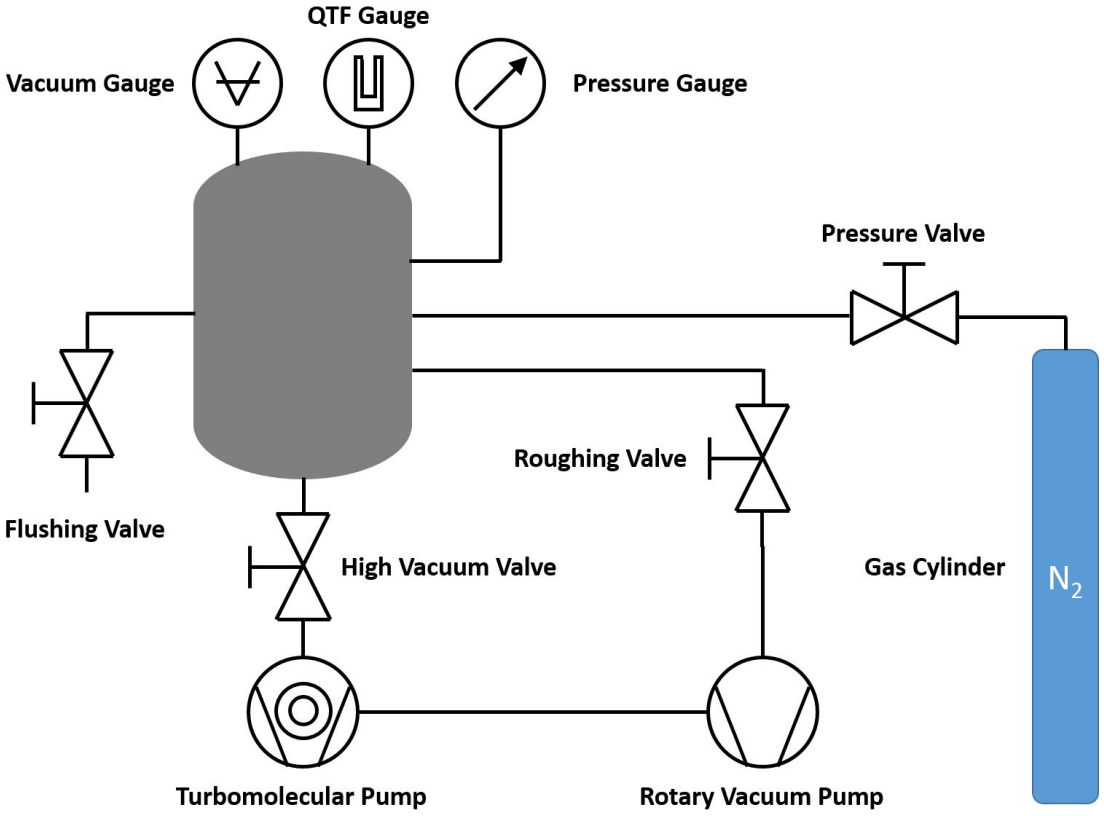

FIGURE 3.13: Schematic of the Test System Used for QTF Gauge

vacuum pumps, gas cylinders, valves and other accessories. The KF ports have O-ring sealing mechanisms to ensure stable vacuum and high-pressure environments during testing.

2. **Pressure Source**

   For positive pressure testing, a high-purity dry nitrogen gas cylinder was connected to the chamber through a pressure-regulated valve. This setup allowed the chamber to be pressurized up to 10 bar in steps, ensuring a controlled and stable pressure environment for the sensor tests. The purity of the nitrogen gas minimizes contamination and ensure repeatable results across multiple testing cycles.

3. **Vacuum Generation**

   A two-stage vacuum generation system was used to achieve vacuum conditions at-least a decade below our specified vacuum range i.e., 10^{-4} mbar as per ISO standards. A rotary vane pump was employed for fine vacuum

generation, while a turbomolecular pump further reduced the pressure in the chamber to achieve the desired high vacuum conditions. A valve assembly is attached to the chamber for isolating it from the vacuum pumps and flushing the chamber with Nitrogen gas. This setup allowed for rapid vacuum generation, enabling testing of the QTF sensor's performance in vacuum conditions.

4. **Temperature Control**

   Since the quartz tuning forks parameters of interest i.e., resonance frequency and impedance, are sensitive to temperature changes, the experimental setup, especially chamber, was maintained at a constant temperature using a thermal control system. A PID-controlled heater kept the chamber at a stable temperature of 25 °C, ensuring that the observed frequency shifts and amplitude changes are solely due to pressure variations and not influenced by temperature-induced fluctuations. This thermal control was critical, as even minor temperature changes could introduce errors in the QTF-based pressure readings.

3.2.2 Data Acquisition Setup

The calibration of the quartz tuning fork sensor's parameters with the stimulation i.e., pressure was essential to ensure the accuracy and reliability of the pressure measurements. The calibration procedure involved comparing the sensor's outputs (resonance frequency and impedance) to high-precision reference gauges over its full operational range, in both vacuum and positive pressures and then comparing the acquired results with established relations or establish a new relationship.

3.2.2.1 Pressure Data Acquisition

In the positive pressure measurement procedure, the focus was on accurately capturing the shift in the quartz tuning fork's resonance frequency as pressure was

applied. This process involved several critical steps to ensure precision and repeatability.

1. **Reference gauge(s) for positive pressure**

   Hydraulic Dead-Weight Tester, 480 Series from Budenberg, was used as reference instrument, offering high precision and resolution in the 1 to 10 bar range. The resonance frequency of the QTF was recorded with an interval of 0.1 bar within the positive pressure range. The frequency shifts are plotted against the applied pressures, generating a calibration curve that maps frequency changes to positive pressure values. This straight line curve is used to determine constant A of equation (3.5) as the slope of the line is equal to A.

2. **Measurement Setup**

   In order to obtain the pressure-dependent frequency data, the quartz tuning fork sensor along with pressure reference were attached to the test chamber capable of withstanding pressures more than 10 bar. The chamber was properly sealed to prevent leaks and ensure stable pressure conditions. A dry nitrogen gas cylinder was connected to the chamber as the pressure source. A flushing valve was also attached to the chamber for releasing the pressure after data acquisition.

3. **Pressure Application**

   Pressure was applied in incremental steps (with a step size of 0.1 bar), starting from atmospheric pressure (1 bar gauge pressure) and gradually increasing up to the maximum desired pressure of 10 bar. Each increment was applied with precise flow control valve to avoid sudden pressure surges that could distort the measurements. At each pressure level, the QTF's resonant frequency was recorded using the above mentioned frequency counter. This device provided accurate real-time readings of the QTF's oscillation frequency, ensuring that even minute frequency shifts caused by the pressure changes are captured.

4. **Data Logging**

   The pressure readings from the reference (dead-weight tester) are logged in tandem with the frequency readings from the quartz tuning fork sensor. The reference gauge provided highly accurate pressure values that are essential for the calibration process. The logged data was later used for post-experiment analysis.

5. **Data Processing** Once the pressure versus frequency data was collected, it was processed develop a linear algorithm which converts the raw frequency readings into pressure values. This algorithm has been discussed in section 3.1.2.2.

3.2.2.2 Vacuum Data Acquisition

In the vacuum region, the objective of data acquisition was to capture the changes in the quartz tuning fork's oscillation amplitude (which corresponds to change in resonance impedance of quartz tuning fork) as the pressure in the chamber is reduced towards high vacuum levels. This involves precise control over the vacuum environment and data recording to ensure the accuracy and reliability of the sensor's vacuum measurements using the acquired data.

1. **Reference gauge(s) for vacuum**

   Capacitance Diaphragm Gauges Make: MKS, Model: 690A01TRA, 690A13TRA) are used as reference instruments due to their high accuracy in low-pressure ranges, making them ideal for providing reference data in the vacuum region. The QTF's oscillation amplitude was recorded at every $1/10^{th}$ of the decade of vacuum level, from 10^{-3} mbar to ambient atmospheric pressure i.e., at every $1/10^{-3}$ mbar step in the range of 10^{-3} to 10^{-2} mbar and every $1/10^{-2}$ mbar step in the range of 10^{-2} to 10^{-1} mbar and so on. This data was used to generate a curve that correlates amplitude variations with vacuum levels and compare the results with the established relation, discussed in section 3.1.2.1.

2. **Measurement Setup**

   The QTF sensor along with reference gauges are mounted inside the test chamber and the chamber was connected to a combination of rotary vane pump for fine vacuum generation and a turbomolecular pump, capable of creating high vacuum conditions up to 10^{-6} mbar. The sensor along with reference gauges are directly exposed to the changing vacuum levels in the chamber without external interference. The setup also incorporated temperature control system, discussed in previous section, to maintain constant thermal conditions, preventing temperature fluctuations from impacting the QTF's oscillation characteristics.

3. **Vacuum Generation**

   To create the vacuum, the chamber was initially evacuated using the rotary pump, followed by the turbomolecular pump to reach the vacuum level in the range of 10^{-6} mbar. Once the chamber reached this low pressure, a controlled leak was introduced using a fine control valve. The pressure was incrementally raised by allowing small amounts of gas into the chamber, carefully controlling the rate of pressure increase. At each incremental pressure level, the oscillation amplitude of the QTF was recorded.

4. **Data Logging**

   During the experiment, the pressure readings from the reference vacuum gauges (Capacitance Diaphragm Gauges) are logged alongside the QTF's oscillation amplitude. The data acquisition system, consisting of a 16-bit ADS1115 Analog-to-Digital Converter (ADC) and a PIC18F4550 microcontroller, was used to capture and digitize the amplitude readings with high precision. This setup allowed for high-resolution monitoring of QTF's oscillation amplitude at each vacuum step.

5. **Data Processing**

   After the vacuum measurements are completed, the data was processed to calculate resonance impedance from the amplitude readings. Since the QTF

is being driven through a constant voltage of 100 mV, the oscillation amplitude corresponds to the current flowing through QTF. Using ohm's law, resonance impedance can be calculated as:

$$Z = \frac{100mV}{I} \tag{3.6}$$

Where, I is the current calculated from amplitude data. The resulting impedance values are validated against the established relation, discussed in section 3.1.2.1 and is discussed in further details in next chapter.

3.3 Challenges and Design Iterations

3.3.1 Challenges

During the design and testing phases, several challenges were encountered:

3.3.1.1 Temperature Sensitivity

Quartz tuning forks are inherently sensitive to temperature fluctuations, which affects their resonant impedance and lead to inaccurate pressure readings particularly in vacuum region. To mitigate this, a temperature control system was integrated into the experimental setup to maintain stable conditions. The temperature dependence of QTF resonance impedance and its mitigation has been discussed in detail in next chapter (chapter 4).

3.3.1.2 Sealing Issues

Achieving a leak-tight seal in the sensor housing was another critical challenge. Initially, adhesive resins like Araldite were employed to seal the sensor housing. However, under high positive pressure conditions, the resin could not maintain the

necessary leak-tight environment, leading to degradation in sensor performance and process safety, as maintaining chamber integrity is crucial.

3.3.1.3 Low Resolution in Amplitude Measurements

The sensor's early design incorporated the built-in 10-bit ADC of the PIC18F4550 microcontroller for both initial data acquisition and vacuum measurement. While sufficient for low vacuum measurements, this resolution proved inadequate for the high vacuum range (10^{-3} to 10^{-2} mbar), where small variations in oscillation amplitude need to be detected. The low resolution made it difficult to capture these subtle changes accurately, particularly in high vacuum conditions where oscillation amplitude variation is very low.

3.3.2 Design Improvements

To address these challenges, several design improvements were implemented after the initial rounds of testing:

3.3.2.1 Improved Sealing

To resolve the issue of maintaining a leak-proof environment, adhesive resins were replaced with Viton O-rings, which provided better durability and sealing capability under both high vacuum and high-pressure conditions. These O-rings are well-known for their excellent chemical resistance and mechanical resilience, ensuring that the sensor housing remained leak tight across whole pressure range. This enhanced the sensor's reliability in extreme environments.

3.3.2.2 Enhanced ADC Resolution

Recognizing the limitations of the built-in 10-bit ADC, the design was upgraded to incorporate an external 16-bit ADC (ADS1115), which provided significantly

better resolution, sufficient for the accurate detection of small oscillation amplitude variations in the high vacuum range. The higher resolution of amplitude shifts, corresponding to pressure changes, enabled improved the accuracy and enhanced measuring limit of the vacuum readings.

Through these design iterations, the sensor was significantly improved in terms of performance, reliability, and accuracy, ensuring that it could function effectively across a wide spectrum of vacuum and positive pressure environments.

3.4 Conclusion

This chapter has outlined the comprehensive process behind the development of the quartz tuning fork-based compound gauge, with a wide operational range. By carefully selecting materials, refining the mechanical and electrical design, and employing precise calibration techniques, it was made sure that the sensor is able to meet the objectives of the research. Challenges encountered during the design process were addressed through iterative improvements, ensuring the sensor's robustness across its operational range.

Chapter 4

Results and Discussion

This chapter presents the results obtained from the experimental evaluation of the quartz tuning fork-based compound pressure gauge and their validation against the theoretical calculations and established standards. The performance of the gauge is analyzed in terms of sensitivity, accuracy, repeatability and stability across the complete range of its measurement; 10^{-3} mbar to 10 bar and the results are compared with conventional pressure and vacuum sensors to validate the accuracy and reliability of the new sensor. Key findings, trends, challenges and their mitigation are discussed in detail.

4.1 QTF Parameters Calculations

There are certain parameters related to the quartz tuning fork sensor and the gas under pressure measurement for measurement of pressure. The calculations/values of such parameters are detailed below.

4.1.1 Parameters for Vacuum Measurement

As described earlier in section 3.1.2.1 that electrical impedance of quartz tuning fork changes with change in vacuum level around it and this change in impedance

is given by the relations:

$$\Delta Z = \frac{2\eta_0 V^2 cos\theta}{A_m^2}.(6\pi\eta' R + 3\pi R^2\sqrt{2\eta'\rho\omega}) \tag{4.1}$$

where,

$$\eta' = \frac{\eta}{1 + (\frac{L}{R})(C_1 + C_2 e^{(-C_3\frac{R}{L})})} \tag{4.2}$$

Following are the calculations and details of different parameters required by equations (4.1) and (4.2) in order to calculate the vacuum from measured oscillation amplitude:

4.1.1.1 Calculation of Intrinsic Impedance of QTF

The QTF crystal, at high vacuum, is driven by a constant voltage of 100 mV_{rms} and using an inverting op-amp configuration the impedance of oscillator is calculated as shown in figure 4.1 below:

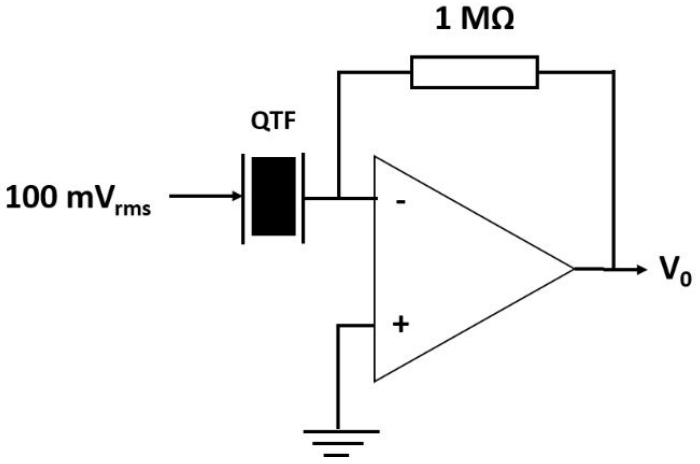

FIGURE 4.1: Schematic for Impedance Calculation of QTF)

Using the equations of an inverting amplifier, QTF's impedance Z_0 can be calculated as:

$$\frac{V_0}{(100mV)} = \frac{1M\Omega}{Z_0} \tag{4.3}$$

$$V_0 = 5.76\ V_{rms}$$

So,

$$Z_0 = \frac{1M\Omega x100mV}{5.76V} \tag{4.4}$$

$$Z_0 = 17.36 \text{ K}\Omega$$

4.1.1.2 Measurement of Mechanical Amplitude of QTF

By using microscope, the vibration amplitude of quartz tuning fork oscillator (being driven by a 100 mV_{rms} signal) is measured to be 2 μm at 10^{-3} mbar and 0.3 μm at 1 x 10^{+3} mbar (atmospheric pressure). The oscillation amplitude of quartz oscillator decreases linearly with pressure. By using the equation of line, following relation is developed between oscillation amplitude A_m and pressure P:

$$A_m = C_a[0.3 + \frac{2 - 0.3}{1000 * P}] \tag{4.5}$$

where,

$$C_a = 2.0067 - 0.743 \ln(\log_{10}(P) + 4) \tag{4.6}$$

4.1.1.3 Calculation of QTF and Test gas Parameters

A. Parameters of Nitrogen Gas:

Pure, dry Nitrogen gas (N_2) has been used as a primary test gas for this research. The parameters of Nitrogen gas required by the equations (4.1) and (4.2) are enlisted in the table 1.1.

TABLE 4.1: List of Nitrogen Gas Parameters

Sr. No.	Parameter	Symbol	Value
1	Molecular Weight	M	28.02 $gmol^{-1}$
2	Coefficient of Viscosity for Nitrogen gas	η	0.0178 mPa.s
3	Density of Nitrogen gas (pressure-dependent)	ρ	1.146 x $\frac{P}{1013}$ kgm^{-3}
4	Mean free path of Nitrogen gas particles (pressure-dependent)	L	$\frac{6x10^{-5}}{P}$ mbar.m

B. Parameters of Quartz Tuning Fork Crystal:

There are several parameters of quartz tuning fork used in the research and required by the equations (4.1) and (4.2). All those parameters are enlisted in the table 4.2.

TABLE 4.2: List of QTF Parameters

Sr. No.	Parameter	Symbol	Value
1	Intrinsic Impedance of QTF at high Vacuum	Z_0	17.36 (KΩ)
2	Resonance Frequency of QTF	f_r	32763.8 Hz
3	Thickness of QTF	R	0.3 cm
4	Conversion Efficiency of the Electric Energy to the Mechanical Energy	η_0	0.90 – 0.95 [76]
5	Phase difference between Voltage and Current	θ	0*
6	Amplitude of the forced vibration of quartz tuning fork's prongs	A_m	Equations (4.5) and (4.6)

* Since the oscillator always vibrate in resonance therefore its voltage and current are always in phase and hence the phase difference is always zero. Therefore term $\cos\theta$ in equation (4.1) is always 1.

C. Other Parameters Required for Calculations

There are some other parameters, indirectly related to either quartz tuning fork or Nitrogen gas (the primary test gas used for this research) which are required for calculations by the equations (4.1) and (4.2). These parameters are enlisted in the table 4.3.

TABLE 4.3: List of Other Vacuum Calculation-Related Parameters

Sr. No.	Parameter	Symbol	Value
1	Excitation Voltage of QTF Oscillator	V	0.1 V_{rms}
2	Ideal Gas constant	R_0	8.31446 $mbar.m^3.mol^{-1}.K^{-1}$
3	Temperature	R	298 K
4	Millikan's Constants	C_1	1.00
5	Millikan's Constants	C_2	1.90
6	Millikan's Constants	C_3	0.88

4.1.2 Parameters calculation for Positive Pressure Measurement

From equation (3.5) in previous chapter, we know that change in resonance frequency of QTF with positive pressure is related as follows:

$$\Delta f_r = A_f P \tag{4.7}$$

The constant A_f can be calculated experimentally by subjecting the quartz oscillator to changing pressures and recording the values of frequency at corresponding pressure levels. The constant A_f is equal to the slope of resulting linear graph. The initial frequency of the QTF at atmospheric pressure is 32.755 kHz.

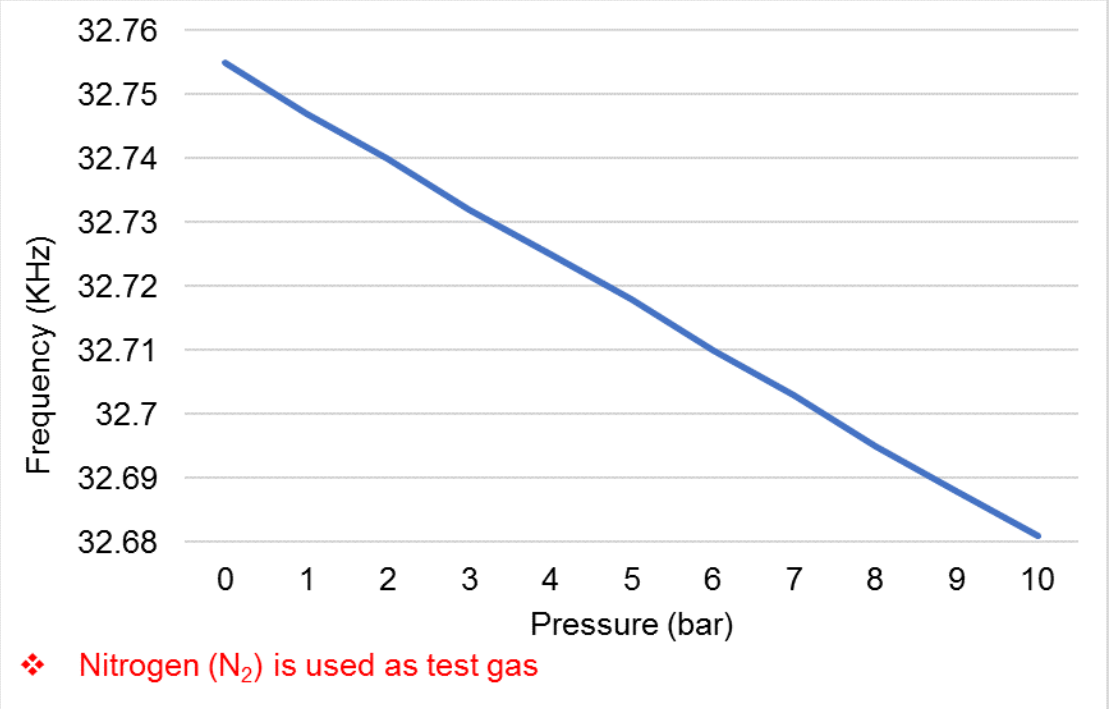

FIGURE 4.2: Variation of QTF Frequency with Positive Pressure

From the linear graph of pressure vs. frequency in figure 4.2, we can calculate the slope of the line that is equal to constant A_f. Therefore,

$$A_f = \text{-}7.4$$

If we put the value of slope A_f, the final relation for pressure from equation (4.7) becomes:

$$P = -\frac{\Delta f_r}{7.4} \tag{4.8}$$

4.2 Measurement Results

This section summarizes the results of QTF in comparison with pressure and vacuum references.

4.2.1 Vacuum Region

The impedance of QTF at different vacuum levels is calculated theoretically and is measured experimentally as well using Nitrogen (N_2) as test gas. The results are summarized in table 4.4 and displayed graphically in figure 4.3.

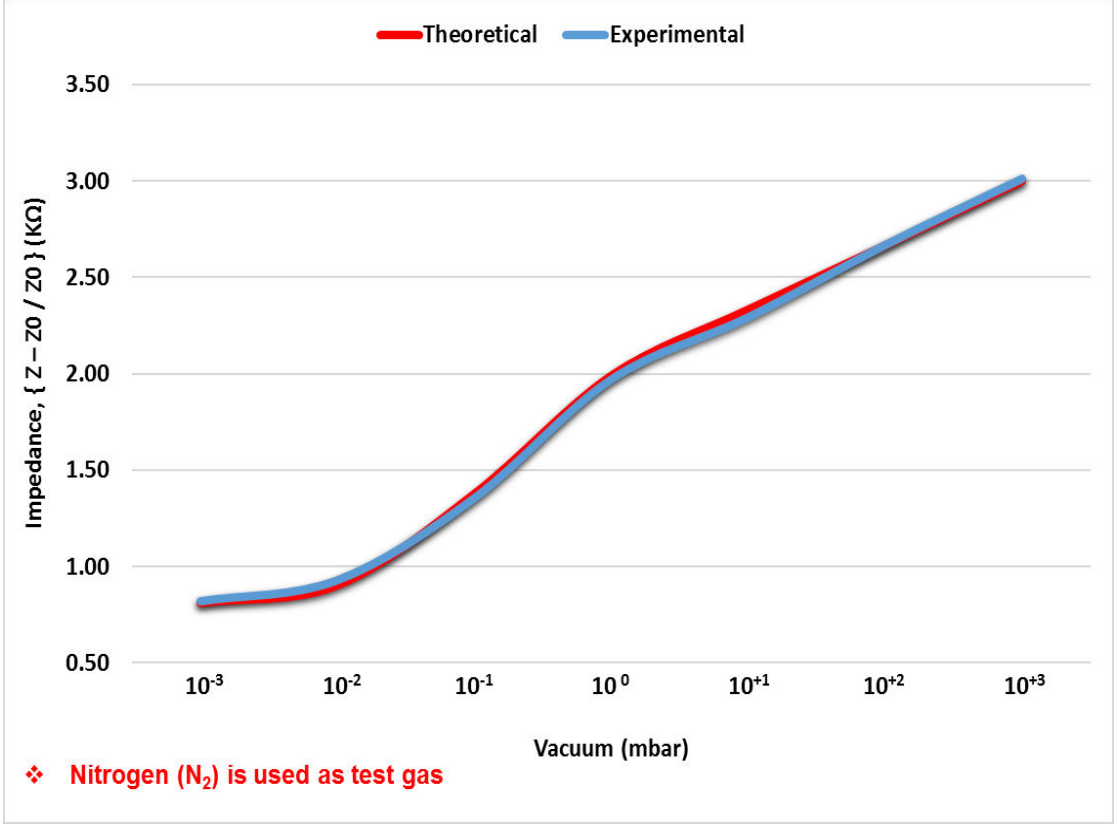

FIGURE 4.3: Experimental vs. Theoretical Results for Change in Impedance of QTF with Vacuum

TABLE 4.4: Experimental vs. Theoretical Results of QTF Impedance Dependence on Vacuum

Vacuum (mbar)	Calculated Impedance (KΩ)	Measured Impedance (KΩ)
10^{-3}	18.27	18.27
10^{-2}	18.48	18.53
10^{0}	30.42	30.23
10^{+1}	45.87	44.39
10^{+2}	78.73	81.38
10^{+3}	150.13	158.70

4.2.2 Positive Pressure Measurement (0 to 10 bar)

From section 4.1.2, the resonance frequency of QTF at different levels of pressure is calculated and is also measured experimentally using Nitrogen (N_2) as test gas. The results are summarized in table 4.5 and displayed graphically as well in figure 4.4.

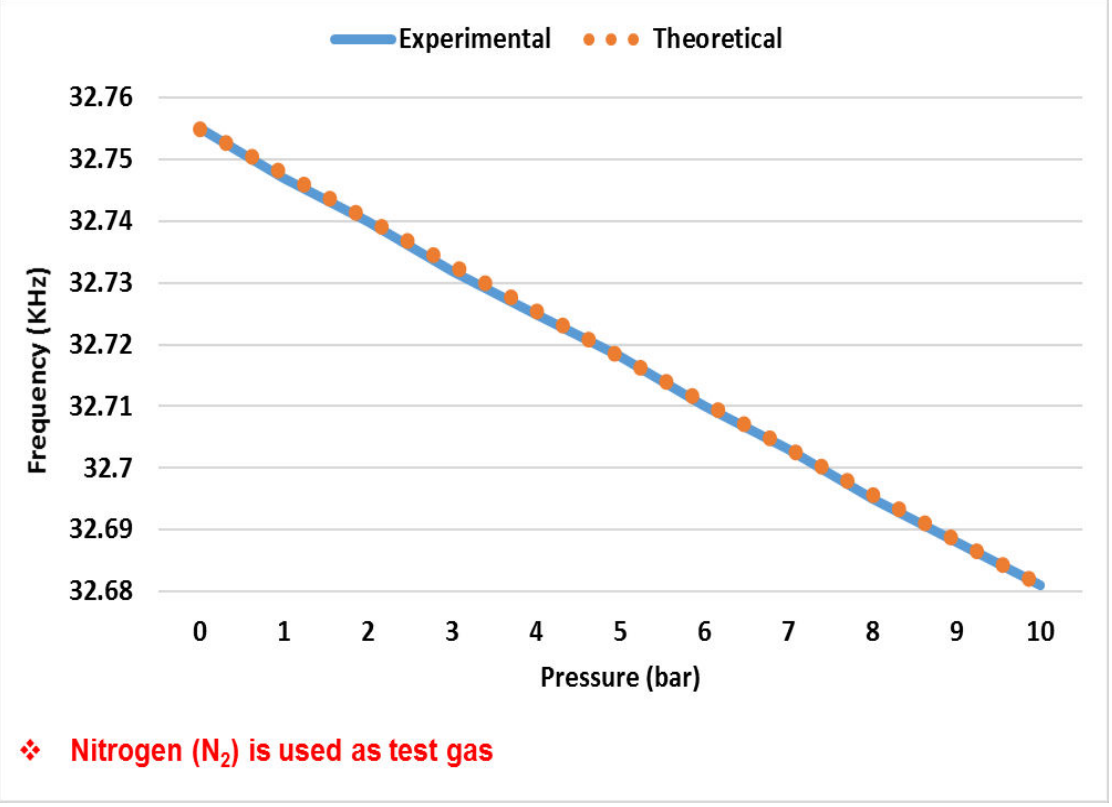

FIGURE 4.4: Experimental vs. Theoretical Results for Change in Frequency of QTF with Pressure

TABLE 4.5: Experimental vs. Theoretical Results of QTF Frequency Dependence on Pressure

Pressure (bar)	Theoretical Frequency (KHz)	Measured Frequency (KHz)
1	32.7476	32.747
2	32.7402	32.740
3	32.7328	32.732
4	32.7254	32.725
5	32.7180	32.718
6	32.7106	32.710
7	32.7032	32.703
8	32.6958	32.695
9	32.6884	32.688
10	32.6810	32.681

4.3 Calibration Results

To verify the accuracy, reliability and repeatability of developed sensor, calibration was performed against standard gauges, with high accuracy, as reference. The quartz tuning fork sensor demonstrated excellent repeatability and high accuracy across the whole pressure range.

4.3.1 Vacuum Calibration

The QTF based vacuum measurement demonstrates high linearity with reference pressure with an accuracy better than ±10% as demonstrated by the calibration curve of QTF in figure 4.5 below.

4.3.2 Positive Pressure Calibration

Just like vacuum, the QTF based positive pressure measurements also demonstrate high linearity with reference pressure with an accuracy of better than ±5% as demonstrated by the calibration curve of QTF in figure 4.6 below.

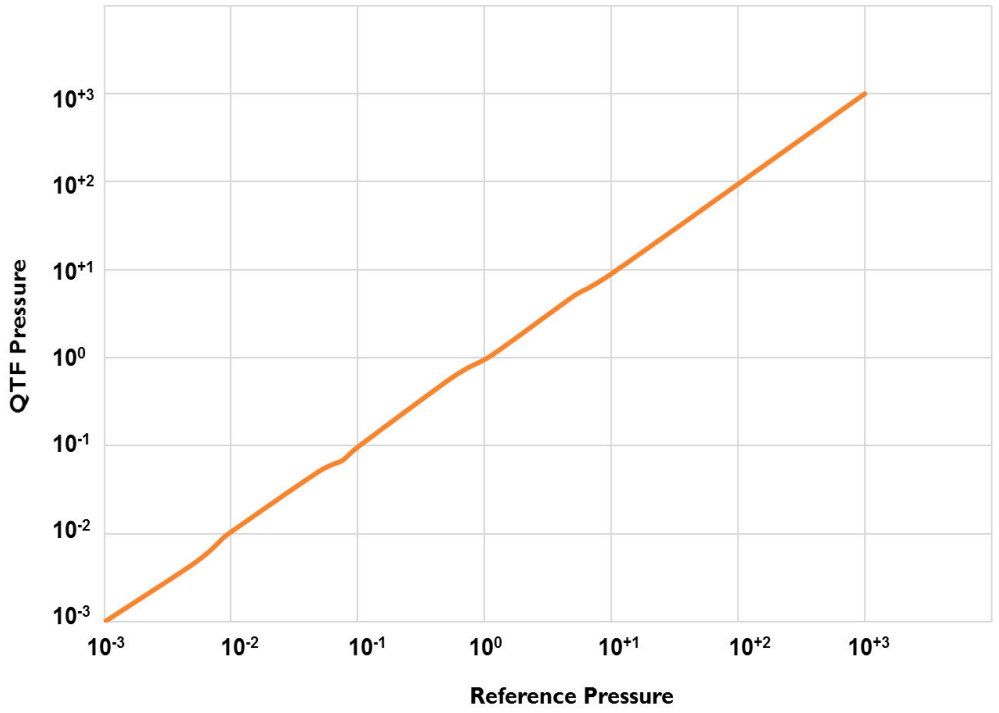

❖ Nitrogen (N_2) is used as test gas

FIGURE 4.5: Calibration Curve of QTF in Vacuum Region

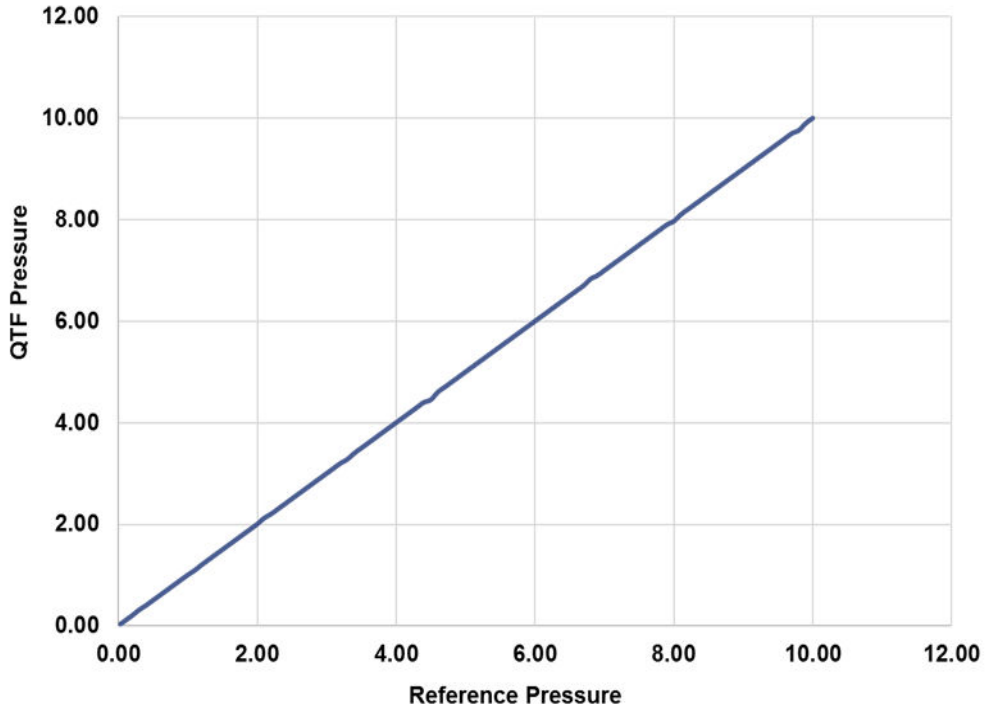

❖ Nitrogen (N_2) is used as test gas

FIGURE 4.6: Calibration Curve of QTF in Positive Pressure Region

4.4 Error Analysis

4.4.1 Sources of Error

Following are some factors which negatively impact QTF's pressure measurement performance:

4.4.1.1 Temperature

Figure 4.7 shows the temperature dependence of quartz oscillator's intrinsic impedance (at pressure ¡ 10^{-3} mbar), measured in the temperature range 20 – 40 °C. The figure shows that, there is almost linear relationship between the impedance and temperature T, which is given as:

$$Z_T = 0.2534T + 12.30 \tag{4.9}$$

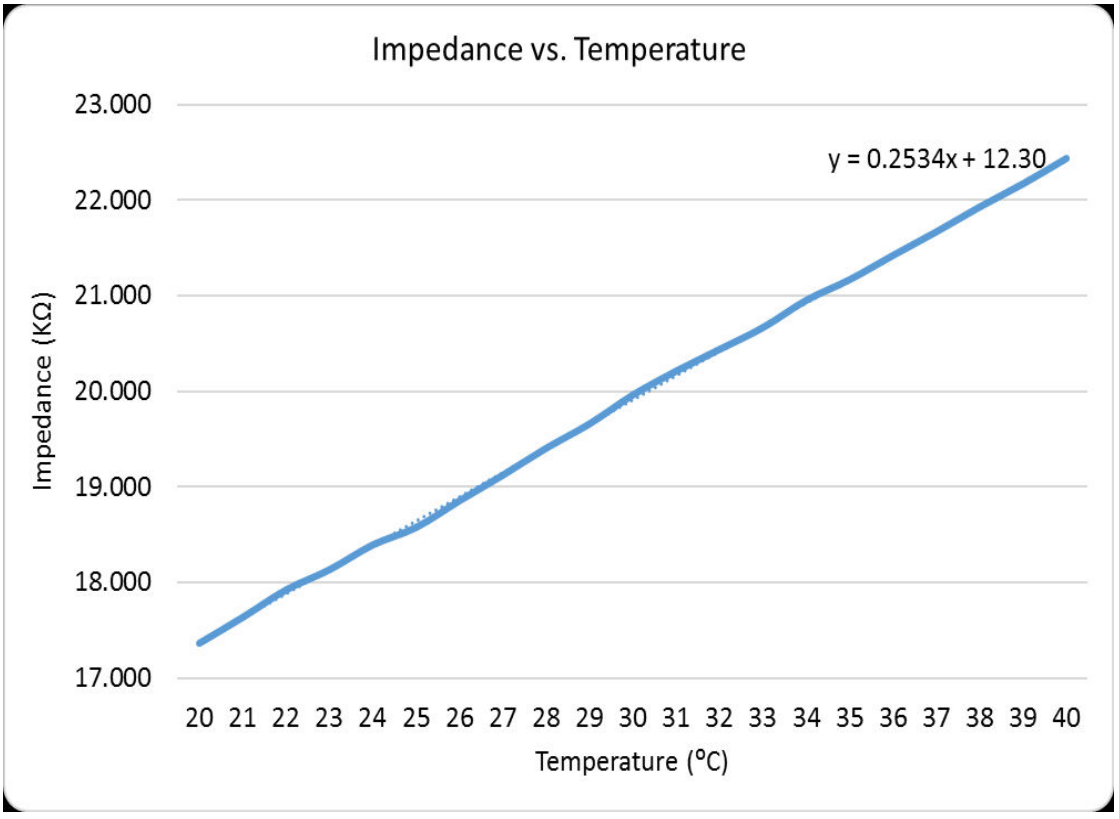

FIGURE 4.7: Temperature Dependence of QTF Impedance

4.4.1.2 Gas Dependence

Like all other indirect-type pressure gauges, the quartz tuning fork sensor is also gas-dependent. From equation (4.1), we can see that:

$$\Delta Z \propto \sqrt{\rho} \tag{4.10}$$

Where,

$$\rho = \frac{PM}{RT} \tag{4.11}$$

With R and T being constant:

$$\Delta Z \propto \sqrt{MP} \tag{4.12}$$

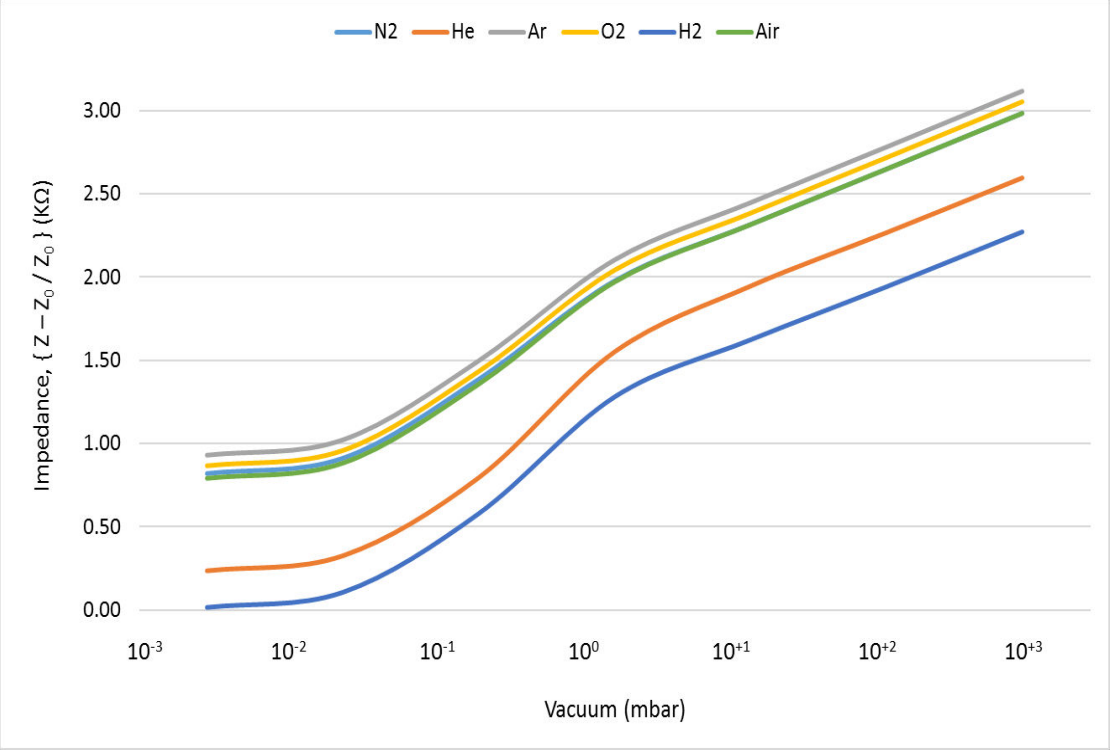

FIGURE 4.8: Gas Dependence of QTF Impedance

The results are displayed graphically in figure 4.8.

Similarly, the change in frequency is also gas dependent [66]:

$$\Delta f_r \propto \rho \propto MP \tag{4.13}$$

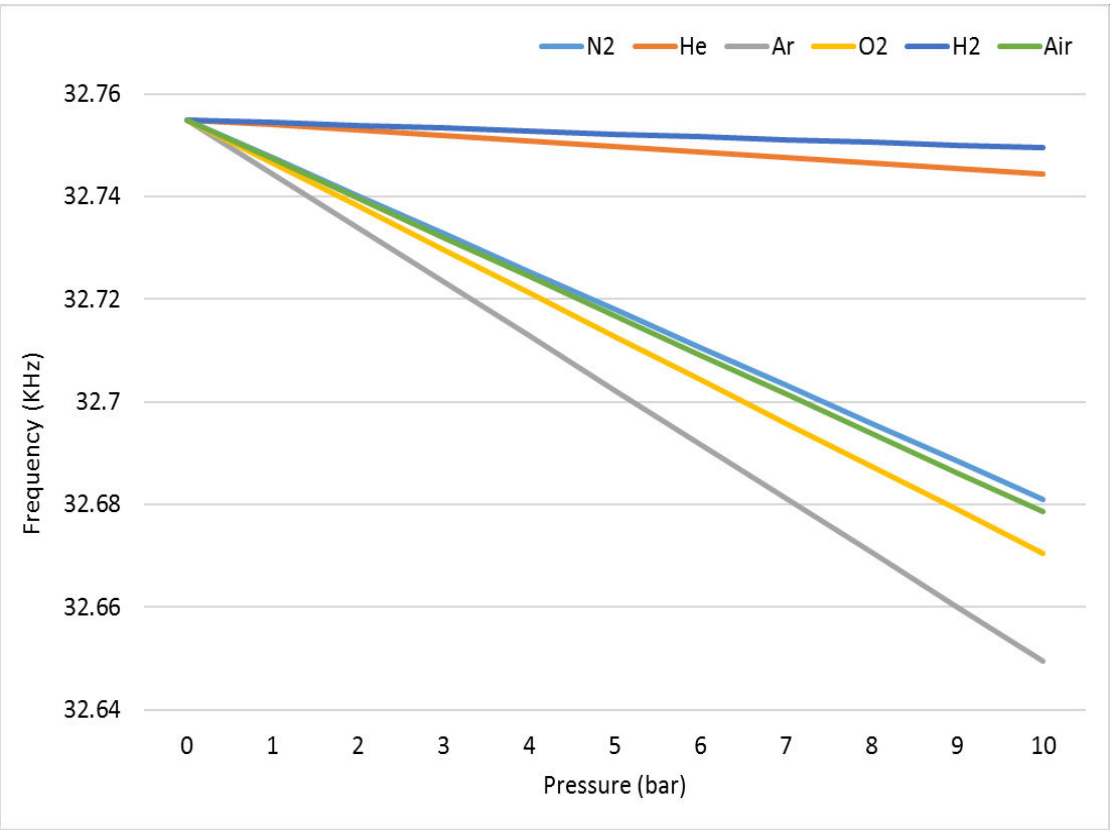

FIGURE 4.9: Gas Dependence of QTF Frequency

Figure 4.9 shows that frequency of quartz oscillator changes linearly with exerted pressure from all gasses but with different mass-dependent slope. The gasses with higher molecular masses have rather higher sensitivity (slope) in terms of frequency change and lighter gasses disturb frequency with lower intensity (slope).

4.4.2 Error Mitigation

For accurate and stable results, the problems caused by factors affecting the gauge's performance need to be addressed. Compensation techniques were applied to account for any variations and negative impact caused by the factors discussed above.

4.4.2.1 Temperature

To compensate for temperature's variation in QTF gauge's pressure reading, the temperature must be known at first hand. For this purpose, a digital, low-cost temperature sensor DS18B20 was used. DS18B20 can measure temperature in the range of -10 – 85 °C with an accuracy of ±5 °C. Once the temperature is known, from equation (4.9) we can calculate the actual impedance value from the measured value.

4.4.2.2 Gas Dependence

For known gas composition or pure gasses (known molecular mass M), we can just put the right value of M in the impedance-vacuum or frequency-pressure formulae to measure the correct value of vacuum or pressure.

4.5 Performance Validation

The performance validation of the quartz tuning fork-based pressure sensor ensures that the design objectives met in terms of accuracy, reliability, and robustness across the full range of pressures. Several aspects of the sensor's performance were evaluated through systematic testing:

4.5.1 Accuracy

In order to evaluate the accuracy of developed sensor, it was calibrated against reference gauges as per established standards of calibration (ISO 17025 and ISO 3567) to ensure reliability and traceability of measurements. In vacuum region, the sensor was calibrated against a series of capacitance diaphragm gauges while positive pressure region was calibrated against dead weight tester. The calibration results, with calculated percentage error, are summarized in tables 4.6 and 4.7.

TABLE 4.6: Calibration Results for Vacuum Region

Ref. Pressure "P_R" (mbar)	QTF Pressure "P_T" (mbar)	% Error $\frac{P_T - P_R}{P_R}$ x 100
2.01E-03	2.00E-03	-0.50
5.02E-03	5.10E-03	1.59
8.01E-03	7.80E-03	-2.62
2.00E-02	1.90E-02	-5.00
5.00E-02	4.80E-02	-4.00
8.01E-02	7.80E-02	-2.62
2.02E-01	2.00E-01	-0.99
5.03E-01	5.10E-01	1.39
8.02E-01	8.10E-01	1.00
2.03E+00	2.10E+00	3.45
5.03E+00	5.10E+00	1.39
8.01E+00	7.90E+00	-1.37
2.01E+01	2.10E+01	4.48
5.01E+01	5.00E+01	-0.20
8.02E+01	8.20E+01	2.24
2.03E+02	2.10E+02	3.45
5.03E+02	5.20E+02	3.38
8.04E+02	8.40E+02	4.48
1.00E+03	1.00E+03	1.00

The calibration results indicate that maximum observed error in the vacuum region is 5% with low-pressure region (below 1 mbar) demonstrating minimal error, reinforcing the sensor's capability for precise vacuum measurement.

The calibration results in pressure region indicate that error is limited to a maximum of 2%, which is comparable to most of the highly accurate pressure sensors being used in industrial and research applications.

These results show that the QTF gauge exhibits high accuracy in both regions of pressure which verify our claim of a compound gauge which is equally specialized in both regions. Also the results show that gauge has superior performance in positive pressure region in terms of accuracy.

TABLE 4.7: Calibration Results for Positive Pressure Region

Ref. Pressure "P_R" (mbar)	QTF Pressure "P_T" (mbar)	% Error $\frac{P_T - P_R}{P_R}$ x 100
1.35	1.37	1.48
2.14	2.17	1.40
3.23	3.29	1.86
4.02	4.1	1.99
5.46	5.51	0.92
6.31	6.33	0.32
7.27	7.26	-0.14
8.38	8.33	-0.60
9.09	9.01	-0.88
10	10.01	0.10

4.5.2 Sensitivity

The sensitivity of the developed quartz tuning fork compound pressure gauge is evaluated based on following two factors:

1. Resolution – the smallest detectable change in pressure.
2. Response Time – the time required to detect the change in pressure.

4.5.2.1 Resolution

The resolution of quartz tuning fork sensor in vacuum region is 1 x 10^{-4} mbar, which is comparable to or better than several commercially available vacuum gauges. For the positive pressure region, the sensor has a resolution of 0.1 bar. While this resolution is lower than some high-precision digital pressure sensors, it is more than adequate for many industrial and scientific applications. However, the slightly lower resolution in this region is not the limitation of sensor itself but rather a constraint imposed by the low-cost frequency measurement mechanism used in this research. With more sophisticated frequency detection systems, this resolution can be significantly enhanced further.

4.5.2.2 Response Time

The quartz tuning fork is much faster than conventional sensors. The response time of developed sensor is less than 100 ms in vacuum region and approximately 10 ms in positive pressure region.

4.5.3 Repeatability

To test the repeatability of sensor, a series of five consecutive measurement cycles were conducted in both the vacuum and positive pressure regions under identical environmental and experimental conditions. The results are very satisfactory and are discussed in following sections.

4.5.3.1 Vacuum Region

The calibration results, shown in figures 4.10, demonstrate that the sensor is highly repeatable. The maximum standard deviation in vacuum region is 4.5% which is well within acceptable range.

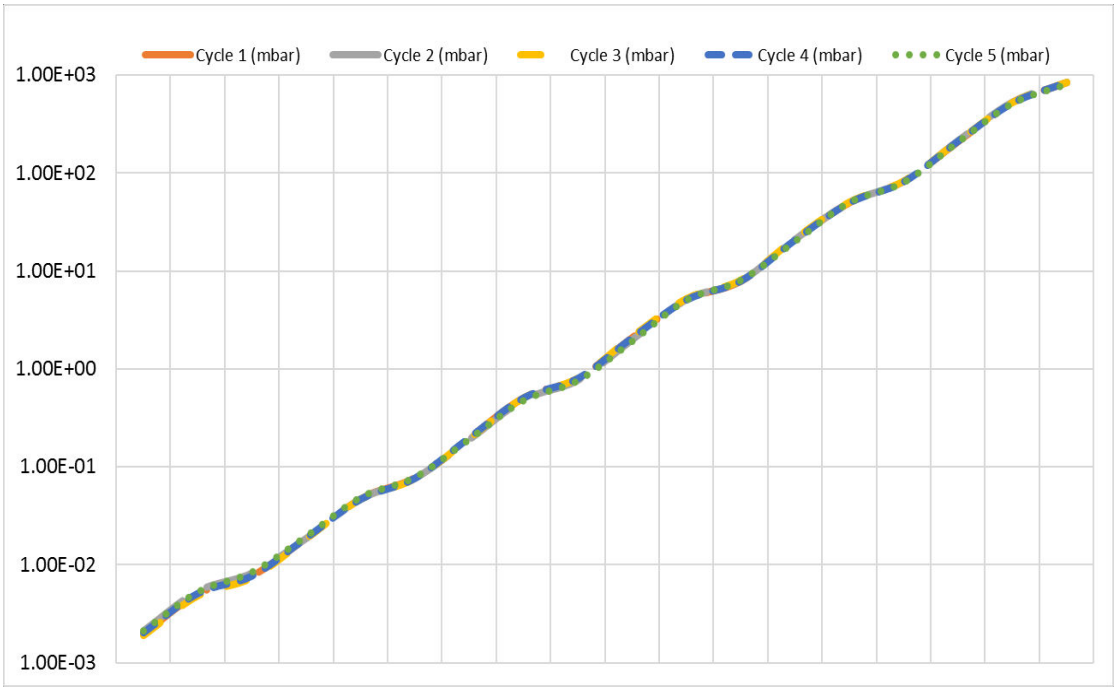

FIGURE 4.10: Repeatability of QTF Calibration in Vacuum Region

4.5.3.2 Positive Pressure Region

The calibration results, shown in figure 4.11, demonstrate that the sensor is very highly repeatable in positive pressure region. The maximum standard deviation in this region is 0.92% only which is comparable to highly precise pressure instruments.

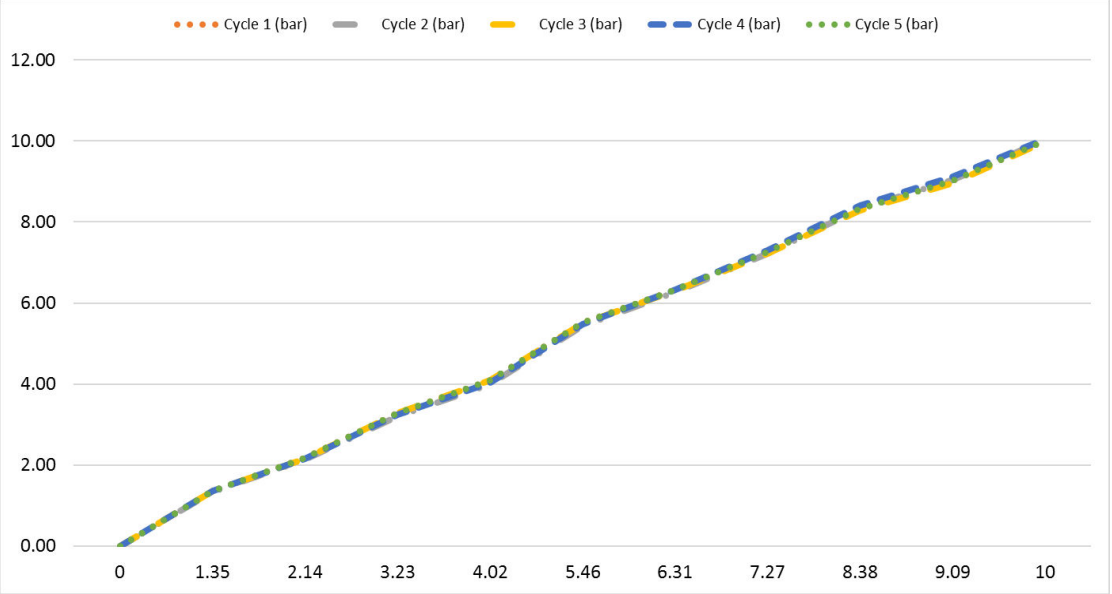

FIGURE 4.11: Repeatability of QTF Calibration in Positive Pressure Region

4.5.4 Stability

Sensor stability is one of the primary demands for industrial environments. Stability test was performed to ensure that the sensor's performance remained robust over extended periods of use, especially under harsh conditions like high vacuum or high pressure. Two types of stability testing was performed:

1. Short-term tests involved subjecting the QTF-based sensor to continuous exposure to both vacuum conditions and positive pressures over 100 hours continuously.

2. Long-term tests involved recalibrating the sensor against the same reference after a gap of 6 months and check for any inconsistencies.

4.5.4.1 Short-Term Stability Test

A. Vacuum Region

The sensor was evacuated to a vacuum level of 2.0 x 10^{-3} mbar for 100 hours under continuous pumping. The results plotted in figure 4.12 show that sensor deviated ±3.0% only which might be due to variation in environmental factors and pump variation.

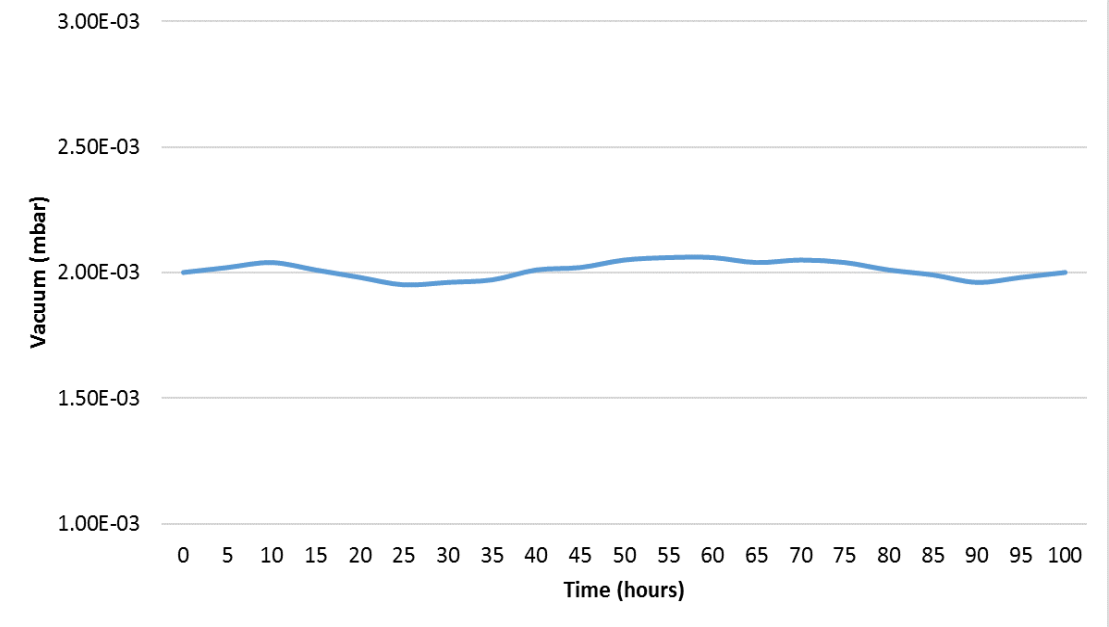

FIGURE 4.12: Stability of QTF Sensor for 100 Hours in Vacuum Region

B. Positive Pressure Region

The sensor was pressurized to 5.51 bar for 100 hours under a leak-tight environment. The results plotted in figure 4.13 show that sensor deviated ±0.54% only which might be due to variation in environmental factors.

4.5.4.2 Long-Term Stability Test

To test the long term reliability of sensor, it was calibrated twice against the same reference setup with a gap of 6 months.

A. Vacuum Region

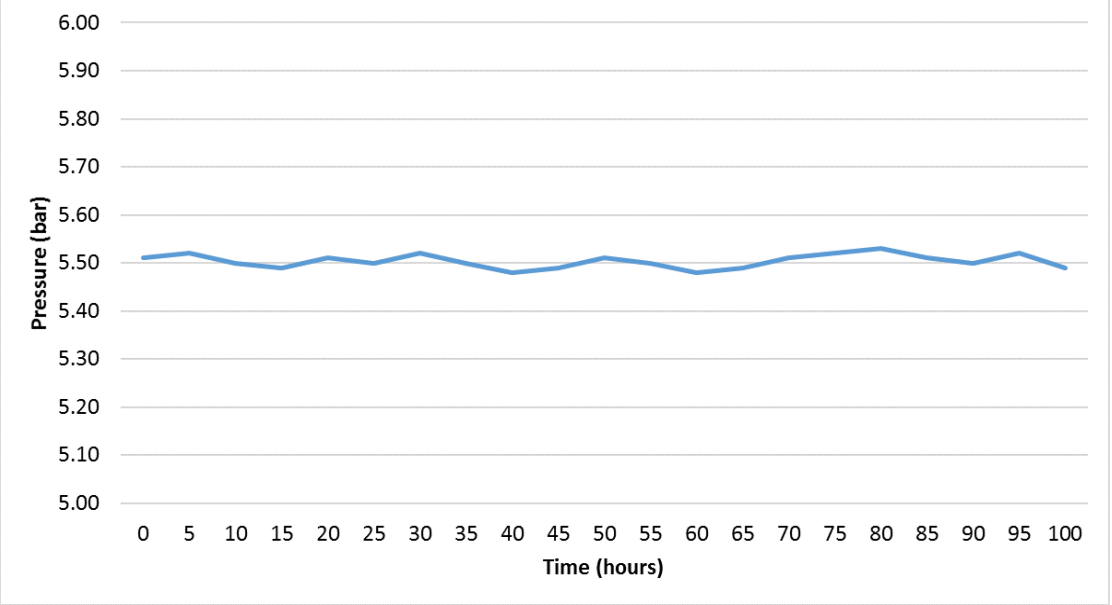

FIGURE 4.13: Stability of QTF Sensor for 100 Hours in Positive Pressure Region

The results plotted in figure 4.14 show that there are only slight differences at some points but overall results are quite satisfactory. There was 8% of maximum deviation from the previous calibration in the viscous flow region. The difference was approximately 2% in the molecular flow region.

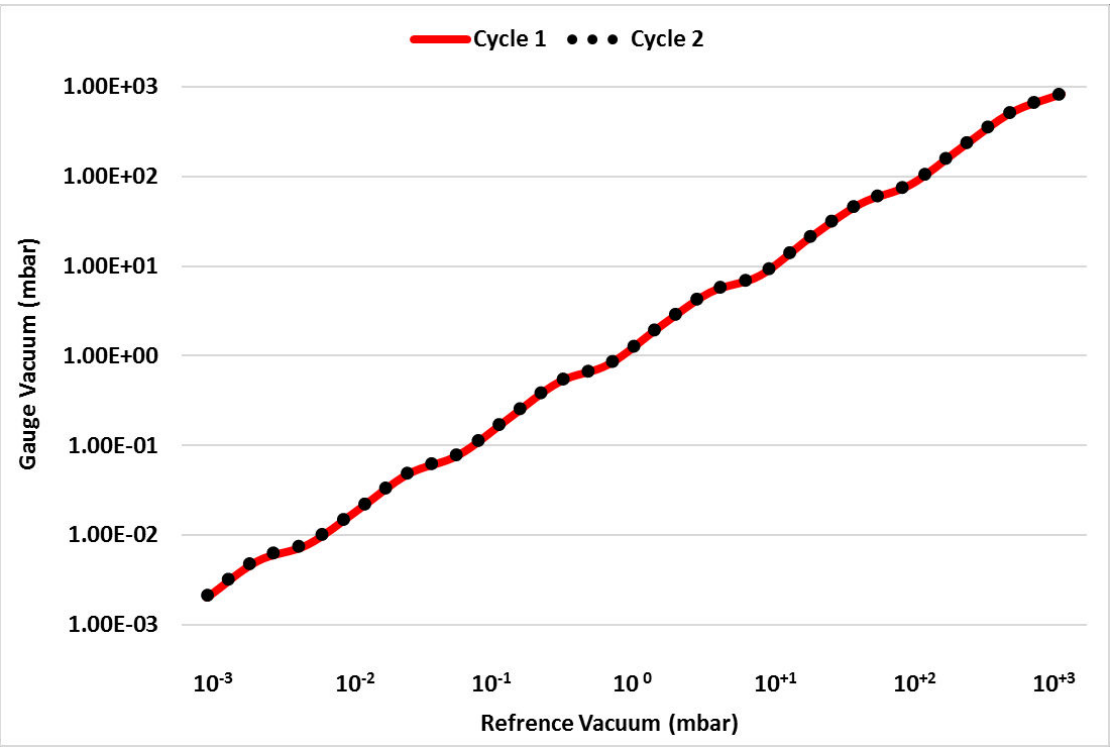

FIGURE 4.14: Calibration Curves of QTF Sensor with 6-Month Gap, in Vacuum Region

B. Positive Pressure Region

The results plotted in figure 4.15 show that the two calibration curves closely follow each other with slight differences at some points. The maximum deviation of second calibration curve was less than 1% which shows that this sensor is very much stable in positive pressure region.

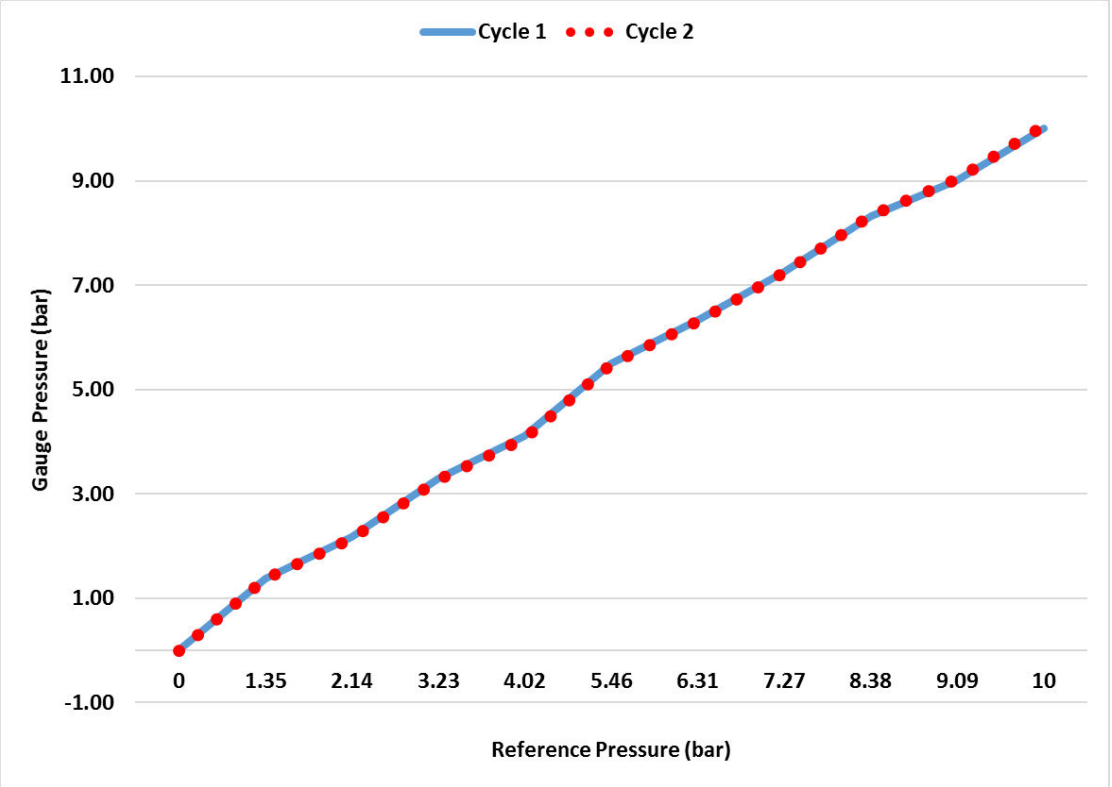

FIGURE 4.15: Calibration Curves of QTF Sensor with 6-Month Gap, in Positive Pressure Region

The stability tests confirmed the sensor's durability and reliability in real-world applications, especially industrial environment, where continuous or long-term pressure monitoring is required.

4.5.5 Comparative Analysis

To evaluate the QTF sensor's superiority, a comparison is made between the quartz tuning fork sensor and conventional pressure gauges in terms of range, accuracy, operational region (vacuum, pressure or compound), operational limitations, principle cost and maintenance cost. This comparative analysis helps establish the

advantages and trade-offs of the developed sensor relative to existing technologies. The results are summarized in table 4.8. The quartz tuning fork sensor not only outperformed existing compound gauges but also other conventional gauges in its region of operation in one way or another.

4.6 Discussion

The results validate the feasibility of using quartz tuning forks as compound pressure sensors. The sensor's ability to measure both vacuum and higher pressures with a single device represents a significant advancement. The dual-mode operation (amplitude for vacuum and frequency for positive pressure) eliminates the need for multiple sensors, reducing cost and complexity. Key advantages of the quartz tuning fork-based sensor include:

1. High sensitivity in the vacuum region
2. Linear response in the positive pressure region
3. Compact design and ease of integration
4. Low cost

However, certain limitations were identified, including susceptibility to environmental factors, especially temperature, and slight deviations at extreme pressure levels. Future iterations will focus on enhancing accuracy and expanding the measurement range.

4.7 Possible Applications of Proposed Research

The quartz tuning fork based compound pressure gauge has a wide range of potential applications across various fields due to its high precision, miniaturization and broader measuring range. Here are some possible applications of the gauge:

4.7.1 Fluid Catalytic Cracking

Fluid Catalytic Cracking (FCC) is a key refining process that breaks down heavy hydrocarbons into smaller, more valuable components. The reactor and regenerator operate at moderate pressures (1.72 barg in the reactor and 2.41 barg in the regenerator) to facilitate the conversion of heavy gas oil into lighter products. To prevent the formation of petroleum coke, which can clog furnace pipes during crude oil distillation, the process is maintained below 380 °C. These unconverted heavy hydrocarbons are then directed to the vacuum distillation unit, which operates at approximately 10 to 50 mbar and lowers the boiling points of these heavy components to well below 380 °C. The compound gauge developed in this research provides an innovative solution for precise measurement of both vacuum and positive pressures in refining applications, ensuring efficient process monitoring and control.

4.7.2 Leak Testing

Industrial chambers, pipes and joints require leak-testing before being employed in the process for safe operation. Gas storage spaces also need leak testing for safety as any leakage could cause severe damage to life and property. Leak testing is done using both vacuum and high pressures for different applications/ processes. Traditionally, different sensors are used for the measurement of both vacuum and pressures. However, a single quartz tuning fork sensor can be used for measurement of both vacuum and high pressures in such applications.

4.7.3 Chemical Industry

Some chemical processes require vacuum to create clean environment or remove any moisture present in the reaction chamber and then require high pressures for efficient chemical processing. Quartz tuning fork, being a compound sensor, is ideal for such applications.

4.7.4 Vacuum Pressure Swing Adsorption (VPSA)

Vacuum Pressure Swing Adsorption (VPSA) is a gas separation process that operates by adsorbing gases at elevated pressures (4–5 bar) and regenerating the adsorbent under vacuum. This technique is commonly used for oxygen and nitrogen separation, utilizing materials like zeolites to selectively adsorb specific gases. The compound gauge developed in this research provides an effective solution for monitoring both the high-pressure adsorption phase and the vacuum regeneration phase.

4.7.5 Scientific Research

In scientific research, that involves accurate and broad pressure measurements, such as in physics experiments or material testing, quartz tuning fork can enhance measuring capabilities.

In summary, the quartz tuning fork-based compound pressure gauge offers versatility that can benefit a wide range of industries and applications. Its ability to provide accurate measurements in a diverse and challenging environment makes it a valuable technology for enhancing performance in numerous fields.

4.8 Conclusion

The experimental results demonstrate that the quartz tuning fork-based compound pressure gauge is a reliable and accurate tool for compound pressure measurement. The sensor's performance meets or exceeds that of conventional gauges, highlighting its potential for industrial and scientific applications, paving the way for future innovations in compound pressure measurement technology.

TABLE 4.8: Comparison of Quartz Tuning Fork Compound Sensor with Conventional Gauges

	Range	Accuracy	Operation	Limitations	Cost	Maintenance Cost
QTF	10^{-3} mbar – 10 bar	10%	Compound		Low	Low
U-Tube	1 mbar – 2 bar	5%	Compound	Toxic Liquid (Mercury)	Low	High
McLeod	10^{-6} mbar – 1 mbar	10%	Vacuum	Toxic Liquid (Mercury)	High	High
Bourdon	1 mbar – 1atm. 1 atm. – 100 bar	>10%	Compound	Mechanical Operation	Low	High
Strain	0 bar – 100 bar	10%	Pressure		Low	Low
Capacitance	10^{-4} mbar – 1 atm. & 0 bar – 100 bar	5%	Vacuum & Pressure	Specialized Materials	High	High
Piezoresistive	10^{-1} mbar – 1 atm. & 0 bar – 1000 bar	10%	Vacuum & Pressure		High	High
Pirani	10^{-3} mbar – 1 atm.	20%	Vacuum	High Temperature	Low	Low
Ionization	10^{-9} – 10^{-3} mbar	20%	Vacuum	Ionization	High	Low
Spinning Rotor	10^{-7} – 10^{-1} mbar	5%	Vacuum	Magnetic Field	High	High

Chapter 5

Alternatives to QTF in Compound Sensing

For the compound pressure gauge, the quartz tuning fork was selected due to its ability in handling both vacuum and positive pressure environments, along with its ability to deliver precise and reliable measurements across a wide pressure range using the same sensor. The quartz tuning fork's ability manifold electrical parameters' variation, prominent being resonance frequency and impedance, allows it to senses both vacuum and positive-pressure variations. Before finalizing the quartz tuning fork as the sensor of choice, other sensing technologies were considered, each offering unique advantages but ultimately falling short for this application. Below is a detailed review of the alternatives that were considered.

5.1 Capacitive Pressure Sensors

Capacitive pressure sensors are widely known for their excellent performance in both positive pressure and vacuum regions. These sensors work by detecting changes in capacitance as the distance, between two conductive plates, changes in response to applied pressure. Capacitive sensors offer high accuracy and can be

fine-tuned for specific ranges of pressure, making them suitable for pressure sensing applications in both vacuum and positive-pressure environments. However, several drawbacks made them less suitable for this compound pressure gauge:

5.1.1 Range Specificity:

Capacitive sensors typically require different sensor design (i.e., thickness) for measuring different pressure ranges. This means separate sensors would be needed for vacuum and positive-pressure regions, complicating the design and reducing the compactness of the system. Achieving a unified sensor capable of spanning the full range from 10^{-3} mbar to 10 bar would have required multiple sensors, defeating the goal of a compact, low-cost, wide-range device.

5.1.2 Cost and Complexity:

Capacitive sensors are relatively expensive compared to quartz tuning forks. They are often constructed from special materials, such as Inconel, which offers superior resistance to corrosion and extreme temperatures but adds to the overall cost of the system. Additionally, specialized machining is required to maintain the precision tolerances necessary for high-performance capacitive sensors, further increasing the cost and complexity of manufacturing.

These limitations made capacitive sensors less ideal for a compact and cost-effective design that could handle a wide range of pressures.

5.2 Piezoresistive Sensors

Piezoresistive sensors were another potential option considered for this research. These sensors are diaphragm type just like capacitance diaphragm sensors and detect pressure by measuring the change in electrical resistance in a material (typically silicon) when it is subjected to mechanical stress. Piezoresistive sensors are

widely used in positive-pressure applications due to their ruggedness, simplicity, wide measuring range and robust performance in harsh environments. Despite their durability and reliability in positive-pressure regions, several factors limited their suitability for this compound pressure gauge:

5.2.1 Limited Range:

Piezoresistive sensors are typically designed for a specific pressure range and struggle to perform across a wide range of pressures. While they are robust in positive-pressure conditions, their performance in vacuum or negative pressure environments is limited. Different designs or sensor configurations would be required for positive and negative pressure regions. For example, a sensor optimized for measuring positive pressures may become insensitive to negative pressures, while one designed for negative pressures may fail to accurately measure higher positive pressures.

This lack of versatility limits their usefulness in applications where a broad range of pressures needs to be measured using a single sensor.

Given these limitations, piezoresistive sensors were deemed unsuitable for a system that required seamless transition and accurate performance across a pressure range, from vacuum to positive pressures.

5.3 The Case for Quartz Tuning Fork

The quartz tuning fork sensor was ultimately selected as the optimal sensor for this research due to its unique ability to operate in both regions of pressure, from 10^{-3} mbar to 10 bar, without requiring multiple sensors or complex configurations. The quartz tuning fork can detect minute changes in oscillation amplitude (because of resonance impedance) in vacuum conditions and frequency shifts in response to positive pressure changes, making it an ideal sensor for dual-mode operation (vacuum and positive pressure sensor).

5.3.1 Sensitivity and Range:

The QTF provides high sensitivity across both vacuum and positive pressure regions, with oscillation amplitude increasing in vacuum conditions due to reduced damping and frequency shifts occurring under positive pressure due to mechanical stress on the prongs. This allows the QTF to offer precise measurements across the entire pressure range with a single sensor.

5.3.2 Compactness and Simplicity:

Unlike capacitive and piezoresistive sensors, which may require separate sensor units or complex compensation mechanisms, the QTF provides a compact and unified solution. Its small size and simple design make it easy to integrate into the housing, reducing overall system complexity while maintaining high performance.

5.3.3 Cost Efficiency:

The QTF is also more cost-effective compared to both piezoresistive and capacitive sensors, particularly because it is widely available in standard frequencies (such as 32.768 KHz) and does not require the use of expensive materials or specialized machining processes.

5.3.4 Reliability and Stability:

Quartz tuning forks are known for their long-term stability and low thermal drift, which are critical for applications that demand consistent performance over time. Unlike the other two, QTF's performance is less affected by environmental factors, ensuring reliable readings without the need for complex compensation techniques.

The quartz tuning fork was selected for its versatility, compactness and cost-efficiency. It provided a balanced solution to the design challenges that capacitive and piezoresistive sensors could not address.

Chapter 6

Conclusion and Future Work

6.1 Conclusion

This research presented the design and development of a novel, wide-range QTF-based compound gauge capable of measuring both vacuum and positive pressures with same proficiency. The sensor operates by detecting amplitude variations, corresponding to electrical impedance variations, in vacuum conditions and frequency shifts in positive pressure region, enabling a broad measurement range from 10^{-3} mbar to atmospheric pressure and further up to 10 bar in positive pressure region. The study demonstrated that the QTF sensor offers significant advantages over conventional pressure gauges. It provides a compact, low-power, and cost-effective solution while maintaining high accuracy across a wide pressure range. Experimental validation confirmed the sensor's ability to deliver high performance results with minimal cost. Calibration procedures and experimental tests were carefully designed to validate the sensor's response under different conditions, ensuring its practical applicability in various industrial and scientific settings. Numerous challenges were encountered during the development and testing, such as environmental influences (especially temperature), mechanical integrity under extreme pressure conditions etc. which were addressed through design iterations and refinements.

Overall, this research contributes to the field of pressure sensing by introducing a novel approach that combines a low-cost, widely available quartz tuning fork technology with pressure measurement principles. The findings lay a strong foundation for future improvements and broader applications in vacuum technology, industrial monitoring, and scientific instrumentation.

6.2 Future Work

While the developed QTF compound gauge has demonstrated promising results, several areas of improvement and further exploration is still there. Future research can focus on:

1. **Extended Pressure Range** Exploring alternative QTF configurations and advanced signal processing techniques could extend the measurable pressure range beyond the current limits.
2. **Environmental Compensation** Investigating the effects of temperature, humidity, and other environmental factors on sensor performance and implementing compensation techniques to improve accuracy.
3. **Internet of Things** Incorporating Internet-of-Things to the sensor for remote monitoring and real-time data acquisition in industrial and research applications.
4. **Commercialization and Field Testing** Conducting extended field trials in diverse environments and evaluating the feasibility of large-scale manufacturing for commercial deployment.

By working on these aspects, future work can further optimize the performance, reliability, and applicability of QTF gauge, making it a viable alternative to conventional pressure measurement technologies and further expanding its possible applications.

Bibliography

[1] ISO, *Vacuum technology – Vocabulary Part 1: General terms, 2nd edition*, International Organization for Standardization Std. ISO 3529-1, 2019-07.

[2] A. Chambers, *Modern Vacuum Physics, ISBN 978-0-8493-2438-3.* CRC Press, 2004.

[3] J. B. West, "Torricelli and the ocean of air: the first measurement of barometric pressure," *Physiology*, vol. 28, pp. 66–73, 2013.

[4] V. Harsch, "Otto von gericke (1602-1686) and his pioneering vacuum experiments." *Aviation, space, and environmental medicine*, vol. 78 11, pp. 1075–7, 2007. [Online]. Available: https://api.semanticscholar.org/CorpusID:21282738

[5] M'Leod, "Apparatus for measurement of low pressures of gas," *Proceedings of the Physical Society of London*, vol. 1, no. 1, p. 30, mar 1874. [Online]. Available: https://dx.doi.org/10.1088/1478-7814/1/1/308

[6] E. da C. Andrade, "The history of the vacuum pump," *Vacuum*, vol. 9, no. 1, pp. 41–47, 1959. [Online]. Available: https://www.sciencedirect.com/science/article/pii/0042207X5990555X

[7] C. F. Roca, "Vacuum-packed, please," *Mètode-110, Climate crisis*, vol. 3, 2021.

[8] J. M. Lafferty, "Review of pressure measurement techniques for ultrahigh vacua," *Journal of Vacuum Science and Technology*, vol. 9, no. 1, pp. 101–107, 01 1972. [Online]. Available: https://doi.org/10.1116/1.1316523

[9] L. GmbH, "Fundamentals of vacuum technology," p. 76, 2016. [Online]. Available: https://www.leybold.com/content/dam/brands/leybold/downloads/brochures/general-brochures/Fundamentals_of_Vacuum_Technology_EN.pdf

[10] A. Thomas and J. L. Cross, "Micrometer u-tube manometers for medium-vacuum measurements," *Journal of Vacuum Science and Technology*, vol. 4, pp. 1–5, 1967.

[11] A. BERMAN, "Chapter 4 - gauges for low-pressure measurement," in *Total Pressure Measurements in Vacuum Technology*, A. BERMAN, Ed. Academic Press, 1985, pp. 121–241. [Online]. Available: https://www.sciencedirect.com/science/article/pii/B9780120924400500107

[12] A. Wolf, "An elementary theory of the bourdon gage," *Journal of Applied Mechanics*, vol. 13, no. 3, pp. A207–A210, 03 1946. [Online]. Available: https://doi.org/10.1115/1.4009563

[13] F. B. Jennings, "Theories on bourdon tubes," *Transactions of the American Society of Mechanical Engineers*, vol. 78, no. 1, pp. 55–62, 02 1956. [Online]. Available: https://doi.org/10.1115/1.4013563

[14] D. J. Hucknall, "4 - pressure measurement," in *Vacuum Technology and Applications*, D. J. Hucknall, Ed. Butterworth-Heinemann, 1991, pp. 126–167. [Online]. Available: https://www.sciencedirect.com/science/article/pii/B978075061145950008X

[15] S. K. D. Ing., *Historical review*. John Wiley & Sons, Ltd, 2017, ch. 1, pp. 1–16. [Online]. Available: https://onlinelibrary.wiley.com/doi/abs/10.1002/9783433606667.ch1

[16] L. GmbH, "Vacuum measuring, controlling," p. 20, 2021. [Online]. Available: https://www.leybold.com/content/dam/brands/leybold/downloads/catalogue-chapters-pdf/060_EN_Measuring_Controlling.pdf

[17] T. C. Catalog, "P101, pressure transducer." [Online]. Available: https://www.te.com/en/product-CAT-PTT0018.html

[18] Z. A. Hasse, "Electric pressure recording device." *Review of Scientific Instruments*, vol. 80, no. 19, pp. 563–564, 09 1936.

[19] V. L. . R. C. J. C. Lilly, "A variable capacitor for measurement of pressure and mechanical displacement; a theoretical analysis and its experimental evaluation." *J. Appl. Physics*, no. 18, pp. 613–628, 1947.

[20] D. Alpert, C. G. Matland, and A. O. McCoubrey, "A null-reading absolute manometer," *Review of Scientific Instruments*, vol. 22, no. 6, pp. 370–371, 06 1951. [Online]. Available: https://doi.org/10.1063/1.1745941

[21] H. W. Drawin, "Electrical capacity -diaphragm vacuum gage. in german. advances in vacuumscience technology, proc. 1st int. cong, on vacuum techniques (1958)." *(PergamonPress, New York*, pp. 274–284, 1960.

[22] R. Hecht, "Apparatus for absolute pressure measurement," US Patent US3,446,075, May, 1969.

[23] C. K. W.R. Macdonald, "An electrostatic feedback transducer for measuring low differential pressures," Royal Aircraft Establishment, Tech. Rep. TR71022, 1971.

[24] K. Jousten, *Handbook of Vacuum Technology*. John Wiley & Sons, Jun 2016.

[25] MKS, "Baratron type 122a, absolute pressure gauge," 1996. [Online]. Available: https://www.mks.com/mam/celum/celum_assets/resources/122A-MAN.pdf

[26] R. W. Hyland and R. L. Shaffer, "Recommended practices for the calibration and use of capacitance diaphragm gages as transfer standards," *Journal of Vacuum Science & Technology A*, vol. 9, no. 6, pp. 2843–2863, 11 1991. [Online]. Available: https://doi.org/10.1116/1.577209

[27] M. S. Pirani, "Continuously indicating vacuum gage. in german." *Deutsche Physikalische Gesellschaft*, vol. 8, pp. 686–694, 1906.

[28] W. J. A. David C. Jacobs, "Miniature silicon based thermal vacuum sensor and method of measuring vacuum pressures," US Patent US5,557,972, Sep, 1996.

[29] W. B. Nottingham, "Electron emission problems," in *Proceedings of 7th Annual Conference on Physical Electronics*, no. 44. Massachusetts Institute of Technology, Cambridge: Research Laboratory of Electronics (RLE) at the Massachusetts Institute of Technology (MIT), Jan 1957, p. 1–2.

[30] R. T. Bayard and D. Alpert, "Extension of the low pressure range of the ionization gauge," *Review of Scientific Instruments*, vol. 21, no. 6, pp. 571–572, 06 1950. [Online]. Available: https://doi.org/10.1063/1.1745653

[31] F. Penning, "Ein neues manometer für niedrige gasdrucke, insbesondere zwischen $l0^{-3}$ und 10^{-5} mm," *Physica*, vol. 4, no. 2, pp. 71–75, 1937. [Online]. Available: https://www.sciencedirect.com/science/article/pii/S0031891437801238

[32] J. P. Hobson and P. A. Redhead, "Operation of an inverted-magnetron gauge in the pressure range 10^{-3} to 10^{-12} mm. hg," *Canadian Journal of Physics*, vol. 36, no. 3, pp. 271–288, 1958. [Online]. Available: https://doi.org/10.1139/p58-031

[33] O. Meyer, "Über die innere reibung der gase," *Pogg. Ann*, vol. 125, p. 177, 1865.

[34] J. C. Maxwell, "Iv. on the dynamical theory of gases," *Philosophical Transactions of the Royal Society of London*, vol. 157, pp. 49–88, 1867. [Online]. Available: https://royalsocietypublishing.org/doi/abs/10.1098/rstl.1867.0004

[35] J. Beams, D. Spitzer Jr, and J. Wade Jr, "Spinning rotor pressure gauge," *Review of Scientific Instruments*, vol. 33, no. 2, pp. 151–155, 1962.

[36] J. Fremerey, "High vacuum gas friction manometer," *Journal of Vacuum Science and Technology*, vol. 9, no. 1, pp. 108–111, 1972.

[37] K. Kokubun, M. Hirata, H. Murakami, Y. Toda, and M. Ono, "A bending and stretching mode crystal oscillator as a friction vacuum gauge," *Vacuum*, vol. 34, no. 8-9, pp. 731–735, 1984.

[38] S. Hansen, "The friction gauge: Pressure transducers that use quartz tuning fork resonators," *Vacuum Technology & Coating*, p. 14–7, Jul 2018. [Online]. Available: https://digital.vtcmag.com/12727/12608/

[39] A. Kundt and E. Warburg, "Ix. on friction and heat-conduction in rarefied gases," *The London, Edinburgh, and Dublin Philosophical Magazine and Journal of Science*, vol. 50, no. 328, pp. 53–62, 1875. [Online]. Available: https://doi.org/10.1080/14786447508641259

[40] J. C. Maxwell, "Xiii. the bakerian lecture.—on the viscosity or internal friction of air and other gases," *Philosophical Transactions of the Royal Society of London*, vol. 156, pp. 249–268, 1866. [Online]. Available: https://royalsocietypublishing.org/doi/abs/10.1098/rstl.1866.0013

[41] W. Sutherland, "Xxxix. thermal transpiration and radiometer motion," *The London, Edinburgh, and Dublin Philosophical Magazine and Journal of Science*, vol. 42, no. 258, pp. 373–391, 1896. [Online]. Available: https://doi.org/10.1080/14786449608620931

[42] J. L. Hogg, "Friction and force due to transpiration as dependent on pressure in gases," *Proceedings of the American Academy of Arts and Sciences*, vol. 42, no. 6, pp. 115–146, 1906. [Online]. Available: http://www.jstor.org/stable/20022193

[43] I. Langmuir, "Chemical reactions at very low pressures. i. the clean-up of oxygen in a tungsten lamp." *Journal of the American Chemical Society*, vol. 35, no. 2, pp. 105–127, 1913. [Online]. Available: https://doi.org/10.1021/ja02191a001

[44] F. Haber and F. Kerschbaum, "The measurement of low pressure in oscillating quartz filaments (determination of the vapour pressure of quicksilver and

iodine)," *ZEITSCHRIFT FUR ELEKTROCHEMIE UND ANGEWANDTE PHYSIKALISCHE CHEMIE*, vol. 20, no. 10, pp. 296–305, 1914.

[45] E. B. King, "Two new types of high vacuum gauge," *Proceedings of the Physical Society of London*, vol. 38, no. 1, p. 80, 1925.

[46] I. Lungmuir, "A new vacuum gage of extreme sensitiveness," *Phys. Rev*, vol. 1, no. 4, pp. 337–338, 1913.

[47] S. Dushman, "Theory and use of the molecular gauge," *Phys. Rev.*, vol. 5, pp. 212–229, Mar 1915. [Online]. Available: https://link.aps.org/doi/10.1103/PhysRev.5.212

[48] J. A. Roberts, "Vacuum gauge," US Patent USUS2 669 124A, Feb, 1954.

[49] W. Becker, "Reibungsyakuummeter "reva"," *Vacuum*, vol. 11, no. 4, pp. 195–204, 1961. [Online]. Available: https://www.sciencedirect.com/science/article/pii/S0042207X6180002X

[50] F. T. Holmes, "Axial magnetic suspensions," *Review of Scientific Instruments*, vol. 8, no. 11, pp. 444–447, 1937.

[51] J. W. Beams, I. Young, J. L., and J. W. Moore, "The production of high centrifugal fields," *Journal of Applied Physics*, vol. 17, no. 11, pp. 886–890, 11 1946. [Online]. Available: https://doi.org/10.1063/1.1707658

[52] J. Fremerey, "Cavity type permanent magnet suspension," *Review of Scientific Instruments*, vol. 44, no. 9, pp. 1396–1397, 1973.

[53] J. K. Fremerey and B. Lindenau, "Gas friction vacuum meter and method of making measuring body," US Patent US4 395 914A, Aug, 1983.

[54] J. Fremerey, "Spinning rotor vacuum gauges," *Vacuum*, vol. 32, no. 10-11, pp. 685–690, 1982.

[55] Fremerey, "The spinning rotor gauge," *Journal of Vacuum Science & Technology A: Vacuum, Surfaces, and Films*, vol. 3, no. 3, pp. 1715–1720, 1985.

[56] D. Pacey, "A piezoelectric oscillator manometer," *Vacuum*, vol. 9, no. 5-6, pp. 261–263, 1959.

[57] M. H. M. O. H. M. Y. Toda and K. Kokubun, "Pressure dependence of quartz crystal resonator characteristics (in japanese)," *Journal of Vacuum Society Japan*, vol. 26, no. 5, p. 526, 1983.

[58] M. Hirata, K. Kokubun, M. Ono, and K. Nakayama, "Size effect of a quartz oscillator on its characteristics as a friction vacuum gauge," *Journal of Vacuum Science & Technology A: Vacuum, Surfaces, and Films*, vol. 3, no. 3, pp. 1742–1745, 1985.

[59] M. Ono, M. Hirata, K. Kokubun, H. Murakami, F. Tamura, H. Hojo, H. Kawashima, and H. Kyogoku, "Design and performance of a quartz oscillator vacuum gauge with a controller," *Journal of Vacuum Science & Technology A: Vacuum, Surfaces, and Films*, vol. 3, no. 3, pp. 1746–1749, 1985.

[60] M. Ono, M. Hirata, K. Kokubun, H. Murakami, H. Hojo, H. Kawashima, and H. Kyogoku, "Quartz friction vacuum gauge for pressure range from 0.001 to 1000 torr," *Journal of Vacuum Science & Technology A*, vol. 4, no. 3, pp. 1728–1731, 05 1986. [Online]. Available: https://doi.org/10.1116/1.573966

[61] M. Hirata, M. Ono, K. Kokubun, M. Abe, N. Maruno, K. Shimizu, and T. Ogawa, "Design and testing of a quartz friction vacuum gauge using a self-oscillating circuit," *Journal of Vacuum Science & Technology A*, vol. 5, no. 4, pp. 2393–2396, 07 1987. [Online]. Available: https://doi.org/10.1116/1.574461

[62] K. Kokubun, M. Hirata, M. Ono, H. Murakami, and Y. Toda, "Unified formula describing the impedance dependence of a quartz oscillator on gas pressure," *Journal of Vacuum Science & Technology A*, vol. 5, no. 4, pp. 2450–2453, 07 1987. [Online]. Available: https://doi.org/10.1116/1.574869

[63] R. Stocker, "The quartz tuning fork as a total pressure gauge: a versatile concept," *Vacuum*, vol. 41, no. 7-9, pp. 2118–2119, 1990.

[64] T. Kobayashi, H. Hojo, and M. Ono, "Pressure measurement from 1 atm to 0.01 pa using a quartz oscillator," *Vacuum*, vol. 44, no. 5-7, pp. 613–616, 1993.

[65] H. E. Karrer and J. G. Leach, "Quartz resonator pressure transducer," US Patent US3 561 832A, Feb, 1971.

[66] R. W. Ward, "Pressure measurement apparatus and method," US Patent US4 644 796A, Feb, 1987.

[67] N. A. Downie and M. Behrens, "Method of and apparatus for measuring the pressure of a gas," US Patent US9 239 271B2, Jan, 2016.

[68] T. Kobayashi, H. Hojo, and M. Ono, "Gas concentration analysis with a quartz friction vacuum gauge," *Vacuum*, vol. 47, no. 6-8, pp. 479–483, 1996.

[69] A. Kurokawa, K. Odaka, and S. Ichimura, "Partial-pressure measurement of atmospheric-pressure binary gas using two pressure gauges," *Vacuum*, vol. 73, no. 2, pp. 301–304, 2004.

[70] A. Suzuki, A. Kurokawa, H. Nonaka, and S. Ichimura, "A possible hydrogen sensing method with dual pressure gauges," *Sensors and Actuators A: Physical*, vol. 127, no. 1, pp. 37–40, 2006.

[71] A. Suzuki and H. Nonaka, "Measurement of a wide range of hydrogen concentration with rapid response using dual pressure gauges," *international journal of hydrogen energy*, vol. 33, no. 21, pp. 6385–6392, 2008.

[72] A. Suzuki, "Hydrogen sensing characteristics of a quartz oscillator," in *Hydrogen Energy*, D. Minic, Ed. Rijeka: IntechOpen, 2012, ch. 14. [Online]. Available: https://doi.org/10.5772/48449

[73] A. Suzuki, H. Hojo, and T. Kobayashi, "Temperature calibration of quartz oscillator for outdoor hydrogen sensing," *Vacuum*, vol. 121, pp. 255–259, 2015.

[74] A. Suzuki, "Temperature-stable quartz oscillator and its applications in pressure gauges, gas sensing, and gas concentration measurements," *Journal of Vacuum Science & Technology A*, vol. 34, no. 3, 2016.

[75] A.Suzuki, "Outdoor use stability improvement of the baseline output from a quartz oscillator pressure sensor," *AIP Advances*, vol. 9, no. 3, 2019.

[76] K. Evans, "Power generation efficiency of piezoelectric crystals," Ph.D. dissertation, ., December 1983.